Energy Research and Development Division
FINAL PROJECT REPORT

A METHOD FOR EVALUATING DIAGNOSTIC PROTOCOLS FOR PACKAGED AIR CONDITIONING EQUIPMENT

Prepared for: California Energy Commission
Prepared by: Purdue University
Project Management: New Buildings Institute

PURDUE UNIVERSITY

nbi new buildings institute

DECEMBER 2012
CEC-500-08-049
DELIVERABLE 5.2

The CEC is in the process of reviewing this final report.

Prepared by: *Purdue University/Herrick Laboratories*
Primary Author(s):
Dr. Jim Braun, David Yuill, Howard Cheung

New Buildings Institute
1601 Broadway
Vancouver, WA 98663
360-567-0950
www.newbuildings.org

Contract Number: 500-08-049

Prepared for:
California Energy Commission

David Weightman
Contract Manager

Chris Scruton
Project Manager

Virgina Law
Office Manager
Energy Efficiency Research Office

Laurie ten Hope
Deputy Director
RESEARCH AND DEVELOPMENT DIVISION

Robert P. Oglesby
Executive Director

Acknowledgements

Special acknowledgements go to the tireless researchers, David Yuill and Howard Cheung, led by Dr. Jim Braun at Herrick Laboratories/Purdue University, in developing the evaluator.

Special thanks to NIST staff Dr. Piotr Domanski and Vance Payne for the close collaboration with the Purdue team and for the significant enhancements that were added to the evaluator functionality.

Thanks also to reviewers of the draft report whose contributions increased the clarity and understanding of the results: Jon Douglas, Lennox International, Sean Gouw, Southern California Edison, Keith Temple, Industry Consultant.

Final thanks to Mark Cherniack, New Buildings Institute, for overall project management.

PREFACE

The California Energy Commission Energy Research and Development Division supports public interest energy research and development that will help improve the quality of life in California by bringing environmentally safe, affordable, and reliable energy services and products to the marketplace.

The Energy Research and Development Division conducts public interest research, development, and demonstration (RD&D) projects to benefit California.

The Energy Research and Development Division strives to conduct the most promising public interest energy research by partnering with RD&D entities, including individuals, businesses, utilities, and public or private research institutions.

Energy Research and Development Division funding efforts are focused on the following RD&D program areas:

- Buildings End-Use Energy Efficiency
- Energy Innovations Small Grants
- Energy-Related Environmental Research
- Energy Systems Integration
- Environmentally Preferred Advanced Generation
- Industrial/Agricultural/Water End-Use Energy Efficiency
- Renewable Energy Technologies
- Transportation

A Method for Evaluation Diagnostic Protocols for Package Air Conditioning Equipment is the final report for the Fault Detection and Diagnostics: Moving the Market and Informing Standards in California project. This is a research project within the Evidence-based Design and Operations Project (CEC contract number 500-08-049) conducted by New Buildings Institute. The information from this project contributes to Energy Research and Development Division's Building End-Use Energy Efficiency Program.

When the source of a table, figure or photo is not otherwise credited, it is the work of the authors of the report.

For more information about the Energy Research and Development Division, please visit the Energy Commission's website at www.energy.ca.gov/research/ or contact the Energy Commission at 916-327-1551.

ABSTRACT

Fault detection and diagnosis (FDD) tools are becoming more widely available for air-conditioning systems in residential and light commercial settings, and FDD is included in California's Title 24 building energy code, but it is not known how effective these FDD tools are. There is no uniform method of evaluating how well FDD tools work. This report describes the development of methods for evaluating the performance of FDD for air-conditioners. A library of data has been developed with laboratory measurement data for systems with several common types of fault. The 607 test cases in the library include a wide range of operating conditions and faults, and nine different air-conditioners. These test cases are fed to an FDD tool and the tool's outputs are compared to the known fault conditions. The results are organized based on the effect that the fault would have on the system's capacity or efficiency. One finding of the study is that simulation data are needed to augment the library of experimental data. Therefore, a gray-box modeling approach has been developed with models generated to accurately model the performance of several systems operating under any conditions with (or without) faults present.

To demonstrate the FDD evaluation method, a case study described in the report, evaluates the performance of the California Refrigeration Charge/Airflow (RCA) FDD approach that is specified in Title 24-2008 and the upcoming Title 24-2013. The RCA is found to perform poorly, flagging faults in up to 46% of the unfaulted cases, misdiagnosing over 25% of cases with faults, and not detecting faults in 32-55% of the cases with faults present.

This work is continuing with federal support from National Institute for Standards and Technology (NIST). The methods will be further refined and performance metrics will be developed. A database of simulation data will be generated.

Keywords: air conditioning, rooftop units, fault detection and diagnosis, FDD, Title 24 FDD

Please use the following citation for this report:

Braun, James, David Yuill, Howard Cheung (Purdue University). 2012. ***A Method for Evaluating Diagnostic Protocols for Packaged Air Conditioning Equipment.*** California Energy Commission. Publication number: CEC-XXX-2010-XXX.

Table of Contents

Figures

Tables

Executive Summary

Background and objectives

Fault detection and diagnostics (FDD) was introduced in the 1970s for nuclear, industrial, aerospace and military applications, but over the past 15 years has been increasingly applied in HVAC. FDD in air-cooled unitary air-conditioning systems, including residential-type split systems and rooftop units (RTU) that are typically used in small commercial buildings, is of particular interest because these systems are so widely deployed and because they often have lower-quality installation and maintenance than larger and more complex systems, hence more undiscovered faults. Several FDD tools are currently available for unitary air-conditioning systems. When a homeowner, facilities manager, utility program manager or regulatory body is considering which tool to use (if any) a key question they must ask is: how well does each tool work? But no system currently exists for evaluating the performance of FDD tools applied to unitary air-conditioners, or for evaluating the performance of FDD tools in other industries. This problem is particularly pressing for California because the Title 24 Building Energy Code includes diagnostics-based installation procedures, and because utility programs have provided incentives for diagnostics-based maintenance programs. The objective of the current project is to address the need to know how well FDD tools work by developing a methodology for evaluating FDD protocols, and software that can conduct the evaluation methodology.

Evaluation method

The evaluation approach is to feed data from a large number of test cases to the candidate FDD protocol (the "protocol" is primarily the algorithm that the tool uses; it does not include the sensor hardware or the hardware interface), and collect the responses. Each test case represents a set of conditions that might be encountered by a FDD tool. The conditions include combinations of: (a) outdoor air temperature; (b) indoor air temperature; (c) indoor air humidity; (d) type of fault present, if any; (e) intensity of the fault; (f) specific unitary system.

For each test case there are five possible outcomes: (i) *No Response* – the FDD can't be applied, or can't give a diagnosis; (ii) *Correct*; (iii) *False Alarm* – a fault is indicated when no fault is present; (iv) *Misdiagnosis* – the wrong fault is diagnosed; (v) *Missed Detection* – the FDD indicates no fault when a fault is present. Percentages are calculated from the collected results of the set of test cases.

The raw results for the evaluation are organized according to the magnitude of the impact that the faults would cause on system performance. Results are presented across a wide range of performance degradation categories. This means that a user of the evaluation results may choose a fault impact threshold of interest. For example, if the user wishes to tolerate faults that cause less than 5% degradation in efficiency, he or she can see what the outcome rates are for this level of degradation.

To carry out the evaluation, a software tool has been developed. The tool contains a data library with the available test cases. The user interface allows selection of conditions (a) to (f) above and the candidate FDD protocol, and conducts the evaluation, producing graphs and tables of the results.

Faults

This project focuses on six common faults that affect unitary air-conditioning systems:

1. Refrigerant under- or overcharge
2. Low-side heat transfer
3. High-side heat transfer
4. Refrigerant liquid line restrictions
5. Non-condensables in the refrigerant
6. Compressor valve leakage

Standard definitions are proposed to quantify the severity of a fault for each fault type, and standard methods for imposing these faults in a laboratory are also proposed. A study of the performance effects of faults was conducted because the fault-imposed degradation strongly affects the utility of a FDD tool and the fault severity levels that should be evaluated. This study bolstered the rationale behind the standard methods of imposing faults in the laboratory. For example, it confirmed that reducing airflow across the evaporator or condenser is a good proxy for all fouling faults that commonly occur in these components.

Fault data library

A data library has been developed to provide input data for the evaluator. This library contains 66 data for each of 607 test cases. The data include measurements (pressure, temperature, humidity, flow rate, mass and power), information about the system (refrigerant type, nominal capacity, expansion device type, etc.), capacity and efficiency, and fault type and intensity (if a fault is present). These data come from experiments conducted on nine systems – 3 rooftop unit (RTU) and 6 split systems – in laboratories in the US. Each of the measurement data is the average of several measurements taken over a period of steady operation. The data have been organized in a standard format developed for this project, and have been carefully vetted for accuracy and consistency. Over 40% of the originally collected data were rejected because of apparent experimental problems.

One question that arose in a review of our work centered on the definition of "correct" refrigerant charge. The experimenters that tested the systems typically charged the unit carefully to the specification of the manufacturer, but in some cases it wasn't well documented. To ensure that the evaluations of undercharge- and overcharge-diagnosing FDD protocols are valid, the nominally correct charge is defined as the charge that gives the maximum efficiency at a standard rating condition (95/80/67).

When a system has a fault that degrades its performance, it is important for the evaluator to know how much the performance is degraded. A new index is proposed to quantify the performance degradation: the Fault Impact Ratio (FIR). Determining FIR experimentally requires exactly matching the operating conditions for a test with a fault and a test without a fault. This is very difficult in practice; typically conditions are close but not exactly the same. To overcome this problem we have built up normal models - models that are based on a regression of the unfaulted data – that simulate performance of the unfaulted system under any set of operating conditions. These models are used to calculate FIR values. All test cases in the library have FIR values, which allows evaluation to be based upon the true significance of the fault.

Simulation

There are several disadvantages to using experimental data for evaluation of FDD. Most significant is that existing data are quite limited, and generating new experimental results is very difficult and costly. To address this problem a method has been developed to model unitary systems operating with or without the faults included in this project. This method is a hybrid of inverse models – based on experimental data – and forward models that are based on physics alone. The method produces models, referred to as gray-box models, using some measurement data, but using physical laws to extend the model to conditions that were not tested experimentally. These models treat each component – compressor, heat exchangers, expansion device and piping – separately.

Additional experimental data that were not used in the modeling are used to validate the model. Models have been completed for all of the systems in the fault data library. These models show good agreement with the experimental data. Future work will include using simulation data generated with these models as inputs for the evaluator.

Case Study

A case study has been conducted to test and refine the evaluation methods developed in this project. The RCA protocol specified in California's Title 24 was evaluated. The RCA protocol is intended to diagnose refrigerant charge and evaporator airflow faults. It includes several different approaches depending on the expansion device, whether being applied by an installer or Home Energy Rating System (HERS) raters, or whether the 2008 or 2013 version of the standard is being used. It includes lookup tables for target values of superheat and temperature split (2008 version only), and uses superheat and subcooling to diagnose charge faults.

Although no metrics exist for categorizing the results of an evaluation, the results of the RCA evaluation can be considered quite poor. The limitations on operating conditions mean that for 21-28% of the test cases the RCA protocol gives *No Response*. The *False Alarm* rates are typically 15-50%, depending on the fault impact threshold of interest and the version of the protocol being considered. This *False Alarm* rate is particularly troubling, since each *False Alarm* results in costly service being done to a system that is performing well.

The *Misdiagnosis* and *Missed Detection* rates are also high. Aggregated summaries are shown in Table 1 for the four versions evaluated. These results, combined with the False Alarm rates paint a picture of a protocol that may not be worth applying.

Table 1: Aggregated summary of Misdiagnosis and Missed Detection rates for the RCA protocol

	2008		2013	
	Installer	HERS	Installer	HERS
Misdiagnosis Rate	26%	25%	32%	29%
Missed Detection Rate	32%	39%	37%	55%

Introduction

Background: FDD in HVAC

Fault detection and diagnostics (FDD) was introduced in the 1970s (Himmelblau 1978; Isermann 1984) for use in life-critical processes such as nuclear power, aerospace, and military applications, in which early detection of a fault may prevent catastrophic failure. FDD compares sensed data to the expected values of these data under given operating conditions to determine whether the data are within the expected ranges, and to determine what might cause them to be out of range. As the cost of sensors and controllers has decreased, FDD has been applied to many other engineering processes such as HVAC (Breuker and Braun 1998a; Katipamula & Brambley 2005). The objectives of applying FDD to HVAC are generally to sense subtle faults that degrade performance or reduce the expected equipment life, since such faults may go unnoticed by equipment operators until they cause outright equipment failure.

FDD has been applied to many kinds of HVAC equipment, such as chillers (Comstock and Braun 1999; Reddy 2007; Zhao et al. 2011), cooling coils (Veronica 2010), VAV air handling systems (Norford et al. 2002; House et al. 1999, Wang et al. 2011) and packaged air-cooled vapor compression air-conditioning equipment (Rossi and Braun 1997; Li and Braun 2003, Kim et al. 2008, Armstrong et al. 2006). The latter type of system, which includes rooftop units and split systems, is the focus of the current project, and will be referred to as a "unitary system." FDD on systems of this type is of particular interest for three reasons. The first is that these systems are very widely deployed, used in most houses and responsible for about 60% of the cooling energy used by commercial buildings in the US (Feng et al. 2005). The second is that these systems are often deployed in applications in which the operator does not provide regular maintenance and may not have the capability to recognize the presence of faults until the system fails (Roth et al. 2006). Finally, these systems have a high incidence of faults because of the lack of maintenance and because of installation issues related to lower-cost and less sophisticated systems (Wiggins and Brodrick 2012). As a result there are currently several companies that market FDD for unitary systems and there are equipment manufacturers that are including FDD capabilities in some of their unitary equipment product lines.

When considering which FDD approach to use, or when considering whether a particular FDD approach meets a code requirement, the obvious question to ask is: how well does it work? Answering this question is not simple. There is currently no standard method of evaluating the performance of FDD applied to unitary equipment, and "there are currently no available military or commercial standards to support a systematic and consistent approach to assessing the performance and effectiveness" of FDD applied to engineered systems in general (Vachtsevanos et al. 2006). This means that an evaluation method can't be adapted from another field or engineering application, in the same way that HVAC FDD itself was adapted from other fields.

There has been some previous research that considered evaluation of FDD for vapor compression air-conditioning equipment. Breuker & Braun (1998b) studied the accuracy of a FDD tool developed by Rossi and Braun (1997) when applied to a specific rooftop unit, and methods of tuning parameters within the tool to achieve optimal performance. Reddy (2007) discusses generic evaluation methodologies for assessing different FDD protocols applied to large chillers. None of the previous research proposed a standard method of test or evaluation and rating system.

FDD has the potential to provide significant benefits. Surveys of air-conditioning systems have found a large fraction to be operating with a fault (Rossi 2004; Breuker et al. 2000) that can have significant effects on capacity, efficiency and equipment life. For example, if refrigerant undercharge faults were eliminated from only the existing residential air conditioners in the US, it is estimated that residential cooling energy consumption would be reduced by 0.1 to 0.2 quad per year, i.e. a 5 to 10% reduction (Roth et al. 2006). However, FDD in unitary equipment is still a somewhat immature technology, as evidenced by the widely varying approaches used and by the low rate of adoption. Developing a method to test and evaluate FDD protocols is expected to help advance the technology in three ways. First, it will allow regulatory bodies to give meaningful specifications for FDD requirements. Second, it will allow users of FDD – including equipment manufacturers, facilities operators, utility incentive managers or equipment owners – to make informed decisions about whether to use FDD and which protocol will work best for them. Finally, it will aid the development and improvement of FDD algorithms by providing a measure by which improvements can be tracked.

California's need for FDD evaluation

California has a current need for methods of evaluating FDD for unitary air-conditioning equipment. The California Energy Commission (CEC) has included requirements for FDD in the Title 24 Building Energy Code, and has diagnostics-based test protocols for installation. There have also been sponsored programs aimed at improving the quality of installation and maintenance of air-conditioners in California, using diagnostics to test whether systems are correctly charged and have the correct indoor coil airflow. However, the effectiveness of the diagnostics methods is unknown, and was called into question as the energy savings fell short of expectations.

Project Objectives

The project described in this report was intended to develop methodologies for evaluating the effectiveness of FDD protocols applied to unitary systems operating in cooling mode that have (a) charge or airflow faults; (b) other commonly occurring faults; and (c) no significant faults. The term "protocol" is used here to refer to the algorithm that generates FDD outputs. A complete FDD tool will also include hardware, such as sensors, signal conditioners, and processors. These components can affect FDD performance, but are not within the scope of the current project.

An additional objective of this project was to develop software that is capable of implementing an evaluation following the evaluation methodology.

Evaluation method

Several approaches to evaluating the effectiveness of FDD protocols have been developed and considered in the current project. There are significant challenges to evaluating FDD because there are so many approaches to conducting FDD, using different inputs, giving different outputs, and having varied objectives. One major division is between protocols intended to be used in maintenance and installation work (typically run on a handheld device), and protocols intended to be used in a permanently-installed onboard application (automated FDD). The focus of this project is on the former – handheld devices – but much of the evaluation methodology could be applied to the latter. This project also focuses on FDD methods that are based on steady-state measurements from unitary equipment operating in cooling mode.

Another example of a challenge in evaluating FDD is that the benefits and costs associated with applying FDD vary for potential applications of a given FDD tool. For something as complex as FDD, ideally an evaluation provides a simple output, such as typical economic benefit from deploying the FDD. However, this value depends on fault prevalence, which is currently not well understood, so the evaluation method that was chosen is one in which the evaluation provides output based on the performance degradation. This allows flexibility in using the evaluation results for a wide range of expected scenarios. The method is summarized below then described in greater detail within the context of a case study on page 47, so that examples of the evaluation calculations are readily available.

Approach summary

The approach to evaluation of FDD protocols is to feed a set of data to each protocol and observe the responses, collecting and categorizing them to develop summary statistics. The data represent typical conditions that a FDD tool may encounter:

- Several different systems with different properties, such as configuration, refrigerant type, SEER rating, and expansion device type
- A range of ambient and indoor thermal conditions
- Different types of faults, or with no fault
- Different intensities of fault

For each test case (a single combination of the conditions above) the protocol gives a response. These responses are tallied and organized to give statistics that reflect the overall utility of the protocol. The evaluation process is summarized in Figure 1.

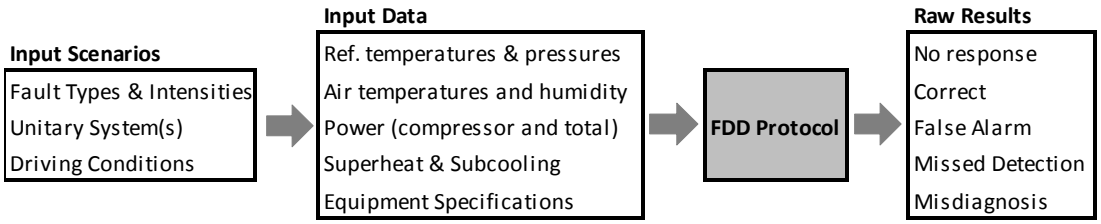

Figure 1: Evaluation method

The following subsections describe the components of the evaluation method in more detail. The library of input data compiled for this project is described in the "Data Library" section of this report. Fault types and their effects on operation of unitary air-conditioners are described in the "Faults" section.

Faulted and unfaulted operation

Faults are conditions that affect performance negatively and they have some level of severity. In this project we have developed two ways to characterize this level of severity. The first is Fault Intensity (FI), which is related to measureable quantities. For example, a 20% undercharge. The second is Fault Impact Ratio (FIR), which is related to equipment performance, and is tied to either capacity or COP. For example, when FIR_{COP} = 95%, it says that the equipment is operating at 95% of its maximum efficiency under a given set of driving conditions. Each of these terms – FI and FIR – are formally defined in later sections of this report.

There is not a direct relationship between FI and FIR. This means that it is possible to have faults that have some FI, but with no measureable degradation of performance. This raises the question of how do we draw a distinction between faulted and unfaulted operation. For the evaluation method developed in this project the answer is that we consider FIR, because the equipment performance is generally what equipment operators and users of FDD are concerned with. This leads to another question, which is: how much performance degradation constitutes faulted operation. Our approach is to leave this as a variable quantity, using FIR *thresholds* to draw the distinction between faulted and unfaulted. We evaluate each protocol at several thresholds so that a user of the results can choose the threshold he or she considers appropriate. If the FIR threshold is 99%, it means that test cases with FIR above this threshold are considered to be unfaulted, regardless of the FI. This threshold concept is important in the consideration of False Alarms, described below.

Test case outcomes

When FDD is applied, there are five possible outcomes with respect to fault isolation:

1. **No response** – the FDD protocol cannot be applied for a given input scenario, or does not give an output because of excessive uncertainty.

2. **Correct** – the operating condition, whether faulted or unfaulted, is correctly identified

3. **False alarm** – no significant fault is present, but the protocol indicates the presence of a fault. More specifically, a False Alarm is indicated when the protocol gives a response that a fault is present and

a. the fault impact is below a given threshold, and

b. the system is not overcharged by 5% or more

The special requirement in bullet b. is included for the following reason. An overcharged system may have a significant fault, but no significant impact on capacity or COP. Consider the example case of a system that is 10% overcharged, but has no significant degradation of capacity or COP. An equipment operator may want to know about the overcharge, since it can be associated with reduction of compressor life, even though it doesn't impact the current performance of the equipment. To address this situation, if the refrigerant is overcharged by more than 5% the system is considered faulted, even if the fault impact is below the given threshold.

4. **Misdiagnosis** – a significant fault is present, but the protocol misdiagnoses what type of fault it is. There are two ways that Misdiagnoses are defined. The first, Misdiagnosis (a), considers test cases with any fault type. The second, Misdiagnosis (b), only considers test cases with faults of a type that the protocol is intended to diagnose. Misdiagnosis (b) can be applied to protocols that are not intended to diagnose all of the fault types represented in the Data Library, to give additional insight into the performance of the protocol. In this study, misdiagnoses rates are presented within specific bands (ranges) of fault impact ratios. With this in mind, the specific criteria for the two misdiagnosis cases are:

   Misdiagnosis (a) is a test case where three criteria are met:

   a. Fault Impact Ratio (FIR) is within the specified range

   b. Experimenter indicated the presence and intensity of a fault

   c. Protocol indicates that the system has a fault different from the type of fault indicated by the experimenter

   Misdiagnosis (b) is a test case where three criteria are met:

   a. Fault Impact Ratio (FIR) is within the specified range

   b. Experimenter indicated the presence and intensity of a fault of a type that the protocol is intended to diagnose

   c. Protocol indicates that the system has a fault different from the type of fault indicated by the experimenter

5. **Missed Detection** – a significant fault is present, but the protocol indicates that no fault is present. Missed Detection rates are presented within specific bands (ranges) of fault impact ratios to better understand where the Missed Detections are most important. Missed Detections are considered for the full data library (Missed Detection (a)) and for the subset of test cases that have faults that the protocol is intended to diagnose (Missed Detection (b)) in the same way that Misdiagnosis results are considered. The criteria for the two Missed Detection cases are:

Missed Detection (a) is a case where three criteria are met:

a. Fault Impact Ratio (FIR) is within the specified range

b. Experimenter indicated the presence and intensity of a fault

c. Protocol indicates that the system has no fault

Missed Detection (b) is a case where three criteria are met:

a. Fault Impact Ratio (FIR) is within the specified range

b. Experimenter indicated the presence and intensity of a fault of a type that the protocol is intended to diagnose

c. Protocol indicates that the system has no fault

To evaluate an FDD protocol, one feeds it multiple input scenarios, each of which gives one of these five test outcomes. Test outcomes 1, and 3 to 5 are gathered and expressed as rates, using percentages. Test outcome 2 is implied by the other outcomes. The rate calculations are provided here and demonstrated within the description of the Case Study.

Test case outcome rate calculations

In rate calculations, the numerator is the number of test cases that have a given test outcome (one of the five listed above). The denominator for each test outcome rate is described below. Each denominator is defined based on determining a meaningful rate. The denominators include only the cases that could apply to each type of outcome. For example, a Misdiagnosis can't be made on a test in which no fault is present, so only those cases determined to be faulted are included in the denominator for Misdiagnosis rate. (If a protocol indicates a fault when none is present, this is a False Alarm, not a Misdiagnosis).

No Response
Numerator: number of cases that meet the "No Response" criteria
Denominator: total number of test cases

False Alarm
Numerator: the number of cases that meet the "False Alarm" criteria
Denominator: the number of cases in which the fault impact is below a specified threshold and the refrigerant is not overcharged by more than 5%

Misdiagnosis (a)
Numerator: the number of cases that meet the "Misdiagnosis (a)" criteria
Denominator: the number of cases that meet the following criteria:

- Fault Impact Ratio (FIR) is within the specified range
- Experimenter indicated the presence and intensity of a fault

- Protocol indicates that the system has a fault

Misdiagnosis (b)
Numerator: the number of cases that meet the "Misdiagnosis (b)" criteria listed in the section above
Denominator: the number of cases in which three criteria are met:

- Fault Impact Ratio (FIR) is within the specified range
- Experimenter indicated the presence and intensity of a fault of a type that the protocol is intended to diagnose
- Protocol indicates that the system has a fault

Missed Detection (a)
Numerator: number of cases that meet the "Missed Detection (a)" criteria
Denominator: the number of cases in which three criteria are met:

- Fault Impact Ratio (FIR) is within the specified range
- Experimenter indicated the presence and intensity of a fault
- Protocol gives a response

Missed Detection (b)
Numerator: number of cases that meet the "Missed Detection (b)" criteria
Denominator: the number of cases in which three criteria are met:

- Fault Impact Ratio (FIR) is within the specified range
- Experimenter indicated the presence and intensity of a fault of a type that the protocol is intended to diagnose
- Protocol gives a response

Software tool

A prototype interactive software tool has been developed that carries out an evaluation of FDD protocols. A schematic diagram shown in Figure 2 describes the flow of information within the evaluator software. The tool uses measurement data for normal and faulty performance that were obtained through laboratory testing in previous studies for a number of different systems where faults were artificially introduced. The data were organized in a common format and are used as inputs to the evaluator. The evaluator interfaces to an FDD protocol by providing measurement data and collecting responses. It then determines overall statistics for false alarm rates, missed detections and misdiagnoses. Originally, false alarm rate was determined using the unfaulted cases specified by the experimenters who performed the experiments. The interactive tool is being updated using the unfaulted definition provided in this report, where the fault impact ratio needs to be less than a specified threshold in order for a case to be considered unfaulted. In addition, future versions will include data generated from equipment simulations based on models developed in this project. The software tool and full data library will be provided as a separate deliverable. A sample protocol (the RCA) will be coded and included with the software.

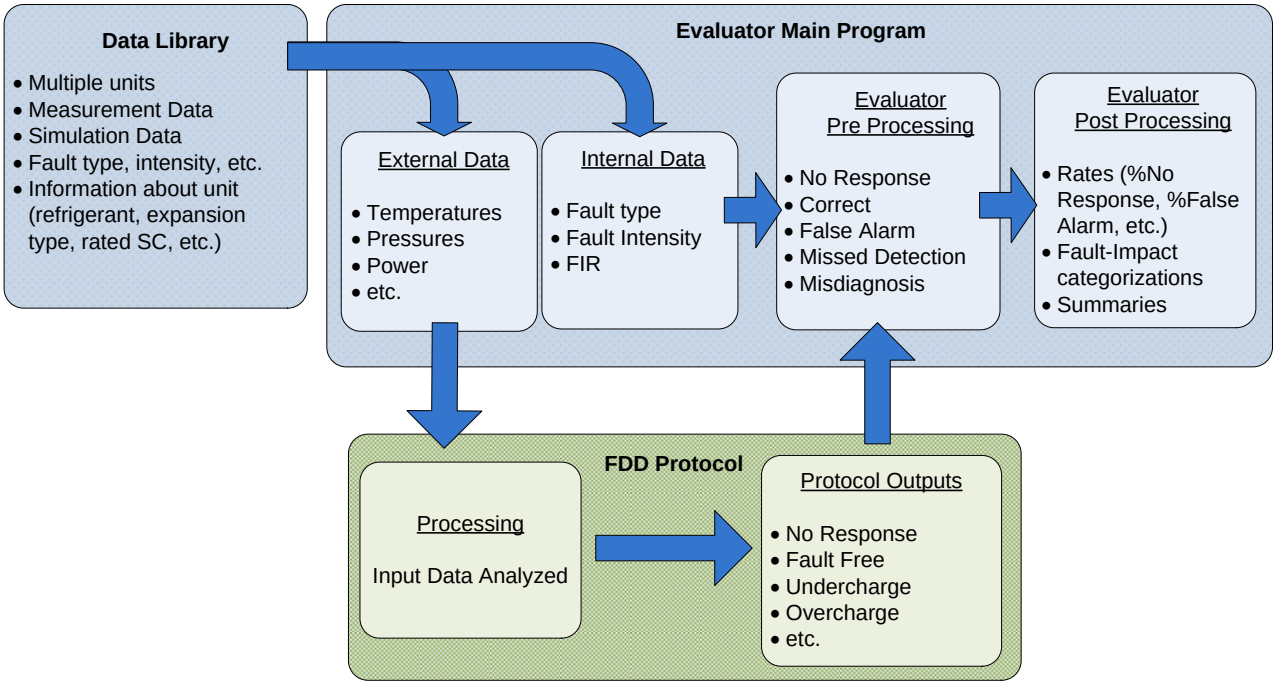

Figure 2: Schematic diagram of evaluator software

Faults

Faults considered in this project

There are six degradation faults that are included in the evaluation. The project's original proposal and contract included only charge and airflow faults. However, because other faults are known to exist in the field, an evaluation should consider the effect these faults have on a protocol, regardless of whether that protocol is intended to detect and diagnose these faults.

The six faults included are listed in Table 2, along with a description of each fault. A diagram showing the components of an air-conditioning system is shown in Figure 3, and referred to in the descriptions of faults and how to impose faults in experiments.

Table 2: Faults included in evaluation of FDD protocols

Fault	Abbr.	Description
Under- or overcharge	UC, OC	A mass of refrigerant that is less or more than the manufacturer specification
Low-side heat transfer	EA	Faults in the evaporator coil such as coil fouling or insufficient airflow
High-side heat transfer	CA	Faults in the condenser coil such as coil fouling or insufficient airflow
Liquid line restriction	LL	Flow restrictions such as crimps or fouled filter/drier in the liquid line (Figure 3)
Non-condensables	NC	The presence of gases that do not condense (e.g. air or nitrogen) in the refrigerant
Compressor valve leakage	VL	Leaks in the compressor from high to low pressure regions, reducing mass flow

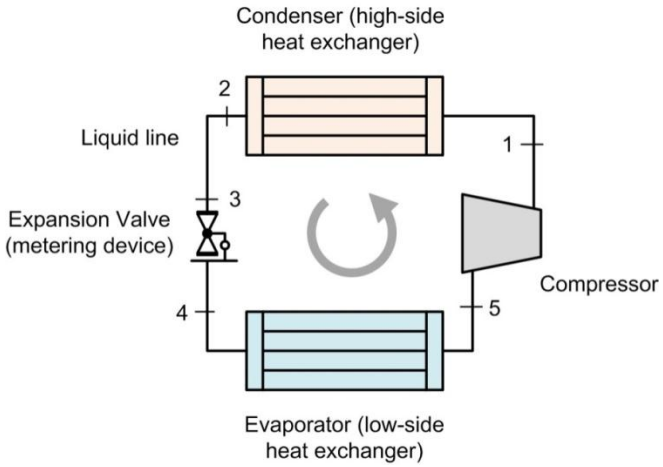

Figure 3: Components of a typical vapor-compression air-conditioner

Imposing faults in laboratory experiments

To provide measurement data as an evaluator input, faults were simulated in a laboratory. We have developed a term to quantify the severity of the fault – Fault Intensity (FI) – and defined FI for each type of fault. A description of how faults were imposed in the laboratory, and the definition of FI for each fault type is provided below.

1. Charge: To impose an under- or overcharge fault, charge is simply removed from or added to the system. The fault intensity is:

$$FI_{charge} = \frac{m_{actual} - m_{nominal}}{m_{nominal}} \quad (1)$$

where m_{actual} is the measured mass of refrigerant in the system

$m_{nominal}$ is the nominally correct mass of refrigerant (see discussion on charge effect on COP and capacity on page 22)

Thus a system designed for 5 lb of charge that had 4.5 lb would be referred to as 10% undercharged or having FI_{charge} = -10%. If manufacturer specifications are not available, an alternate definition for nominal mass can be based on the refrigerant mass that provides the maximum capacity or efficiency.

2. Low-side heat transfer faults: In a typical laboratory setup the airflow across the evaporator coil can be modulated using a variable speed booster fan or dampers. Reducing the airflow accurately duplicates the effect of most faults in this category: airflow reduction from fan or distribution system design problems, obstructions or filter fouling. The effect of evaporator coil air-side fouling is also assumed to be well represented by reducing airflow, particularly if the fouling is assumed to be evenly distributed across the face of the heat exchanger. The fault intensity is defined analogously to FI_{charge} using either mass flow rate or volumetric airflow rate.

$$FI_{EA} = \frac{\dot{V}_{actual} - \dot{V}_{nominal}}{\dot{V}_{nominal}} \quad (2)$$

3. High-side heat transfer faults: Similarly to low-side faults, a reduction in airflow is used to implement high-side heat transfer faults. Some experimenters have simulated blockage by large-scale debris, such as leaves, by covering the face of the condenser coil with paper or mesh. Although this may, in some cases, more realistically represent the fault physically, it is not repeatable nor easily quantified as a fault intensity. Furthermore, the general effect – to increase the refrigerant's high-side pressure – is the same as with reduced airflow. Therefore, reduced airflow is proposed as the standard means of imposing this fault in the laboratory. Accordingly, the fault intensity is defined with airflow rates in the same manner as with low-side heat transfer faults.

$$FI_{CA} = \frac{\dot{V}_{actual} - \dot{V}_{nominal}}{\dot{V}_{nominal}} \quad (3)$$

4. Liquid line restriction: A liquid line restriction is implemented by using one or more valves to impose the desired pressure loss. The fault intensity is defined using the ratio of the increase in pressure drop through the liquid line caused by the faulted condition to the liquid line pressure drop under non-faulted operation and at the same operating condition.

$$FI_{LL} = \frac{\Delta P_{LL,faulted} - \Delta P_{LL,unfaulted}}{\Delta P_{LL,unfaulted}} \quad (4)$$

5. Non-condensables in the refrigerant: A non-condensables fault is imposed by introducing nitrogen into the refrigerant line. The maximum amount of non-condensables to be expected is in the case where a system has been open to the atmosphere and not evacuated prior to charging. Therefore, the fault is defined with a mass of nitrogen compared to the mass of nitrogen that would fill the system at atmospheric pressure.

$$FI_{NC} = \frac{m_{N_2,fault}}{m_{N_2,ref}} \quad (5)$$

6. Compressor valve leakage: Compressor valve leakage is simulated with the use of a hot gas bypass – a pipe carrying refrigerant from the discharge to the inlet of the compressor (from point 1 to point 5 in Figure 3). The fault intensity for this fault is defined as the change in mass flow rate (at a given operating condition) to the original mass flow rate.

$$FI_{VL} = \frac{\dot{m}_{faulted} - \dot{m}_{unfaulted}}{\dot{m}_{unfaulted}} \quad (6)$$

Faults not considered in this project

There are many possible faults that occur in unitary air-conditioners. The faults that are used in the evaluator are controlled largely by the available experimental data. Previous researchers have considered these six faults important, and have conducted experiments to quantify their effects. The results of these experiments are included in the data library.

Some other faults that are not included in the evaluation method developed here are

- Economizer faults
- Thermostatic Expansion Valve (TXV) faults
- Control faults, such as short cycling, sensor failure or degradation, etc.

These faults can have major impacts on performance, and anecdotal evidence suggests that they may be quite prevalent. The evaluation method presented here can be adapted to include these faults when appropriate input data become available.

Fault effects literature

We conducted a review of literature on the effects of faults. The papers gathered and reviewed are listed at the end of this section.

One thing we were looking for in this review is methods to generalize the magnitude of fault impacts on performance (capacity and efficiency). For example, in Figure 4 we have conducted a least-squares linear regression on the relative capacity as a function of relative charge for four units in our data library that have fixed-orifice expansion (FXO) devices. These data all come from tests conducted at the standard rating condition (95°F ambient, 80°F indoor drybulb, and 67°F indoor wet-bulb). The regression equation in the figure can be used to predict performance within the charge range. It would be useful if there were some similarly simple method to generalize these effects across a range of operating conditions, and to discuss the limitations with respect to generalizing performance in different systems.

No such methods were found. However, being able to estimate fault impacts in general could be very useful for researchers, equipment developers, FDD developers, energy simulators, and regulatory bodies. Therefore we plan to develop a paper intended to provide correlations for estimated fault impacts, based on the body of data we have gathered into our data library.

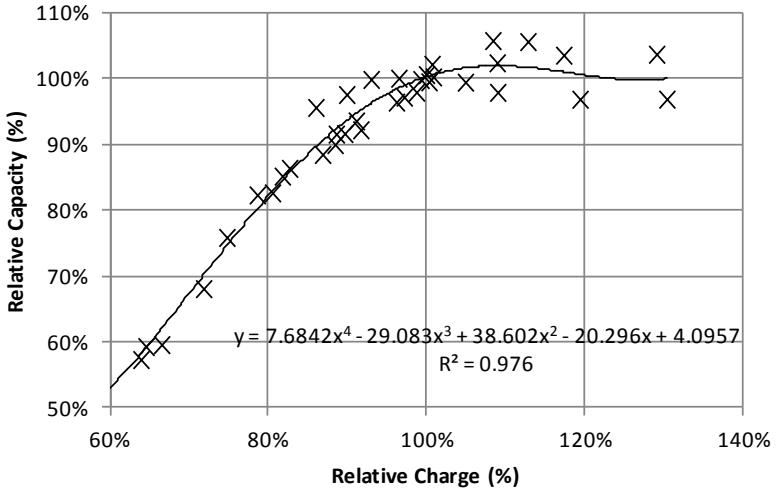

Figure 4: Effect of relative charge level on capacity of four FXO units at rating conditions

Another purpose of the review was to investigate an important question in the current project: is airflow reduction an appropriate proxy for air-side coil fouling? Ali and Ismail (2008) suggest that it is not. However, Bell et al. (2012) and Yang et al. (2007a) both conclude that the effect of fouling on the heat transfer coefficient is small, but the impact on air pressure drop across the coil is large and dominant in the fouling degradation effect for constant speed fan systems. We did a review and analysis of Ali and Ismail and concluded their results aren't applicable to the systems we are considering, and do not affect our assumption that reduced airflow is indeed a good proxy for all air-side heat transfer impediments.

One reason is that the system they studied is a window-mounted air-conditioner. Another is that their conclusions are based in part on performance at very high face velocities. Typical face velocities are about 1.5 m/s, whereas Figure 5 shows that the face velocities in their experiment range up to 5 m/s. The scatter in the 1 to 2 m/s range is larger than the effects being measured. Furthermore, the data show a trend of reduced COP for a given mass of fouling as airflow rates get higher than 2.5 m/s. This suggests that fan power is included in the COP calculation, which would blur the effect being considered.

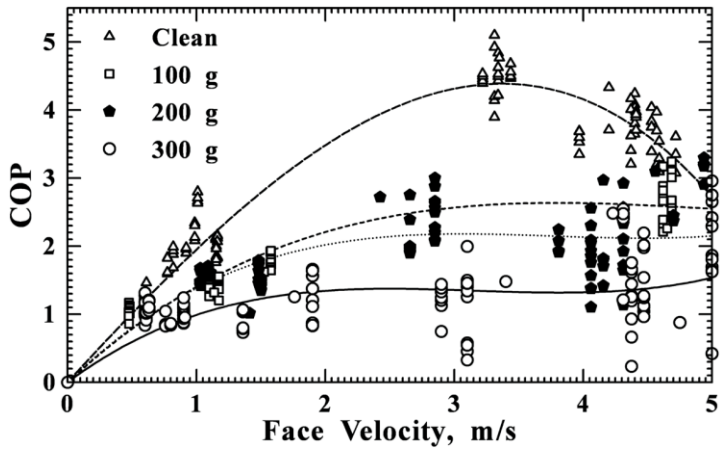

Figure 5: Results of a coil fouling experiment from Ali and Ismail (2008)

Therefore, based on the results of Bell et al. (2012) and Yang et al. (2007a), it is concluded that reduced airflow is an appropriate and reliable proxy for coil fouling faults.

Fault Effect Literature Reviewed:

Ali, A.H.H. and I.M. Ismail. 2008. Evaporator Air-Side Fouling: Effect on Performance of Room Air Conditioners and Impact on Indoor Air Quality, *HVAC&R Research*, 14:2, 209-219

Bell, I.H., Groll, E.A., König, H. 2012. Experimental Analysis of the Effects of Particulate Fouling on Heat Exchanger Heat Transfer and Air-Side Pressure Drop for a Hybrid Dry Cooler. *Heat Transfer Engineering*, 32(3–4): p. 264–271.

Breuker, M.S. 1997. Evaluation of a Statistical, Rule-Based Fault Detection and Diagnostics Method for Vapor Compression Air Conditioners. Master's Thesis, School of Mechanical Engineering, Purdue University, IN.

Breuker, M.S. and J.E. Braun. 1998. Common faults and their impacts for rooftop air conditioners. *Int. J. HVAC&R Research* 4 (3): 303-318.

Bultman, D.H., L.C. Burmeister, V. Bortone, and P.W. TenPas. 1993. Vapor-Compression Refrigerator Performance Degradation due to Condenser Airflow Blockage. *Proceedings of the National Heat Transfer Conference*. New York: ASME

Farzad, M. and O'Neal, D. L. 1991. System performance characteristics of an air conditioner over a range of charging conditions," *International Journal of Refrigeration*, vol. 14, pp. 321-328.

Farzad, M. and D.L. O'Neal. 1990. The effect of improper refrigerant charging on the performance of an air conditioner with capillary tube expansion. *Energy and Buildings*, 14(4): 363–371

Farzad, M. and O'Neal, D. L. 1993. Influence of the expansion device on air-conditioner system performance characteristics under a range of charging conditions, *ASHRAE Transactions*, vol. 99, pp. 3-13.

Grace, I. N., Datta, D., and Tassou, S. A. 2005. Sensitivity of refrigeration system performance to charge levels and parameters for on-line leak detection, *Applied Thermal Engineering*, vol. 25, no. 4, pp. 557-566.

Kim, M., W.V. Payne, P.A. Domanski, S.H. Yoon, and C.J.L. Hermes. 2009. Performance of a residential heat pump operating in the cooling mode with single faults imposed. *Applied Thermal Engineering* 29(2009): 770-778.

Krafthefer, B., C. Rask, and D.R. Bonne. 1987. Air-Conditioning and Heat Pump Operating Cost Savings by Maintaining Coil Cleanliness. *ASHRAE Transactions* 93(1): 1458-1473.

Pak, B.C., E.A. Groll, and J.E. Braun. 2005. Impact of fouling and cleaning on plate fin and spine fin heat exchanger performance. *ASHRAE Transactions* 111(1):496–504.

Palmiter, L., J-H. Kim, B. Larson, P.W. Francisco, E.A. Groll, and J.E. Braun. 2011. Measured effect of airflow and refrigerant charge on the seasonal performance of an air-source heat pump using R-410A. *Energy and Buildings* 43(2011): 1802–1810.

Rossi, T.M., and J.E. Braun. 1996. Minimizing Operating Costs of Vapor Compression Equipment with Optimal Service Scheduling. *Int. J. HVAC&R Research* 2(1): 23-47.

Yang L., J.E. Braun, and E.A. Groll. 2007a. The impact of evaporator fouling and filtration on the performance of packaged air conditioners. *International Journal of Refrigeration* 30(2007) 506-514.

Yang L., J.E. Braun, and E.A. Groll. 2007b. The impact of fouling on the performance of filter-evaporator combinations. *International Journal of Refrigeration* 30(2007): 489-498.

Yoon, S.H., W.V. Payne and P.A. Domanski. 2011. Residential heat pump heating performance with single faults imposed. *Applied Thermal Engineering* 31(2011): 765-771

Data library

One of the most significant outputs from this project is the development of a data library. The library supplies input data for evaluation. It consists of both experimental and simulation data for unitary systems operating at steady state over a range of operating conditions and fault conditions.

Summary of data library

Table 3 shows a summary of the units and numbers of test cases contained in the experimental data library. The number of tests is separated to show the number for each fault type for each system, using the fault type abbreviations given in Table 2. There are a total of 607 test cases, gathered from experiments on nine unitary systems. Three of the systems are rooftop units (RTU), but the tests on these three make up 60% of the total test cases.

Table 3: Summary of test cases in experimental data library

							Number of tests								Temp.	
#	ID	Type	Capacity [tons]	Refrig.	Exp. Device	Comp. Type	No Fault	UC	OC	EA	CA	LL	NC	VL	Min. [°F]	Max. [°F]
1	RTU 3	RTU	3	R410a	FXO	Scroll	24	25	12	21	6	0	0	0	67	125
2	RTU 7	RTU	3	R22	FXO	Recip.	39	34	0	26	36	34	0	33	60	100
3	RTU 4	RTU	5	R407c	FXO	Scroll	17	15	12	19	8	0	0	0	67	116
4	Split 1	Split	3	R410a	FXO	Recip.	1	29	1	0	0	0	0	0	82	127
5	RTU 2[1]	Split	2.5	R410a	TXV	Scroll	16	12	12	21	15	16	15	16	70	100
6	Split 2	Split	3	R410a	TXV	Recip.	2	30	7	0	0	0	0	0	83	127
7	Split 3	Split	3	R410a	TXV	Scroll	4	4	7	0	0	0	0	0	82	125
8	Split 4	Split	3	R22	TXV	Scroll	4	8	0	8	0	0	0	0	82	125
9	Split 5	Split	3	R22	TXV	Scroll	4	4	4	6	0	0	0	0	82	125
						Total:	111	161	55	101	65	50	15	49		

Note 1: RTU 2 is a split system, but was named using a previous naming convention.

The rightmost columns show the limits of the range of ambient temperature during testing for each of the test units in the library. The distribution of tests by return air wet-bulb temperature and by ambient temperature (among the entire set of 607) is shown in Table 4.

Table 4: Distribution of tests by return air wet-bulb temperature (left) and ambient temperature (right)

Return air wet-bulb

Range [°F]	Number of occurrences
50-55	16
55-60	260
60-65	85
65-70	240
70-75	6
	607

Ambient Temperature

Range [°F]	Number of occurrences
60-70	53
70-80	58
80-90	223
90-100	186
100-110	26
110-120	39
>120	22
	607

Description of data

The data in the library represent steady-state cooling operation. Each datum is an average of multiple measurements – from 8 to several hundred – taken while the equipment was operating steadily. The experimenters followed the same standards that equipment performance rating experiments follow, such as AHRI Standard 210/240 (AHRI 2008) and ASHRAE Standard 37 (ASHRAE 2009). More details on the experimental approaches of the data included in the data library can be found in the following references: Breuker (1997), Kim et al. (2006), Shen et al. (2006), Palmiter et al. (2011).

The data library contains measurement data and system information. The types of measurement (and calculated) data are listed in Table 5 in IP units. The entire data library also has an SI-unit version so that inputs are readily available for protocols that use these units, such as European protocols.

Table 5: Data library measurement data types

Variable ID	IP Units	Description
T_RA	[°F]	Return Air dry bulb temperature (evaporator inlet)
DP_RA	[°F]	Return Air dewpoint temperature (evaporator inlet)
WB_RA	[°F]	Return Air wet bulb temperature (evaporator inlet)
RH_RA	[%]	Return Air relative humidity (evaporator inlet)
T_SA	[°F]	Supply Air dry bulb temperature (evaporator outlet)
DP_SA	[°F]	Supply Air dewpoint temperature (evaporator outlet)
WB_SA	[°F]	Supply Air wet bulb temperature (evaporator outlet)
RH_SA	[%]	Supply Air relative humidity (evaporator outlet)
T_amb	[°F]	Ambient air dry bulb temperature
P_LL	[psia]	Liquid line pressure
T_LL	[°F]	Liquid line temperature
P_suc	[psia]	Suction pressure
T_suc	[°F]	Suction temperature
P_dischg	[psia]	Compressor discharge pressure
T_dischg	[°F]	Compressor discharge temperature

Power	[W]	Total electrical power of system
T_air_ce	[°F]	Condenser exiting air temperature
T_sat_e	[°F]	Refrigerant saturation temperature in the evaporator
T_sat_c	[°F]	Refrigerant saturation temperature in the condenser
Power_comp	[W]	Compressor power
Fault	[-]	Experimenter's identified fault type (or unfaulted)
Q_ref	[Btu/hr]	Refrigerant side capacity
Q_air	[Btu/hr]	Air-side capacity
SHR	[-]	Sensible Heat Ratio
COP	[-]	Coefficient of performance
SH	[°F]	Suction Superheat
SC	[°F]	Subcooling
m_ref	[lbm/min]	Refrigerant mass flow rate
Chrg	[lbm]	Mass of refrigerant charge
Chrg%	[%]	Charge as a percentage of nominally correct charge
V_i	[CFM]	Indoor coil volumetric airflow rate
V_i_nom	[CFM]	Nominal indoor coil volumetric airflow rate
V_i_%	[%]	Indoor coil volumetric airflow rate as percentage of nominal
V_o	[CFM]	Outdoor coil volumetric airflow rate
V_o_nom	[CFM]	Nominal outdoor coil volumetric airflow rate
V_o_%	[%]	Outdoor coil volumetric airflow rate as a percentage of nominal
Blk%	[%]	Portion of outdoor coil blocked
LL restr.	[psia]	Pressure loss through liquid line restriction
NonCond	[lbm/lbm]	Mass fraction of non-condensables in the refrigerant
NonCond%	[%]	Mass of non-condensables as a percentage of reference mass
VlvLeak	[lbm/min]	Compressor hot-gas bypass mass flow rate
VlvLeak	[%]	Compressor hot-gas bypass mass flow rate as % of total mass flow
$FIR_{capacity}$	[%]	Fault Impact Ratio for capacity
FIR_{COP}	[%]	Fault Impact Ratio for COP

For each test case there are also pieces of system information about the test unit. The types of system information are described in Table 6.

Table 6: Data library system information

Variable ID	Description
Expansion Type	Expansion valve type (TXV, FXO or EEV)
Manufacturer	Manufacturer
Model (indoor)	Model of indoor unit (for split systems)
Model (outdoor)	Split system outdoor unit model or RTU model

Nominal Capacity	Nominal Capacity (tons)
Refrigerant	Refrigerant
Operating Mode	Cooling or heating
Compressor Type	Reciprocating, scroll, etc.
Compressor Model	Compressor Model
Target SC	Target subcooling rate (for TXV systems)
EER	Energy efficiency ratio
SEER	Seasonal energy efficiency ratio
C1 to C10	Compressor map coefficients

Some of the test units in the data library do not have all of the types of data listed in these tables.

Data vetting, uncertainty and removal of questionable data

FDD protocols use different inputs to detect and diagnose faults. To ensure that the evaluations are meaningful they must be fair, which requires consistent data. A great deal of effort has gone into studying the data to look for inconsistencies because of the importance of using reliable input data. This was done manually.

In conducting and reporting on experiments, results can't be removed from the dataset without justification because this could skew the overall results or conclusions of the experiment. However, in vetting the data for the evaluator, removal of a test case doesn't necessarily skew results because it is removed for all protocols that will be evaluated.

Of more than 1000 test cases that were collected for 14 units, about 40% were removed. Some of the reasons for removal:

- *Data that don't follow physical laws* – for example if significant refrigerant pressure increases occur in locations other than the compressor, if energy is not conserved, humidity is generated across the evaporator, etc.

- *Data that show too much scatter, or are obvious outliers when compared to other data within the set*. For unfaulted tests, a normal model (described below) was an effective tool for assessing outliers. One of the test units was rejected completely because of questionable data.

- *Data that are not self-consistent* – as with fault detection, redundancy in data can be used to detect problems. For example, in cases where an experimenter provided two forms of humidity, such as wet-bulb and relative humidity, each was checked using psychrometric relationships and the associated pressure and dry-bulb temperature. If they didn't agree, the test was further investigated by comparing to air-side capacity or sensible heat ratio if sufficient data were available. If it was unclear which variable was flawed, the test case was removed. Similar approaches were used to check other calculated data, such as capacity and COP.

- *Insufficient data* – some data sets did not contain enough data to determine the impact of a fault. Four of the 14 test units were removed for this reason.

Charge effect on COP and capacity

For faults such as the presence of non-condensable gas in the refrigerant, compressor valve leakage, or reduced airflow across the outdoor coil, the unfaulted condition is clear. However, the unfaulted or "correct" mass of refrigerant charge in a system is less clear. The experimenters have charged their experimental units by methods that they may not have detailed within their description of the experiments. Their data sets usually identify which tests they consider to be conducted with correct charge. However, when evaluating FDD protocols that are attempting to diagnose charge faults, it's imperative that the experiments with nominally correct charge truly have correct charge.

An earlier approach to defining the correct charge was to use the experimenters' nominally correct values. However, this was criticized because we can't be certain that the experimenters' values were correct. To provide a consistent approach, we currently define the correct charge as being **the mass of charge that gives the maximum COP at the standard rating condition (95/80/67).** In most cases this approach agrees with the experimenter value. For example, consider Figure 6. Although the COP flattens out around 100% of nominal charge for the rating condition (purple line), there is a point at 100% that gives the highest COP (2.5). However, there are four units in the data library for which the experimenter's nominally correct value gave the maximal capacity, but not the maximal COP.

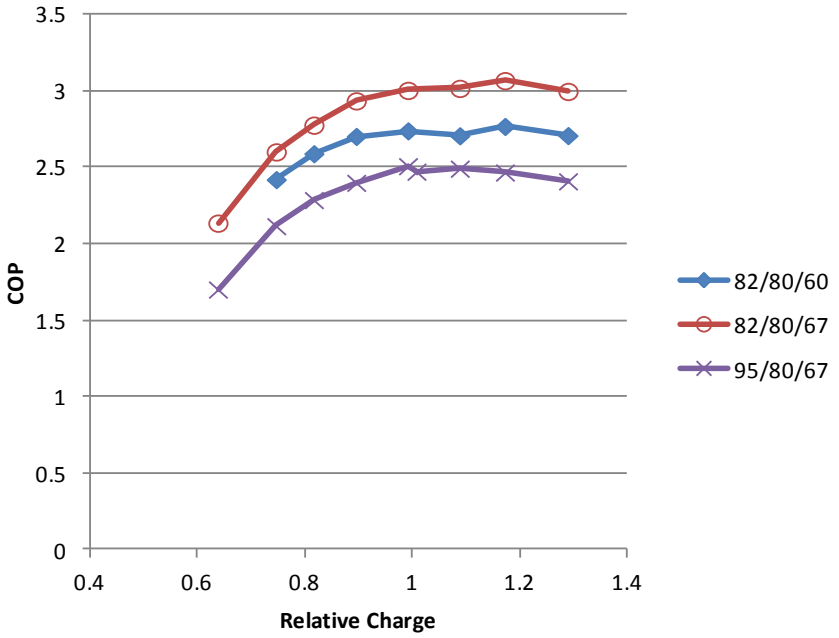

Figure 6[1]: Relative COP as a function of charge at three conditions for a FXO RTU

[1] Plots similar to Figure 6 showing the capacity and COP as a function of relative charge at the standard condition and all other conditions for which there are sufficient data, have been generated for each applicable unit. These are provided in the appendix.

In the four test units for which the maximal COP at the rating condition was not reached at the experimenter's nominal charge, the nominal charge was updated to match the charge for which the maximum COP was achieved. In this report "nominal charge" refers to the maximal-COP charge.

The updated nominal charge for the four units changes the fault category for many of the tests in the affected dataset. One complication of this update is that the other fault test cases became multiple fault cases. For example, cases with evaporator airflow faults imposed became evaporator airflow and over-charge or under-charge fault cases. These tests were removed from the evaluation inputs.

Normal model & FIR

In six of the nine systems in the data library there was a sufficient set of no-fault tests to enable development of a normal model[2]. The six modeled systems are numbers 1 to 6 in Table 3. A normal model is a multiple linear regression of the driving conditions that predicts capacity or COP, as shown in Eqs. 7 and 8, where the coefficients α_i and β_i are found using a least squares approach. The normal model is developed using unfaulted tests (those with no faults imposed, and with maximal-COP charge), so that it can be used to assess what the capacity or COP degradation is for faulted tests at any given condition. The normal model approach for determining degradation is preferable to a measurement-based approach for two reasons. The first is that it significantly reduces bias error, because it obviates the problem of trying to exactly match the test conditions for a faulted and an unfaulted test. The second is that it reduces or eliminates one half of the random error associated with a comparison of two test results (faulted and unfaulted tests at the same conditions).

$$Q = \alpha_0 + \alpha_1 \cdot wb_{ra} + \alpha_2 \cdot wb_{ra}^2 + \alpha_3 \cdot wb_{ra} \cdot T_{amb} + \alpha_4 \cdot T_{amb} + \alpha_5 \cdot T_{amb}^2 \quad (7)$$

$$COP = \beta_0 + \beta_1 \cdot wb_{ra} + \beta_2 \cdot wb_{ra}^2 + \beta_3 \cdot wb_{ra} \cdot T_{amb} + \beta_4 \cdot T_{amb} + \beta_5 \cdot T_{amb}^2 \quad (8)$$

For wet-coil cases, the two external driving conditions are ambient air dry bulb and return air wet bulb temperature. For dry-coil cases, the two driving conditions are ambient dry bulb and return air dry bulb. To use a single two-input model (as shown in Eqs. 7 and 8) to represent both dry- and wet-coil cases, an approach has been followed in which a fictitious return air wet bulb temperature, $wb_{ra,f}$, is used in place of the actual return air wet bulb temperature, wb_{ra} for all dry-coil cases (see Brandemuehl (1993) for details). This $wb_{ra,f}$ is calculated using an iterative approach that involves a bypass factor (BF). BF indicates the fraction of air that would need to bypass an ideal coil, $\dot{m}_{byp}/\dot{m}_{lvg}$, to give equivalent

[2] Systems 4 and 6 from Table 3 are among the four that had their nominal charge adjusted to give maximal COP at the rating condition. These systems had a large number of tests conducted with the experimenter's original nominal charge, but only one or two tests with the maximal-COP charge. For these two cases the normal model was conducted using the original nominal charge. To adjust the FIR values for the updated nominal charge level, each FIR value was divided by the FIR at the maximal-COP charge. For example, in system #4, the maximal-COP charge gave a FIR_{COP} of 104%. Therefore, all FIR_{COP} values were divided by 104% when the nominally correct charge level was adjusted. Although the resulting FIR values are not exact, this method correctly represents the trends caused by adjusting charge, and the magnitude of the inaccuracies introduced by this method is small. The effect of the inaccuracies on an FDD evaluation is insignificant.

performance to the real coil. Using energy and mass balances and psychrometric relationships, BF can also be expressed in terms of specific enthalpies, *h*, or humidity ratios, ω, as shown in Eq. 9.

$$BF = \frac{\dot{m}_{byp}}{\dot{m}_{lvg}} = \frac{h_{lvg} - h_{adp}}{h_{ra} - h_{adp}} = \frac{\omega_{lvg} - \omega_{adp}}{\omega_{ra} - \omega_{adp}} \quad (9)$$

For a wet coil condition, the air leaving an ideal coil will have a dewpoint temperature equal to the surface temperature of the coil – the apparatus dewpoint (*adp*). In the fictitious wet bulb approach, BF is iteratively varied until the enthalpy calculations of Eq. 9 give the same result as the humidity ratio calculations with an assumption of 100% relative humidity for the air at the apparatus dewpoint.

The BF values calculated for the wet coil cases are averaged, and this average is then used to calculate sensible heat ratios for each dry coil test using Eq. 10. In Eq. 10, ω_{adp} is calculated using Eq. 9, and the fictitious return air enthalpy, $h_{ra,f}$, is varied until SHR converges to 1.0. Finally, the fictitious wet bulb, $wb_{ra,f}$, is calculated from $h_{ra,f}$ and T_{ra} and is used in Eqs. 7 and 8 for any dry coil cases in the data set.

$$SHR = \frac{h(T_{ra}, \omega_{adp}) - h_{adp}}{h_{ra,f} - h_{adp}} \quad (10)$$

This approach is described in more detail by Brandemuehl (1993).

During model validation, the measured unfaulted cases (the basis for the model) are compared with model outputs for the same set of conditions. The capacity and COP are compared, and residuals calculated. For example, Eq. 11 shows the calculation for capacity.

$$Residual = \frac{capacity_{model} - capacity_{measured}}{capacity_{measured}} \quad (11)$$

An example plot, showing the residuals for the normal model of capacity for RTU 3, is shown in Figure 7. This plot indicates the level of scatter for this unit, which is typical for a laboratory-tested unit. The dry coil and wet coil data are shown separately to illuminate any difference that could be caused by problems associated with the fictitious wet-bulb approach to model generation. The wet and dry coil cases are very similarly distributed, indicating that this modeling approach hasn't introduced any obvious bias or scatter error. The dry coil cases are associated with lower-capacity cases on average, as one would expect because unitary system capacity decreases with decreasing indoor humidity.

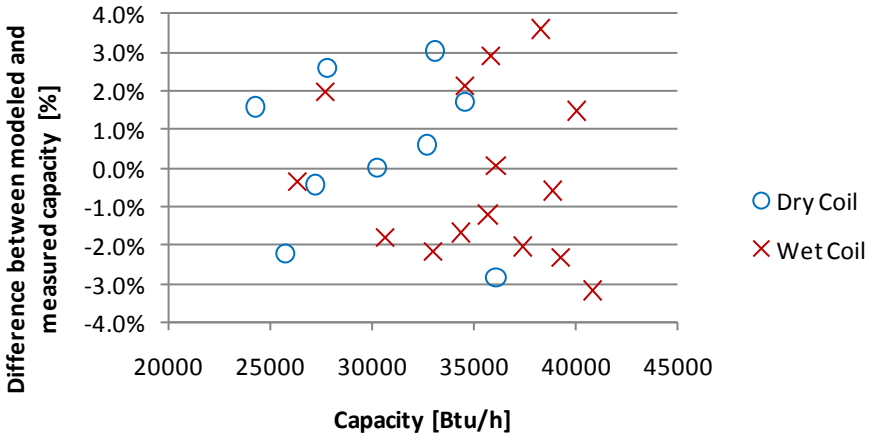

Figure 7: Normal model residuals as a function of capacity for RTU 3

An example of a normal model from RTU 3 is shown in Figure 8. The mesh surface is the model and the circular markers are the measurement data upon which the model is based. This figure is typical of normal models; it has a fairly planar shape, with a slight increase in COP as return air wet bulb increases, and a strong decrease in COP as ambient temperature increases. If the surface is rotated so that it can be viewed from the side, there is typically a very small amount of twist to the planar shape. This is demonstrated in Figure 9. Similar figures showing the normal models of other units are provided in the appendices.

The completed model is used to calculate fault impact ratios (FIR), which form the basis of fault-impact based evaluations, as discussed earlier. FIR are defined as:

$$FIR_{COP} = \frac{COP_{faulted}}{COP_{unfaulted}} \qquad FIR_{capacity} = \frac{capacity_{faulted}}{capacity_{unfaulted}} \tag{12}$$

where the *faulted* COP and capacity values come from measurements, and the *unfaulted* values come from the normal model. The FIR values are included in the data library, and form the basis of the impact-based evaluation approach.

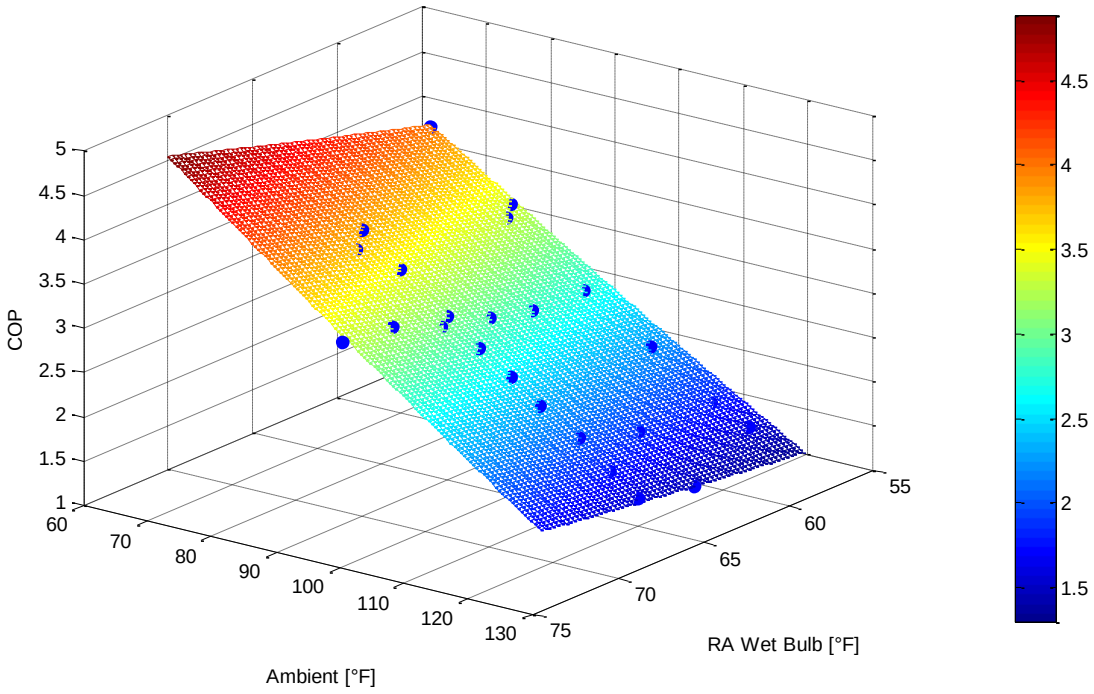

Figure 8: RTU 3 normal model of COP and unfaulted measurement data

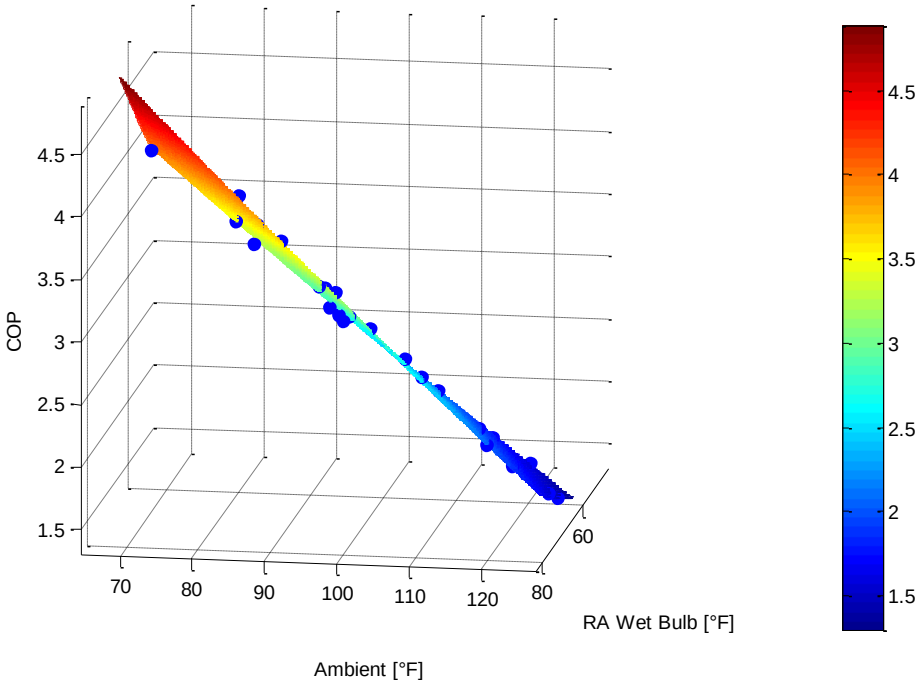

Figure 9: RTU 3 normal model of COP and unfaulted measurement data – side view

Simulation

As the methods developed in this project have progressed, we have become increasingly convinced that the future of FDD evaluation needs to use complete system models to generate input data, rather than relying on measurements. The arguments in favor of using simulation data are summarized below. The main argument against this approach is typically that engineers find it difficult to believe in simulations that they aren't deeply familiar with. To paraphrase William Beveridge: Everybody believes an experiment except the experimenter; nobody believes a model except the modeler. A second argument against the approach is that it is too difficult and time consuming to generate models that can accurately model faulted system operation. This second argument has been addressed in the current project by developing a new method for rapidly simulating unitary systems, using an inverse modeling approach. This method is described below. The method's development has been completed very recently, so evaluations using simulation data have not yet been carried out. However, under research funding from the National Institute of Standards and Technology (NIST) we are continuing work on evaluation of FDD, and will introduce simulation data into the FDD evaluation process.

Arguments in favor of using simulation data for FDD evaluation

Reliability of data – The exercise of vetting the data for this project has shown that measurement data have significantly uncertain results. We also are aware through direct experience that obtaining accurate results for air-conditioning systems under varying driving conditions and with faults imposed is extremely difficult. Since errors typically don't affect all variables equally, a protocol that relies on an error-affected variable may perform worse than a protocol that uses a different variable as its input.

Additional systems – The current database has just nine systems, and represents all of the known data that is sufficiently reliable and detailed. This may not be a large enough sample, since protocols perform better with some systems than others. The cost of conducting additional experiments is prohibitive. Simulation can be conducted with much less expense.

Finer resolution of driving conditions – It is likely that a developer or potential user of a protocol may be interested in an exact condition that hasn't been tested, or may wish to know a more precise fault intensity for which a protocol begins to flag faults than what the data can provide. A simulation can be set to give any reasonable conditions.

Multiple faults – Multiple faults are known to exist in the field and methods of diagnosing multiple faults are being developed (Li and Braun 2007). Adding combinations of faults at varying intensity drastically increases the number of test cases required for even the coarsest evaluation. However, multiple faults can be simulated quite accurately.

Gaming – The input data for an evaluation are analogous to the answers to a test. A finite set of input data, such as the set contained in the data library, can quite easily be programmed into a protocol so that it recognizes the conditions and gives the correct response. This will render evaluation meaningless, because the ability to get perfect evaluation results isn't related to the ability to detect and diagnose faults in the field. With simulation data, tables of correct answers won't exist.

Overview of inverse model approach

A purely physics-based model – one that uses known theoretical relationships and exact knowledge of geometry and material properties – is extremely difficult to build and can take a long time to converge; sometimes on the order of hours for each test case. Once it's complete, it needs a physical experiment to provide validation data, or it can't be relied upon. Such a model is sometimes called a white-box model.

Conversely, a pure black-box model is one that intuits a relationship between inputs and outputs without concern for what it physically represents. A regression of experimental data is an example of a black box model.

The model that has been developed to provide input data to the evaluator is referred to as a gray box model. This model breaks the system into components – compressor, evaporator, refrigerant lines, etc. – and models each one using black box model techniques. However, physical constraints are added to the components, and to the overall system model. For example, refrigerant mass is conserved, heat exchangers are divided into regions with different convection coefficients depending on the refrigerant phase in that section, etc.

Although the model still requires some experimental data, it can generate more reliable results by imposing physical constraints and removing scatter. The components can be switched and combined, so that a large number of different systems can simulated with experimental data from a small number.

There is a great deal of mathematics involved in this model; hundreds of equations. This detail is omitted in the current report, but can be found in a report that will be submitted to NIST in December 2012. The preliminary model is also described in Cheung and Braun (2012a, 2012b).

Model description

To provide a comprehensive database of simulated system performance for various types of systems under a wide range of environmental conditions and fault levels, a fast, robust and accurate model is achieved by inverse modeling based on experimental data from faulted systems in laboratory studies. Inverse modeling is an approach where parameters of the model are trained from experimental data instead of estimating them by the specifications of the systems and existing correlations. Since inverse modeling makes use of simplified models, the solution process is computationally less expensive. The robustness of the model is maintained by using semi-empirical component models built with some physical principles that give reliable results at conditions not included in the experimental data, such as multiple fault scenarios.

The stages of modeling can be described using the flowchart in Figure 10.

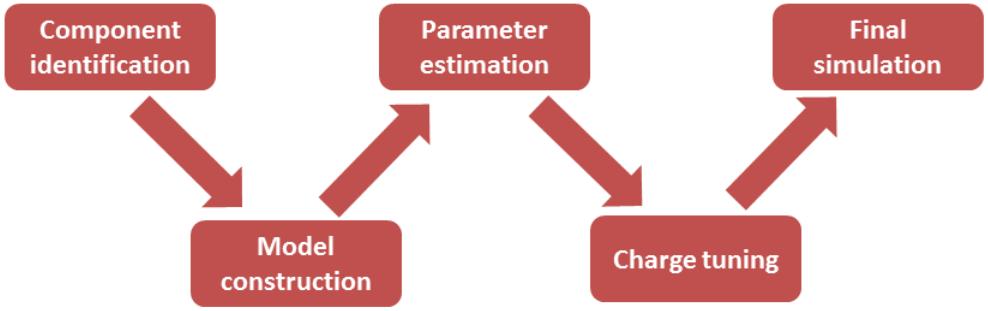

Figure 10: Stages of inverse modeling.

In Figure 10, the first step of modeling is the identification of the common components in various types of vapor compression systems. In different systems, mufflers, strainers, refrigerant pipelines and other components may be assembled differently. For consistency and generality, these minor components are combined into major components and modeled as a few major components, which are modeled in the same manner for all systems.

The second step is the construction of component models with semi-empirical models. The existing semi-empirical models from literature are studied and additional parameters may be added to explain phenomena not covered by the original models. The geometrical parameters of the models are simplified to reduce the difficulty of parameter estimation by optimization.

The third stage involves the estimation of parameters. The parameters of the models are estimated by minimizing the sum of squares of the differences between the experimental and predicted values at the component level. Since data are obtained from experiments of the entire systems, some data are unreliable for training at the component level and are filtered out to avoid unrealistic results. Weighting functions are also added to the optimization process to enhance accuracy of the model under faulted conditions.

The fourth stage is the charge tuning stage. After combining the component models into a cycle model, the charge of the system can be solved by summing the amount of charge inside the refrigerant pipelines and the heat exchangers. However, Shen (2006) showed that the estimation of charge amount by this method often results in large biases in charge estimation. Shen proposes a charge tuning method to eliminate the bias. This method allows the amount of charge to be estimated accurately inside the system, so the amount of charge inside the system can be imposed as a simulation input.

The fifth step is the final simulation stage. In this stage, empirical equations for good initial guesses of the solution process are established to speed up the calculation. Since some faults, such as compressor valve leakage and liquid line restriction, require additional models for simulation, the fault models are constructed based on their physical impacts to the system and are imposed after the completion of the cycle model.

Component identification

Different types of vapor compression systems are generalized into component models as shown by the schematic in Figure 11

.

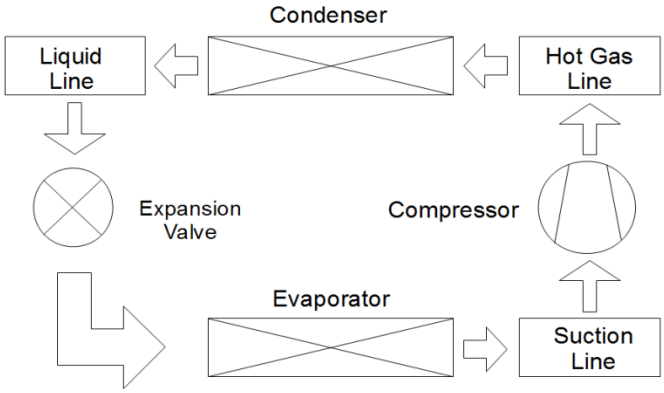

Figure 11: Schematic of component models in a generalized vapor compression system

In a model of a vapor compression system, the major components are the compressor, condenser, expansion device, and evaporator. For faulted systems, superheat and subcooling change significantly and could not be generalized directly from the experimental data. An expansion valve model is needed to simulate the effect of the faults on superheat. The hot gas line in Figure 11 is modeled to account for the heat loss from the pipeline to the surroundings and gives a more accurate estimation of the condenser heat transfer rate. The same is done for the suction line to estimate the evaporator heat transfer rate more accurately. The liquid line is modeled separately because the charge contained in the pipeline and the liquid line pressure drop are important for modeling of the system at different charge and liquid line restriction levels. However, the pipeline between the expansion valve and the evaporator is not modeled as no systems provide data across the pipeline and its performance cannot be understood.

Model construction

Each component in Figure 11 is simulated by a component model. While the compressor, condenser and evaporator are modeled in the same way for all systems, different models of the expansion valve are used depending on the type of valve and the hot gas line, the liquid line and the suction line are modeled by the same refrigerant pipeline model.

Compressor model

A compressor model accepts refrigerant inlet condition, outlet pressure and the ambient temperature as inputs to estimate the refrigerant mass flow rate, the power consumption and the refrigerant enthalpy at compressor discharge. The block diagram of the compressor model is shown in Figure 12.

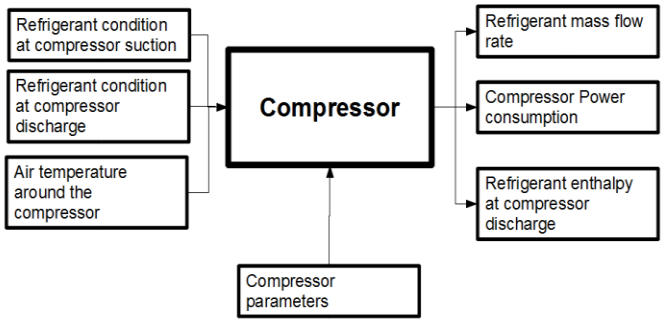

Figure 12: Input and output diagram of compressor model.

The compressor model is developed from Zakula *et al.* (2011), which describes modeling a variable speed compressor. The model was derived from a polytropic compression model with the addition of re-expansion and back-leakage loss. The exponential term depending on the suction pressure from Jähnig et al. (2000) was also used to account for the mechanical and electrical loss of the compressor. In this case, modification is made so that the polytropic coefficient is related to the compressor suction and discharge pressure by empirical equations. An exponential term depending on the discharge pressure is added to account for the mechanical and electrical loss of the compressor. A heat loss model is also constructed based on the natural convection of air side and forced convection of the refrigerant side along the compressor shell to estimate the refrigerant enthalpy at the compressor discharge.

Condenser model

A condenser model predicts the heat transfer rate and pressure drop across the condenser as shown in Figure 13.

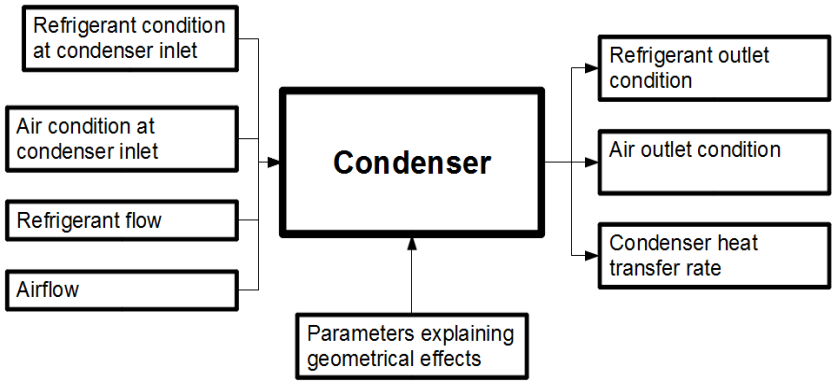

Figure 13: Input and output diagram of condenser model

The condenser heat transfer model is constructed assuming crossflow heat exchanger configuration by moving boundary method. The moving boundary method was suggested by MacArthur and Grald (1989) to section a heat exchanger according to the refrigerant phase. To simplify the analysis, the pressure drop was assumed to be negligible in terms of evaluating the heat transfer characteristics of the heat exchanger. The size and heat transfer rate of each refrigerant phase section were solved by ε-NTU method (Incropera et al. 2007) assuming a crossflow configuration. The resultant schematic of the condenser model is shown as Figure 14.

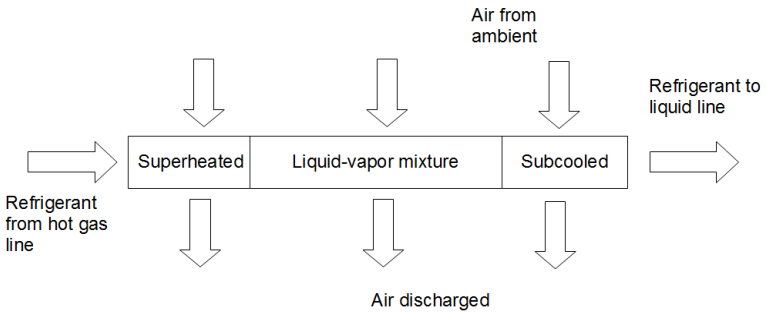

Figure 14: Condenser model schematic for moving boundary method.

Since the geometry of a heat exchanger affects the heat transfer characteristics through the heat transfer coefficients and fin efficiency, their correlations were investigated to generate a simplified model of heat transfer coefficient of the air side and refrigerant side with unknown geometrical parameters.

The condenser pressure drop model is constructed based on the pressure drop characteristics of flows in different refrigerant phases. According to Wallis (1969), pressure drops are divided into frictional loss, accelerational loss and the gravitational loss. Neglecting gravitational loss, the condenser pressure drop model is decomposed into the superheated section frictional pressure drop, two-phase section frictional pressure drop, subcooled section frictional pressure drop and overall accelerational pressure drop. The correlations of each part of the pressure drop model were investigated and the geometrical and empirical parameters in these correlations are lumped together to form the parameters of the model.

Evaporator model

The evaporator model predicts the total heat transfer rate, the sensible heat transfer rate and the pressure drop. This is illustrated by the block diagram of the model shown in Figure 15.

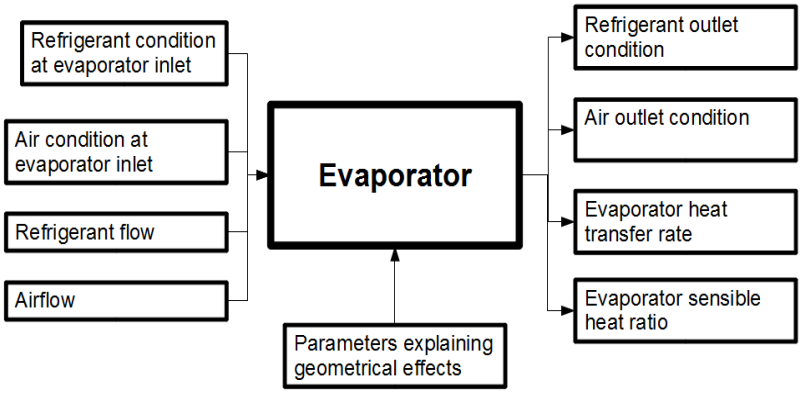

Figure 15: Input and output diagram of evaporator model

The evaporator model also utilizes the moving boundary method, which assumes the evaporator coil heat transfer rate to be solved at the evaporator outlet pressure, to speed up the calculation. Since the evaporator heat transfer model estimates both the sensible heat ratio and the heat transfer rate, a partial-wet-partial-dry method from Braun (1989) is used. Air-to-refrigerant evaporator modeling traditionally involves either dry coil or wet coil analysis, which assumes either no condensation or full of condensation

on the entire evaporator coil. With a partial-wet-partial-dry method, one can divide the coil into a dry section and a wet section and analyze the performance of the evaporator between a completely dry coil and wet coil. The dry and wet sections are considered as individual ε-NTU counterflow heat exchangers and the system of equations are simplified analytically before numerical computation. This saves the computational effort to segment the evaporator into multiple elements for accurate wet performance prediction. The schematic of the method is shown as Figure 16.

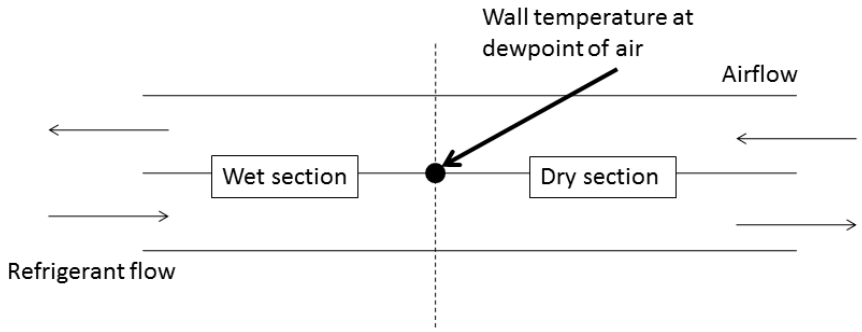

Figure 16: Schematic of partial-wet-partial-dry method

Since the partial-wet-partial dry method is derived in a counterflow configuration and the air-to-refrigerant heat exchangers are modeled as crossflow heat exchangers, the evaporator model combines the two features together to form a schematic shown in Figure 17.

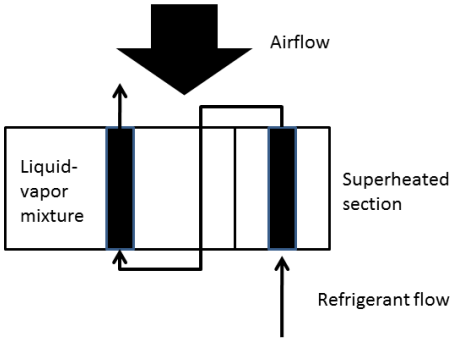

Figure 17: Evaporator model schematic for moving boundary method

The relationship between the parameters and the evaporator heat transfer model are obtained in the same manner as the condenser model from different correlations. The pressure drop model and the parameters associated are also formulated by the same method as the one of the condenser pressure drop model.

Expansion device model

Two types of expansion device are utilized in the equipment within the data library: fixed orifices (FXO) and thermostatic expansion valves (TXV). An FXO is an expansion device with no control inputs and the refrigerant flow is throttled according to the inlet and outlet condition. A TXV works similarly as FXO but the opening area is adjust mechanically in response to the evaporator outlet superheat. An expansion device model predicts the mass flow rate across the valve and assumes adiabatic expansion to estimate the outlet enthalpy. The general block diagram of the model is shown in Figure 18.

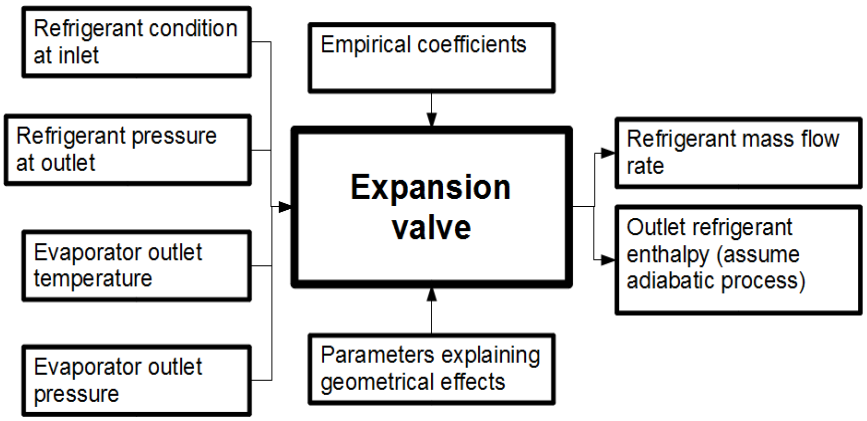

Figure 18: Input and output diagram for expansion valve model

FXO model

To model the mass flow rate across an FXO, a semi-empirical model constructed by Buckingham-PI theorem from Payne an O'Neal (2004) is employed. It is suitable for various types of refrigerant and can model mass flow rate with two-phase refrigerant at the inlet of the FXO. The model requires the diameter and the length of the FXO and the refrigerant conditions at the inlet and outlet of the expansion valve. Since the diameter and the length of the FXO are unknown, they become parameters to be learned from the experimental data. In order to match the FXO model performance at out-of-range conditions, a few more empirical parameters are also introduced into the original FXO model.

TXV model

The modeling of mass flow rate across the TXV is developed from the FXO model with the addition of a quadratic relationship between the diameter of the expansion valve and the evaporator superheat. A maximum diameter is also set as a parameter to be learned from the data since the valve is forced to open fully very often when the system is undercharged.

Refrigerant pipeline model

The refrigerant pipeline model consists of a pressure drop model and a heat loss model and the block diagram of the model is shown in Figure 19.

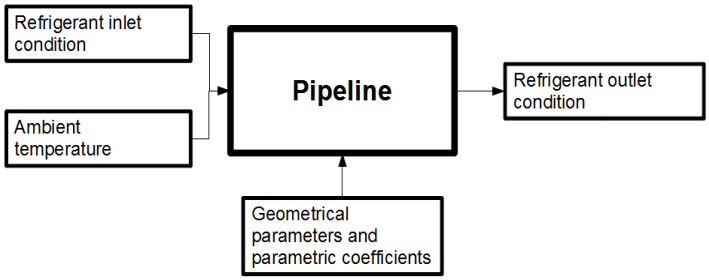

Figure 19: Input and output diagram for refrigerant pipeline model

The refrigerant pipeline pressure drop model is developed in the same way as the heat exchanger pressure drop model but only the single-phase frictional and accelerational pressure drop components are

considered. The heat loss model is formulated based on the natural convection of air around the pipeline and the forced convection of refrigerant flow in the pipeline. The parameters in the model are established by considering the correlations of pressure drop, external natural convection around horizontal cylinders and internal forced convection of refrigerant flow.

Parameter estimation

In the parameter estimation process, parameters are estimated at the component level by considering the inlet and outlet data in the experiments for each of the component. However, since the experiments concern system performance, not all the inlet and outlet data at the component level are valid for parameter estimation. One example is the refrigerant enthalpy at the compressor suction. If the superheat at the location is smaller than 1K, then the condition could be two-phase and therefore the uncertainty of the estimated enthalpy is large. In this case, the data points are removed to reduce the uncertainty of the parameters. Data with compressor valve leakage, liquid line restriction and the presence of non-condensables are also removed from the parameter estimation of component models as they require additional models for simulation. However, they are used for system model validation.

After data filtering, a residual function is constructed for each model that calculates the sum of squares of the differences between the predicted and measured values. Since the test matrix for each of the systems is not balanced and most of them give a heavy emphasis on the non-faulted conditions, weighting functions are also imposed in the residual functions to enhance the accuracy in the modeling of faulted conditions. For example, when estimating the parameters of the compressor mass flow rate model, the residual function involves the difference between the measured and the predicted mass flow rate by the compressor model. Since most experimental cases involve compressor mass flow rate around the rated condition and only a few of them give extreme values of refrigerant mass flow rate, a weighting function is given to the residual function to more heavily weight the points with less occurrence in the experimental cases.

Charge tuning

Charge tuning is a technique to offset the bias in charge estimation as a consequence of factors such as unaccounted refrigerant volume and deviation in void fraction models. It compares the simulated amount of charge and the measured one to find an empirical formula to offset the bias. The empirical formula helps unbiased estimation of the amount of charge in the simulation and the amount of charge can then be used as an input to the simulation. The charge tuning is divided two stages: pre-tuning simulation and establishment of the charge tuning equation.

Pre-tuning simulation

In the pre-tuning simulation, the trained component models are connected to form a cycle model. Various independent variables and residuals along the circuit are identified. The input and output diagram of the pre-tuning simulation is shown in Figure 20.

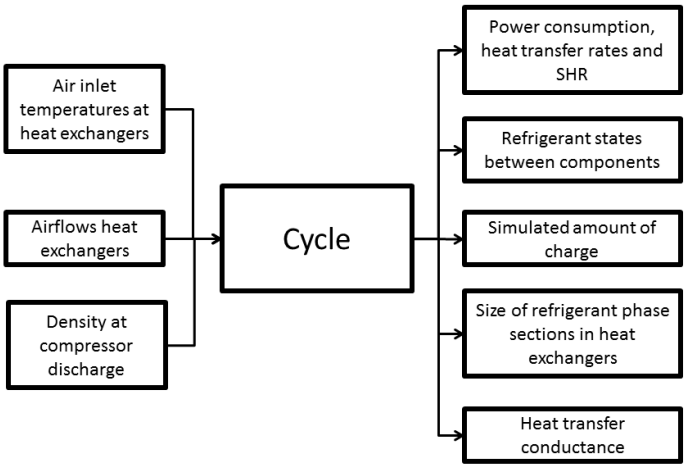

Figure 20: Input and output diagram of pre-tuning simulation

In Figure 20, the density at the compressor discharge is used as an input rather than the subcooling suggested in Shen (2006). Subcooling disappears in seriously undercharged cases as observed in Shen (2006) and cannot be used as an input in undercharged scenarios. Unlike the two-point charging method in Shen (2006), all experimental cases are considered in the pre-tuning simulation and a property along the refrigerant circuit that is valid in all scenarios is needed. Since the compressor discharge is highly superheated in all vapor compression system, the density at the compressor discharge is chosen as an input.

The solution process of a cycle model is implicit and an optimization routine is used to find the solution under various environmental and faulted conditions by reducing the residual to zero. The eight independent variables and the solution routine of the simulation are shown in Figure 21 and Figure 22.

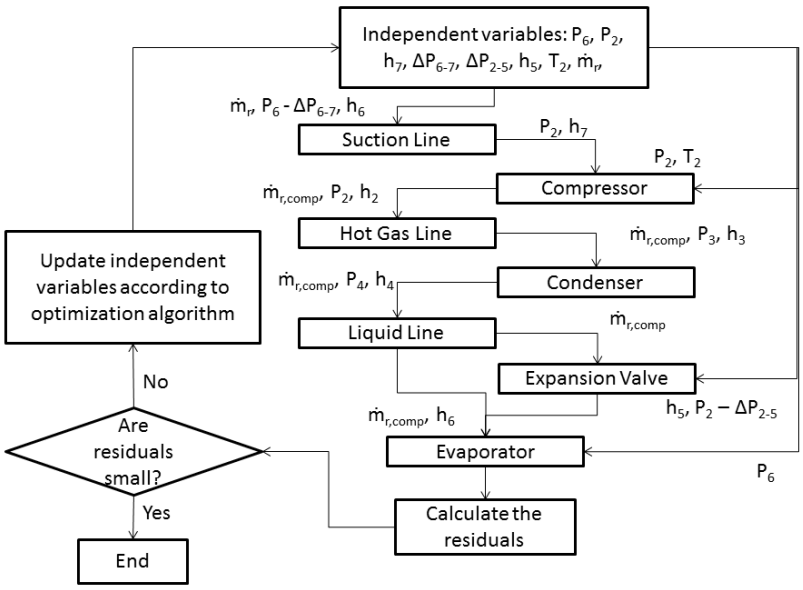

Figure 21: Solution procedure in flowchart for the cycle model

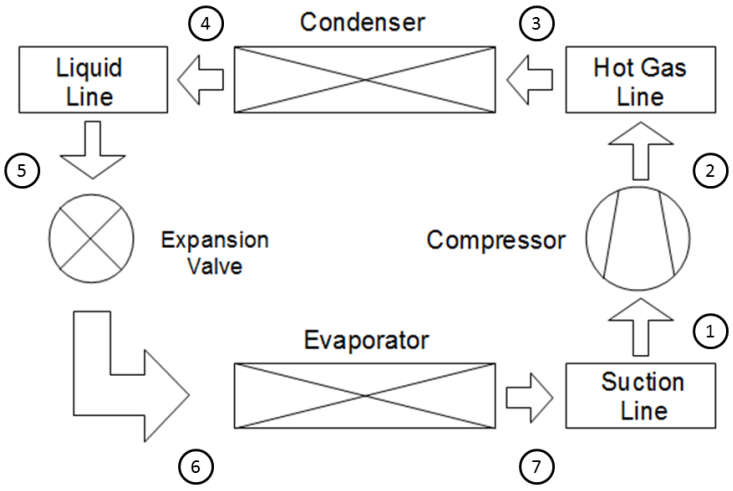

Figure 22: Locations of properties in Figure 21

The independent variables in Figure 21 are pressure at expansion valve outlet, pressure at compressor discharge, enthalpy at suction line inlet, pressure drop across the evaporator, pressure drop from compressor discharge to the expansion valve inlet, enthalpy at expansion valve inlet, compressor outlet temperature and refrigerant mass flow rate. The suction line is solved initially with the refrigerant mass flow rate and the suction line inlet condition from the independent variables. This gives the inlet condition of the compressor model to model the compressor mass flow rate and provides all the inputs necessary to simulate different types of expansion valve. The component models are solved from the suction line outlet in the order of refrigerant flow till the expansion valve inlet. The expansion valve is solved with refrigerant inlet condition given by the independent variables. This avoids potential mathematical errors from the liquid line model as a consequence of poor guesses of the other independent variables. The evaporator model is the last component model to be solved.

The eight residuals of the pre-tuning simulation, to fulfill the degree of freedom from the eight independent variables, are calculated according to Table 7. The optimization routine keeps iterating with different independent variables until the magnitudes of the independent variables are close to zero.

Table 7: Residuals calculated to solve a pre-tuning simulation.

Difference between the imposed enthalpy at expansion valve inlet and the estimated enthalpy at the liquid line outlet	Difference between the imposed suction line inlet enthalpy and the estimated enthalpy at the evaporator outlet
Difference between the mass flow rate of the expansion valve model and compressor model	Difference between the estimated pressure at the liquid line outlet and the imposed pressure at the expansion valve inlet
Difference between the estimated pressure at the evaporator inlet and the imposed one at the expansion valve outlet	Difference between the density at compressor discharge observed from the experiments and the estimated one
Difference between the estimated temperature at the compressor outlet and the imposed one	Difference between the imposed mass flow rate and the estimated one from the compressor model

Establishment of the charge tuning equation

With the solution process, the amount of charge estimated by the cycle model in each experimental scenario can be solved. The original charge tuning equation from Shen (2006) was modified by relaxing the assumption of constant conductance and the inputs and outputs of the charge tuning equation are illustrated as Figure 23.

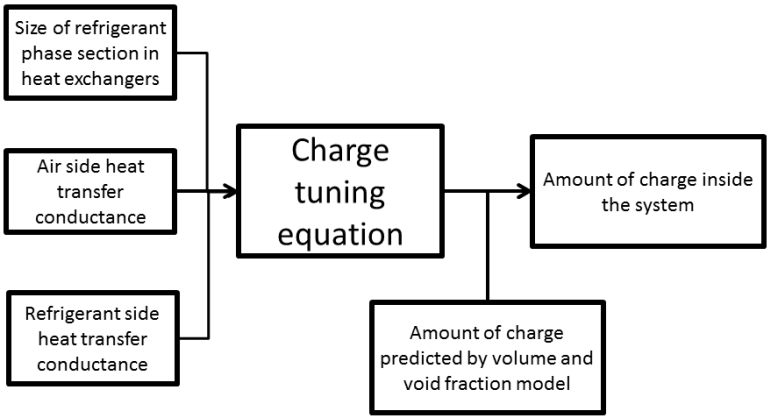

Figure 23: Input and output diagram of charge tuning equation.

The parameters in the charge tuning equation are established by minimizing the sum of squares of the differences between the predicted and real amount of charge in Figure 23. As the number of tests at each charge level is different, a weighing function is added to the residual to avoid over-emphasis on re-occurring charge levels. Since the size of the subcooled section increases with charge level and the size of the superheated section decreases with increasing charge level according to Shen (2006), the parameters are constrained accordingly during the minimization process to avoid capturing parameters violating this physical principle.

Final simulation

After charge tuning, the simulation can operate with imposed charge levels. Further work is done to simulate faults not covered in the parameter estimation process and to speed up the calculation process.

Solution procedure

The independent variables and the solution procedure of the final simulation are the same as Figure 21. Since no experimental cases are available to give the density at the compressor discharge, the residual with the density calculation in Table 7 is replaced by the difference between the charge imposed and the charge calculated after charge tuning.

Fault modeling

The faults of non-standard charging, heat exchanger fouling, compressor valve leakage and liquid line restriction are modeled as described below.

Non-standard charging

After charge tuning, the charge level becomes an input to the simulation and cases with undercharged or overcharged conditions can be solved by imposing the corresponding charge level to the simulation.

Heat exchanger fouling

Yang et al. (2007) and Bell et al. (2012) showed that the impact of heat exchanger fouling was dominated by the decrease of airflow across the heat exchanger. Since the effect of airflow on the heat exchanger is embedded in the condenser and evaporator model, the heat exchanger fouling effect is estimated by imposing a smaller airflow to the heat exchangers.

Compressor valve leakage

Breuker (1997) described compressor valve leakage as the reduction of mass flow rate from the compressor due to the refrigerant backflow from the compressor discharge to the compression chamber and from the compression chamber to the compressor suction. The fault will also superheat the compressor suction refrigerant by the refrigerant backflow from the compressor discharge. This is modeled by increasing the compressor suction enthalpy and suppressing the compressor mass flow rate in accordance with the valve leakage level as illustrated in Figure 24.

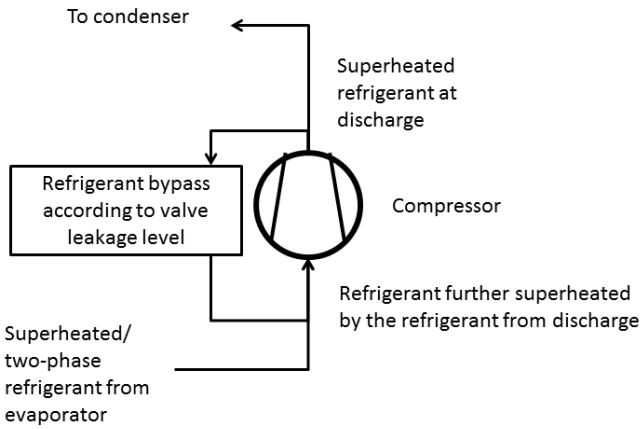

Figure 24: Compressor valve leakage schematic.

Liquid line restriction

Liquid line restriction is described by Breuker (1997) as the increase of flow resistance and pressure drop in the liquid line due to blockage of flow by sediments or contaminants at filters along the liquid line. In this section, it is characterized using the ratio of the additional pressure drop associated with the restriction to the liquid line pressure drop without a restriction, under the same operating conditions. To solve for the fault, the denominator of the liquid line restriction definition is needed and is obtained by solving the cycle once without the liquid line restriction. With the pressure drop across the liquid line from the first cycle solution and the imposed liquid line restriction level, the additional pressure drop across the liquid line is known and a second solution of the cycle is solved with the refrigerant pressure and density at the inlet of the expansion valve decreased by the additional pressure drop.

Empirical equations for initial guesses

To obtain a good initial guess close to the solution for the final simulation and shorten the simulation time, empirical and linear equations for the initial guesses in Figure 21 are constructed from experimental data by linear regression. The inputs and outputs of the equations are shown in Figure 25.

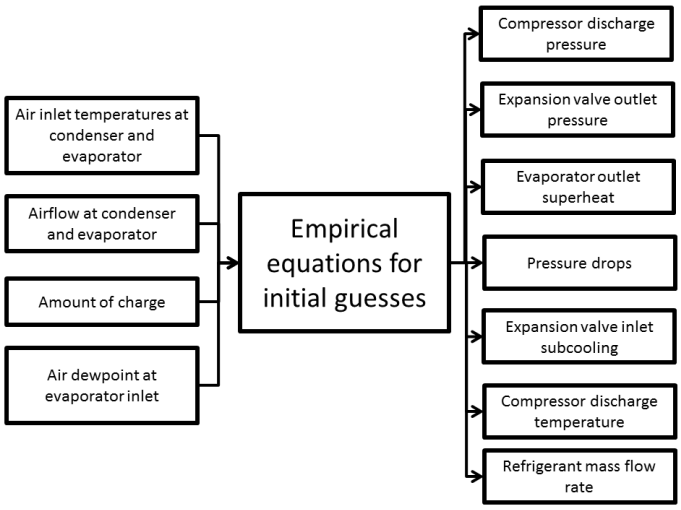

Figure 25: Input and output diagram of empirical equations for initial guesses of the final simulation

The subcooling and superheat in Figure 25 are converted into enthalpy with the pressure values before they were used as initial guesses of the final simulation.

Example simulation on fault impacts

This section provides some sample comparisons of experimental and simulated results for the effects of faults on system variables. For system #6 with a TXV from Table 3, results are presented for the impacts of refrigerant charge, evaporator fouling, and condenser fouling. For system #6 with a TXV, sample results are given for compressor valve leakage.

Non-standard charging

The experimental observations with charge level variation under indoor dry-bulb temperature 80°F, indoor wet-bulb temperature 60°F and outdoor temperature 95°F were compared with the simulation results for COP, evaporator outlet superheat and liquid line outlet subcooling as shown from Figure 26 to Figure 28. Overall, the simulation tracks the trends in performance impacts for these faults. At low refrigerant charge, the TXV is fully open and the evaporator exit superheat is uncontrolled. The COP increases with charge until a peak COP is achieved and then decreases as the condenser subcooling increases.

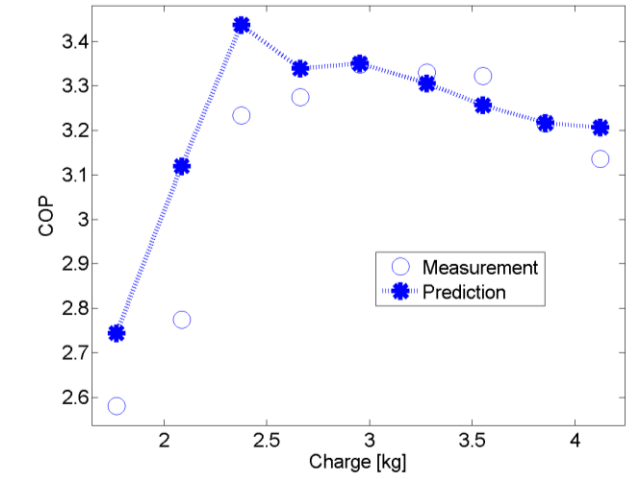

Figure 26: Comparison between experimental and simulated COP at different charge levels

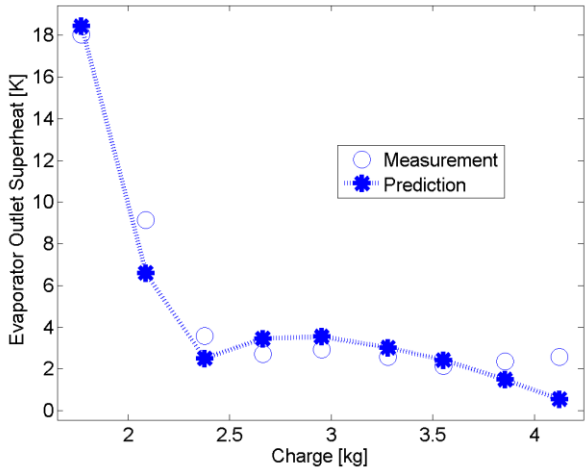

Figure 27: Comparison between experimental and simulated evaporator outlet superheat at different charge levels

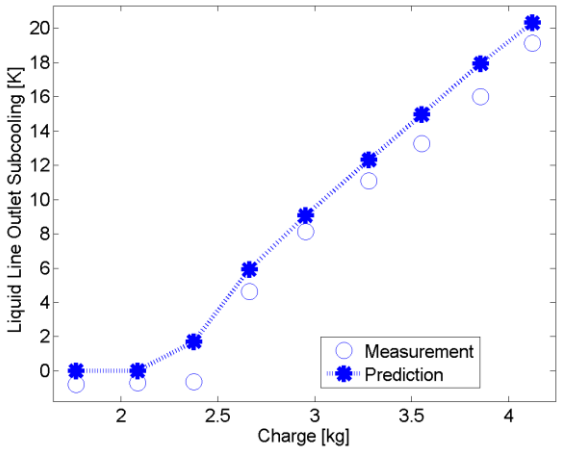

Figure 28: Comparison between experimental and simulated liquid line outlet subcooling at different charge levels

Evaporator fouling

Simulation was conducted at experimental cases with varying evaporator airflow rate tested under indoor dry-bulb temperature 80°F, indoor wet-bulb temperature 67°F and outdoor dry-bulb temperature 95°F. The comparisons of the COP, SHR, compressor discharge pressure and compressor suction pressure are shown from Figure 29 to Figure 32. The simulated results at different evaporator airflow followed the experimental observations as shown from Figure 29 to Figure 32. As the level of evaporator fouling increased, the evaporator airflow dropped and the COP deteriorated in Figure 29. The compressor suction pressure and compressor discharge pressure also decreased with the airflow in Figure 31 and Figure 32. The lower evaporating pressure induced lower evaporator coil surface temperature and a lower SHR as shown by Figure 30.

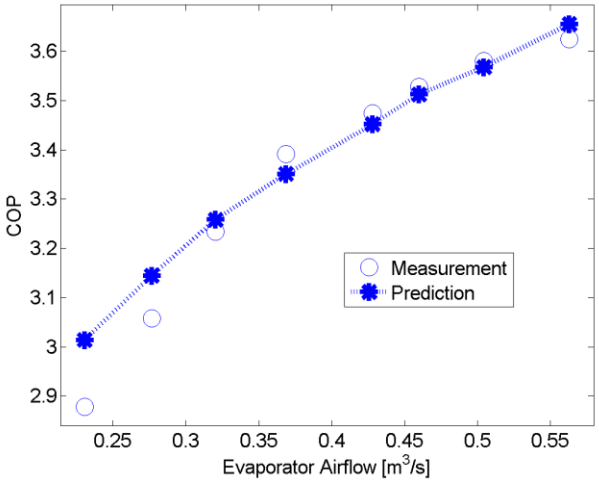

Figure 29: Comparison between experimental and simulated COP at different evaporator airflow rates

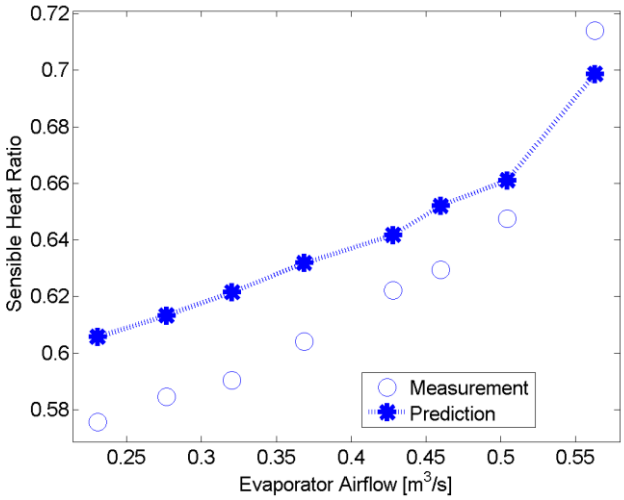

Figure 30: Comparison between experimental and simulated SHR at different evaporator airflow rates

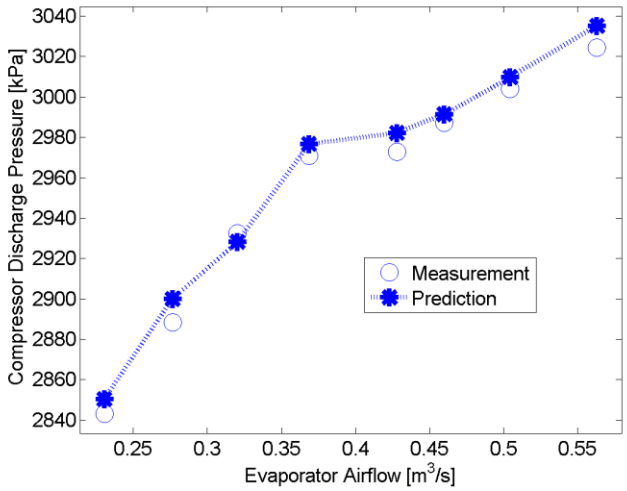

Figure 31: Comparison between experimental and simulated compressor discharge pressure at different evaporator airflow rates

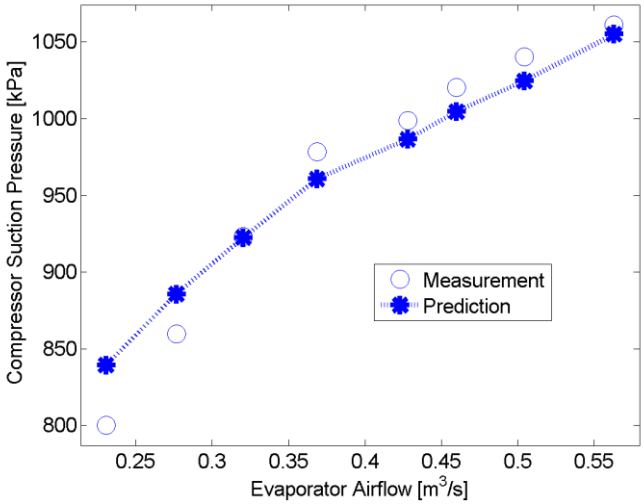

Figure 32: Comparison between experimental and simulated compressor suction pressure at different evaporator airflow rates

Condenser fouling

Condenser fouling was tested with different condenser airflow rates under indoor dry-bulb temperature 80°F, indoor wet-bulb temperature 67°F and outdoor dry-bulb temperature 95°F. The simulation and experimental observations for COP, compressor discharge temperature and compressor discharge pressure are plotted from Figure 33 to Figure 35. Figure 33. In general, the simulation results follow the experimental observations as the condenser airflow rate is decreased. With increasing condenser fouling level and decreasing condenser airflow rate, the compressor discharge temperature and pressure increased in Figure 34 and Figure 35. The increasing fault level resulted in a decreasing COP as shown by Figure 33.

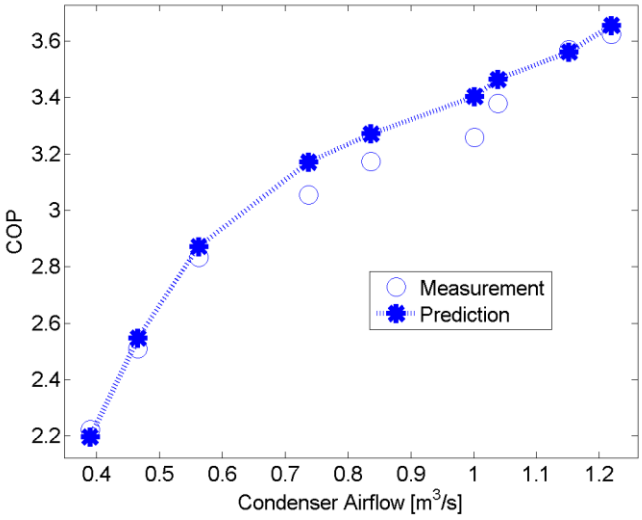

Figure 33: Comparison between experimental and simulated COP at different condenser airflow rates

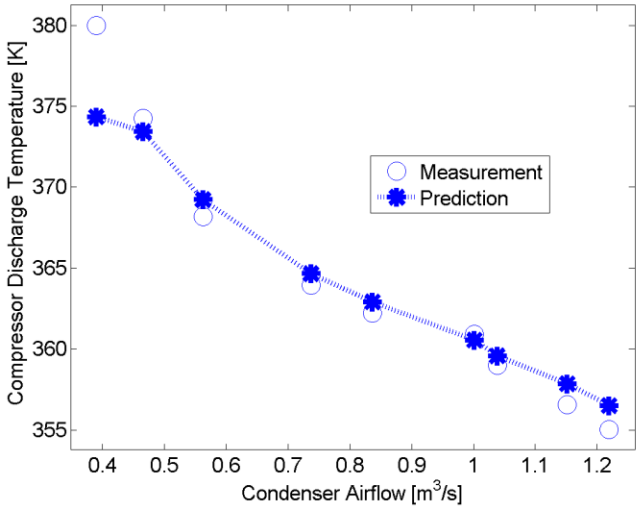

Figure 34: Comparison between the experimental and simulated compressor discharge temperature at different condenser airflow rates

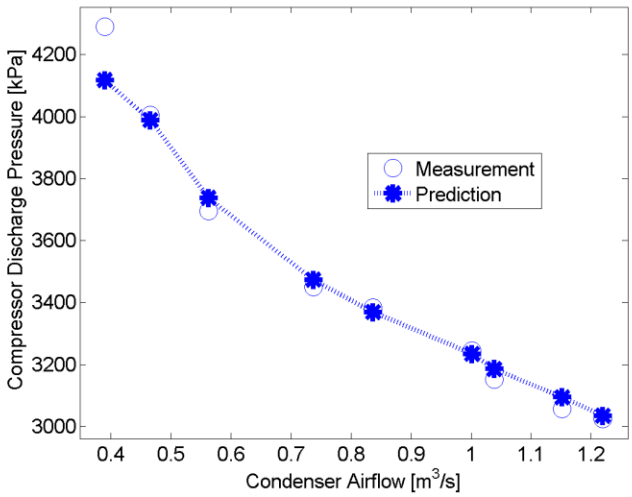

Figure 35: Comparison between the experimental and simulated compressor discharge pressure at different condenser airflow rates

Compressor valve leakage

Simulation was conducted with compressor valve leakage cases evaluated under indoor dry-bulb temperature 80°F, indoor wet-bulb temperature 67°F and outdoor dry-bulb temperature 80°F. The comparison between the experimental observations and the simulation results for COP and compressor pressures are shown from Figure 36 to Figure 38. In this case, the simulated COP and the compressor discharge and suction pressures follow the experimental trends. As the compressor valve leakage level increased, the pressure across the compressor dropped. This reduced the temperature difference between the refrigerant and the surroundings, the heat transfer and the COP of the system.

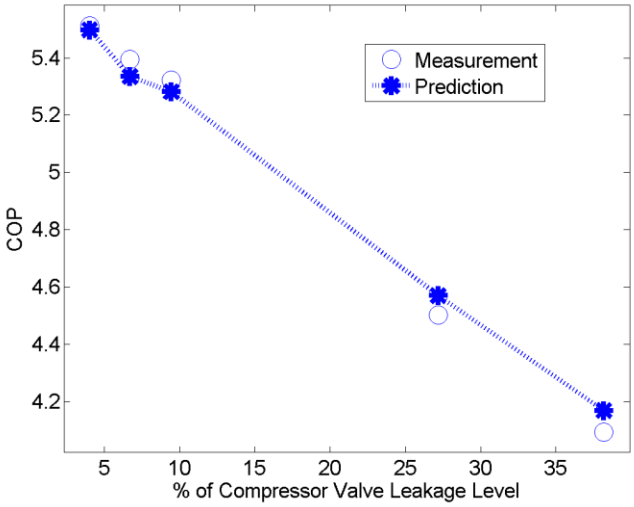

Figure 36: Comparison between the experimental and simulated COP at different compressor valve leakage levels

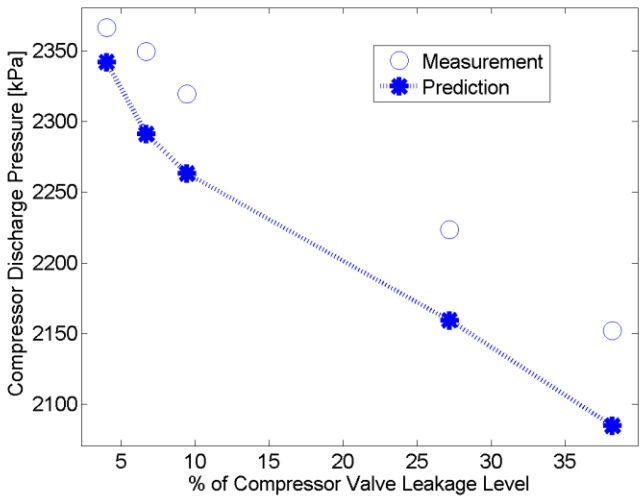

Figure 37: Comparison between the experimental and simulated compressor discharge pressure at different compressor valve leakage levels

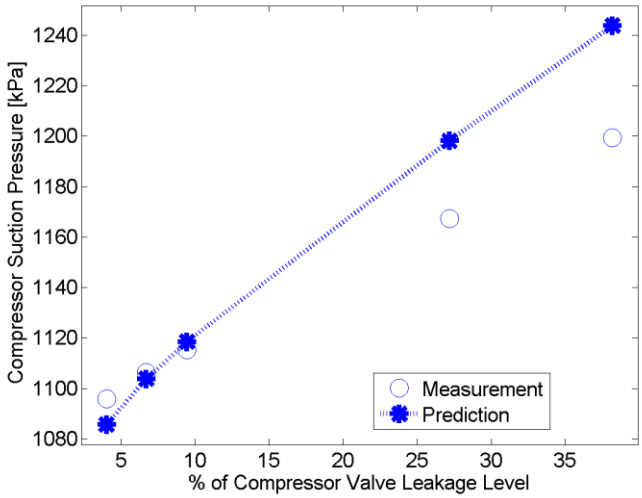

Figure 38: Comparison between the experimental and simulated compressor suction pressure at different compressor valve leakage levels

Case study

The California Title 24 HVAC Refrigerant Charge and Airflow (RCA) diagnostic protocol was used as an experimental subject during the development of the evaluation methods in this project. It was chosen because it is readily available and is in current widespread use. This section describes an evaluation of this protocol based on the performance criteria and data library previously described. In applying the method, data were supplied to the FDD method from the laboratory measurements. In determining fault impact ratios for any fault, the measurement results were compared to the outputs from the normal model determined from regression as previously described.

RCA background

The RCA protocol is specified in California's current Title 24 – 2008 building energy code (CEC 2008). It was included in the 2005 version of the code and is included in a modified form in the 2013 version of the code that will be implemented 2014. RCA, as its name implies, is intended only to detect and diagnose high or low refrigerant charge and low evaporator airflow. The airflow diagnostic is intended to ensure that the evaporator has sufficient airflow for the charge diagnostics to be applied. It is an available option if direct measurement of the airflow isn't conducted. The RCA protocol is based primarily on manufacturer's installation guidelines.

Title 24 specifies that the RCA protocol is to be applied to residential systems. However, it has been used as the basis for utility-incentivized maintenance programs on residential and commercial unitary systems. For this reason, and because there is no fundamental difference between commercial and residential unitary systems, the input data from both RTU and split systems were used in the evaluation.

The protocol is applied sequentially. The evaporator airflow is checked first. If the airflow is deemed acceptable, then the charge algorithm is applied. The RCA uses the following as its inputs: (1) return air dry bulb and wet bulb; (2) supply air dry bulb; (3) ambient air dry bulb; (4) either evaporator superheat for FXO systems, or subcooling for TXV systems; and (5) the manufacturer's specified target subcooling value (for TXV systems). Some of these inputs are used to gather target temperature split and target superheat values from two lookup tables. The inputs, and the values from lookup tables, are used to determine whether temperature split (the air temperature difference across the indoor unit) and superheat (for FXO systems) or subcooling (for TXV systems) are within acceptable ranges, using a difference (Δ) between the measured and target values. For example, ΔSH is calculated as: $\Delta SH = SH_{measured} - SH_{target}$.

The range of driving conditions for the lookup tables is limited, which means that the protocol can't be applied to some tests in the data library (i.e. gives *No Response* outcomes). A flow diagram of the RCA protocol logic is shown in Figure 39. In this figure the inputs listed above are shown in red. The RCA output results are shown in grey boxes. The process starts in the top left corner (if the temperature-split airflow diagnostic is used), with return air dry bulb and wet bulb temperatures as inputs.

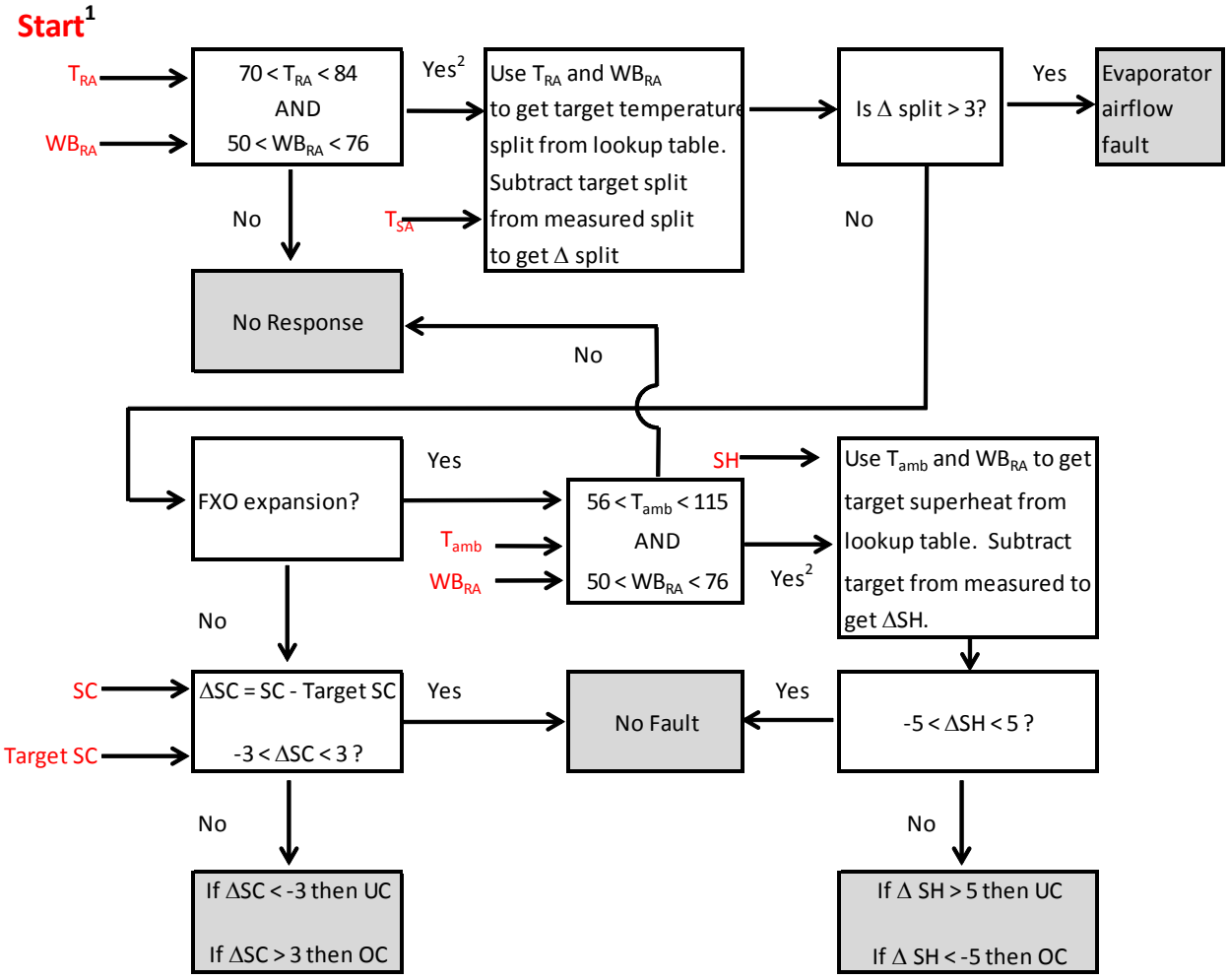

Note 1: The first part of the protocol, intended to determine whether there is sufficient evaporator airflow, is an optional approach that can be used if direct airflow measurement isn't conducted. If the evaporator airflow diagnostic isn't used, the process starts in the box labeled "FXO expansion?"
Note 2: The lookup tables cover the ranges specified above, but there are several cells on each table that contain dash marks, indicating that the protocol should not be applied. In these cases the result is "No Response".

Figure 39: Flow diagram of logic for applying the RCA protocol (using 2008 Installer's version)

RCA versions: 2008, 2013, Installer & HERS

The RCA protocol has been modified with each new version of Title 24. In the 2008 energy code, a special version of the protocol was given for use by Home Energy Rating System (HERS) raters, who provide field verification and diagnostic testing to demonstrate compliance with the standard. This version was identical except that it included looser tolerances when comparing measured and target values of superheat, subcooling, and temperature split. The standard provides a rationale for the different tolerances:

"*In order to allow for inevitable differences in measurements, the Pass/Fail criteria are different for the Installer and the HERS Rater*." (RA 3.2.2.6.1, note #5).

For example, the charge diagnostic for FXO systems is:

$$-5°F < \left(SH_{measured} - SH_{target}\right) < 5°F \rightarrow \ No\ charge\ fault \quad (7)$$

while for the HERS rater the tolerance is increased 1°F above and below the target:

$$-6°F < \left(SH_{measured} - SH_{target}\right) < 6°F \rightarrow \ No\ charge\ fault \quad (8)$$

The 2013 version of Title 24 has removed the temperature-split evaporator airflow diagnostics option. There are other compliance options available to confirm that sufficient airflow is attained prior to diagnosing charge faults. These generally involve showing by direct measurement that the evaporator airflow is above 300 or in some cases 350 CFM per nominal ton of cooling capacity.

The 2013 version also has additional restrictions on the driving conditions under which the protocol can be applied, such as a maximum outdoor (condenser inlet) air temperature of 120°F for TXV-equipped systems, and a minimum return air (indoor) dry-bulb temperature of 70°F (whereas the 2008 protocol had this limitation only for outdoor air temperatures from 55 – 65°F).

A summary of the differences in tolerances within the four versions of the RCA protocol in the current (2008) version and the future (2013) version is shown in Table 8.

Table 8: Tolerances for 2008 and 2013 Installer and HERS versions of the RCA protocol

	2008		2013	
Charge	**Installer**	**HERS**	**Installer**	**HERS**
FXO (Δ superheat)	±5°F	±6°F	±5°F	±8°F
TXV (Δ subcooling)	±3°F	±4°F	±3°F	±6°F
Airflow				
(Δ temperature split)	+3°F	+4°F	-	-

In the case of charge, if a fault is detected, it is diagnosed as "undercharged" if the difference in Equation 7 is above 5°F and "overcharged" if the difference is below -5°F. This distinction is not specified for the HERS rater; the system simply fails the charge test. However, to present a more meaningful evaluation here, the distinction is taken as implied in the results presented below.

Test results

Results of the tests are presented for each of the four RCA versions' with respect to the evaluation outcome categories *No Response, False Alarm, Missed Detection* and *Misdiagnosis*.

No Response

The *No Response* rates for the four RCA versions are shown in Table 9.

Table 9: Total test cases, and No Response results for four RCA versions

	2008		2013	
	Installer	HERS	Installer	HERS
Test Cases	607	607	572	572
No Response	127	128	158	158
No Response Rate	**21%**	**21%**	**28%**	**28%**

In the RCA protocol, a *No Response* result is generated when the driving conditions – ambient air temperature, indoor wet-bulb temperature, and indoor dry-bulb temperature – are not within the range of the lookup tables that are used to determine target temperature split and superheat values, or when they are outside of the limits discussed above. A higher rate of *No Response* means that the protocol is less useful, particularly for maintenance technicians, as detailed by Temple (2008). However, since the rate is dependent on the conditions of the input data, the rates themselves aren't very meaningful because the distribution of input data conditions may not exactly represent the typical conditions when a technician might want to deploy the protocol. A comparison of rates from one protocol to the next would be more meaningful.

The number of test cases and responses differ in the versions of the RCA presented in Table 9. In the 2013 version, all cases with indoor airflow rates below 300 CFM/nominal ton are assumed to be eliminated by direct measurement of airflow, and so they have been removed from the input data (35 test cases were below this criterion). The number of responses varies in the 2008 version because the temperature split (airflow diagnostic) table has a wider range of acceptable conditions. This means that a test case can be flagged as having an airflow fault under conditions where the charge diagnostic would give *No Response*. Since the protocol is sequential (airflow diagnostic first), the charge diagnostic isn't applied if an airflow fault is flagged. With the looser tolerance of the HERS version, some test cases passed the airflow diagnostic (which hadn't passed for the Installer version) and were then flagged as *No Response* when the charge diagnostic was applied.

False Alarm

The *False Alarm* results for each of the four RCA versions are presented in separate plots in Figure 40 to Figure 43. Below Figure 40 the data that form the basis of the figure are also presented, in Table 10, to indicate the sample sizes.

Calculation of *False Alarm* Rate

The *False Alarm* rate is calculated at several Fault Impact Ratio (FIR) thresholds. Test cases with FIR above the threshold are considered unfaulted. The rate calculations follow the procedure described in the section *Test Case Outcome Rate Calculations* on page 9. Referring to Figure 40, the *False Alarm* rate is 45% for the 95% FIR_{COP} threshold, which refers to all test cases in which COP is degraded by 5% or less. Some of these *False Alarms* are cases where the experimenter had imposed a fault, but it wasn't significant enough to cause a 5% degradation in performance, and the others are cases in which the experimenter did not impose a fault.

There is experimental uncertainty in all measurements, including the measurements used in calculating capacity and COP. With randomly distributed error, about half of the unfaulted tests will give FIR values

above 100%, and half below 100%. All of the data with values above 100% are included in the calculations. Since these cases are overwhelmingly unfaulted cases (as opposed to cases slightly below 100%, many of which have small faults imposed), including them gives lower *False Alarm* rates than if these cases were omitted.

Results and Discussion

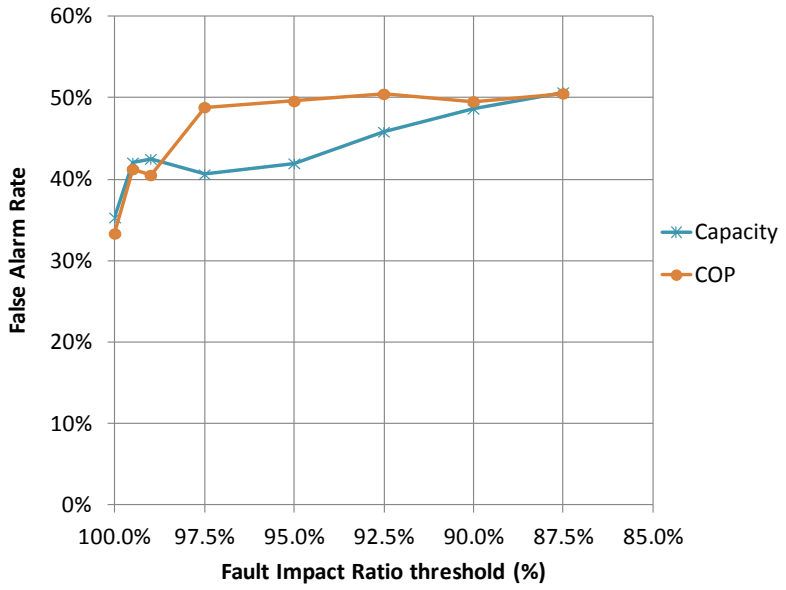

Figure 40: RCA 2008 Installer *False Alarm* rate as a function of FIR threshold

Table 10: Numerical results for RCA 2008 Installer False Alarm rate as a function of Fault Impact Ratio thresholds

	FIR threshold:	100.0%	99.5%	99.0%	97.5%	95.0%	92.5%	90.0%	87.5%
Capacity	Responses	68	107	120	165	236	288	335	361
	False Alarms	24	45	51	67	99	132	163	183
		35%	**42%**	**43%**	**41%**	**42%**	**46%**	**49%**	**51%**
COP	Responses	63	97	116	174	254	311	343	370
	False Alarms	21	40	47	85	126	157	170	187
		33%	**41%**	**41%**	**49%**	**50%**	**50%**	**50%**	**51%**

The results for the 2008 Installer version, in Figure 40, are surprisingly high (the numerical basis of these results is shown in Table 10. In a third of the cases in which the system performs at 100% efficiency, the RCA diagnoses a fault. For systems performing at 97.5% or greater efficiency, the RCA diagnoses about half with a fault. When the protocol is applied in the field, each *False Alarm* is associated with costly and unnecessary service (which may degrade performance), so this result suggests a very poorly performing protocol.

The *False Alarm* rate stays fairly constant, which is surprising. We would expect that as we move to the right across the plot (i.e. consider larger and larger fault impact cases to be unfaulted) that the rate of *False Alarm* would increase significantly.

The *False Alarm* rate at the 100% FIR threshold in Figure 40 is not 0%. As noted above, the 100% threshold includes all test cases for which the FIR is above 100%. If these test cases were not included, then besides increasing the *False Alarm* rate at lower thresholds (as explained above) the 100% point would be undefined (0/0), since there are no cases with FIR between 100% and 100%.

An earlier evaluation approach, in which fault impact was not considered, was presented at a conference (Yuill and Braun 2012). The *False Alarm* rate presented at that time was 26%, which is lower than the rate currently calculated. Apart from the difference in definition of "correct" charge, discussed in the Data Library section above, the current evaluation method gives a different result because many tests with very small faults imposed are now considered unfaulted because they have no significant effect on performance. The current method makes more sense from a user's perspective because users are typically not concerned with operating conditions that don't affect performance (except for the case of overcharge, as noted in the definition of *False Alarms*).

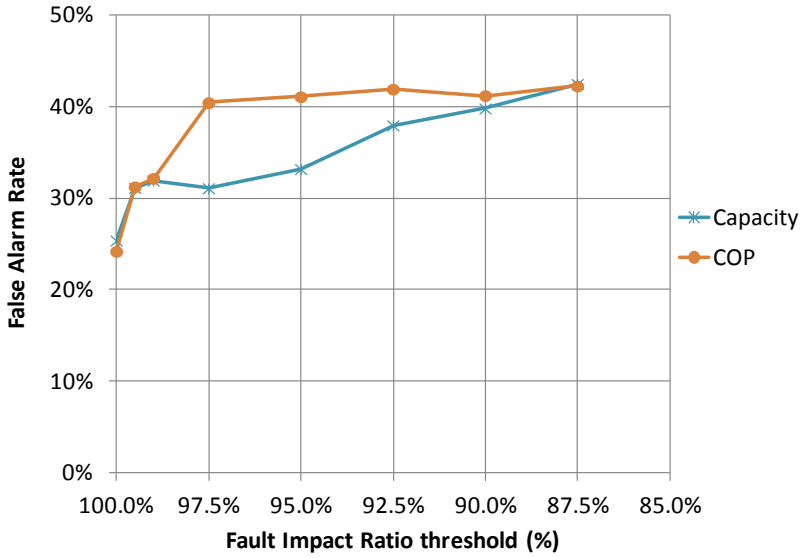

Figure 41: RCA 2008 HERS *False Alarm* rate as a function of FIR threshold

Comparing Figure 40 and Figure 41 we see an improvement in performance with respect to *False Alarm* rate – almost 10% in most cases. The only difference between these versions is the tolerances applied, as shown in Table 8. This suggests that the protocol is overly sensitive. Looser tolerances will reduce the *False Alarm* rate, although they may also have a detrimental effect on the ability to detect and correctly diagnose faults.

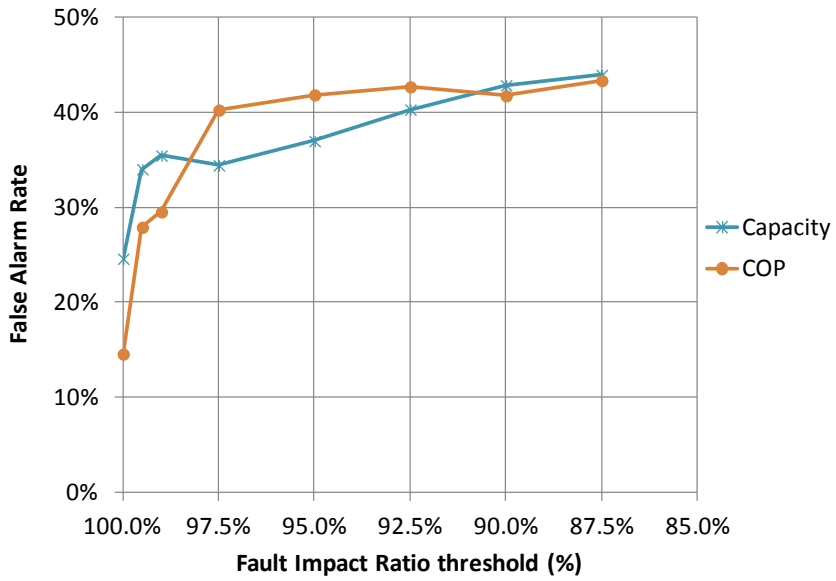

Figure 42: RCA 2013 Installer *False Alarm* rate as a function of FIR threshold

Comparing Figure 40 and Figure 42 we again see improvement. The only difference between these versions is that the airflow fault diagnosis module is removed in the 2013 protocol (Figure 42). This brings reductions in the *False Alarm* rate of 5 – 10%, in most cases.

Although the removal of the temperature-split airflow diagnostic reduces the *False Alarm* rate, it is not necessarily an overall improvement to the protocol, because it reduces the utility of the protocol. The temperature split method is generally easier to apply than the alternative (directly measuring the airflow). Furthermore, the present evaluation necessarily assumes that the direct airflow measurement approach does not provide any *False Alarms*, but this may not be true in actual application of the protocol.

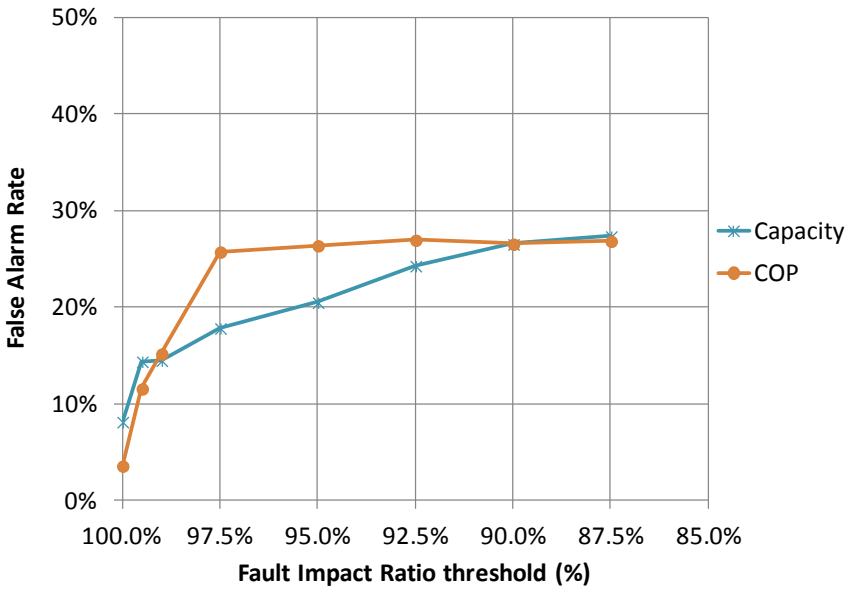

Figure 43: RCA 2013 HERS *False Alarm* rate as a function of FIR threshold

In Figure 43 we see the best performance, with respect to *False Alarms,* of the four versions. This can be attributed to the even looser tolerances for the 2013 HERS version. Although these results are improvements over the other versions, they still seem far too high to be able to consider this an effective protocol. Considering the 95% FIR_{COP} threshold, we still have over 1 in 4 cases falsely flagged as having a charge fault (since there is no airflow diagnostic evaluation in this version), meaning that charge would be added to or removed from a system that is operating acceptably.

Misdiagnosis

Calculation of *Misdiagnosis* rate

As noted in the evaluation outcomes definitions, a Misdiagnosis is a test case in which the following criteria are true:

- The RCA flags a fault
- The experimenter identifies the system as having a fault (or in the units in which we have determined that the maximum COP at the standard 95/80/67 condition occurs at a charge level different from what the experimenter considered to be 100% charged, we have redefined the "correct" charge to coincide with the charge level at maximum COP. When these systems have a charge level different from this "correct" charge, they are classified as having a charge fault)
- The RCA-flagged fault is not the same as the experimenter-identified fault

The rate is calculated as the number of *Misdiagnoses* divided by the number of tests for which the first two criteria are true. The *Misdiagnosis* rate addresses the question: if the protocol is applied to a system operating with a fault, how often will it diagnose a different fault?

The enumeration of misdiagnoses is divided into *Misdiagnosis (a)* and *Misdiagnosis (b)*. The former considers all test cases in the data library. The latter uses only those test cases in the data library that have faults that the protocol is intended to diagnose. For example, in the RCA 2008 protocols, only test cases with refrigerant charge or evaporator airflow faults are included in the *Misdiagnosis (b)* evaluation results. The *Misdiagnosis (b)* results are intended to give further insight into a protocol's performance, but not necessarily to reflect on the overall utility of the protocol, since it is known that other faults exist in the field, and the utility of the protocol depends on how it responds to these other faults.

For evaluation of *Misdiagnosis* rates, we group results into five FIR bins: <75%, 75-85%, 85-95%, 95-105%, and >105%. The *Misdiagnosis* rates for each FIR bin are shown as bars in Figure 44 to Figure 51. The figures represent *Misdiagnosis A* and *B* for each of the four different RCA versions. The number of responses (meeting the first two criteria listed above) is shown in the base of each bar. For example, in Figure 44 the bin for $FIR_{capacity}$ from 95 – 105% shows that there are 118 cases in which the RCA flags a fault and the experimenter has indicated the presence of a fault. Of these, 83 were correctly diagnosed and 35 were misdiagnosed, which gives 30%. In the bin for $FIR_{capacity}$ greater than 105% there were four cases, all of which were correctly diagnosed.

Results and Discussion

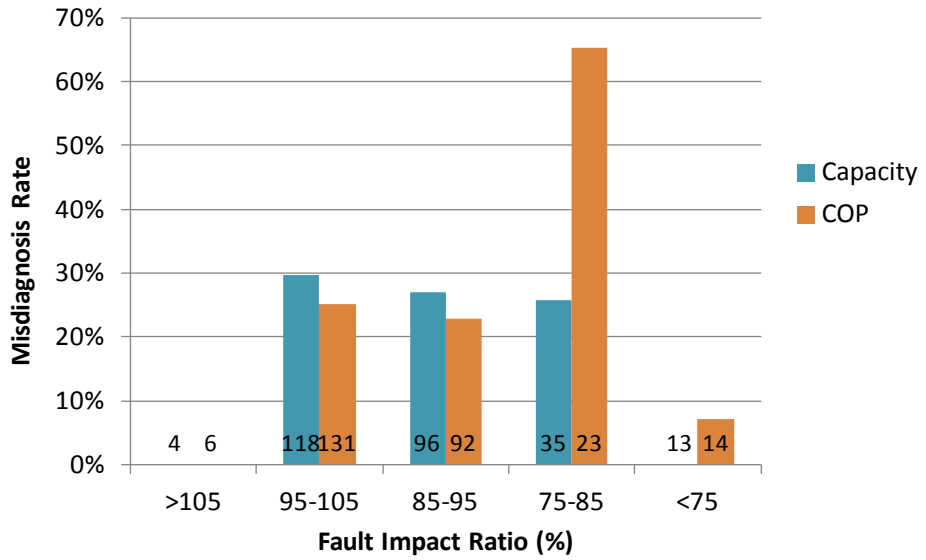

Figure 44: RCA 2008 Installer *Misdiagnosis (a)* rates as a function of Fault Impact Ratio (FIR)

In Figure 44 the *Misdiagnosis* rate for FIR_{COP} in the 75-85% bin is very high: 65%. This bin contains six cases of condenser airflow and six cases of compressor valve leakage faults, all of which the RCA diagnoses as overcharged, contributing to this unusually high rate. However, the overall rate for all data is 26%, which is also quite high.

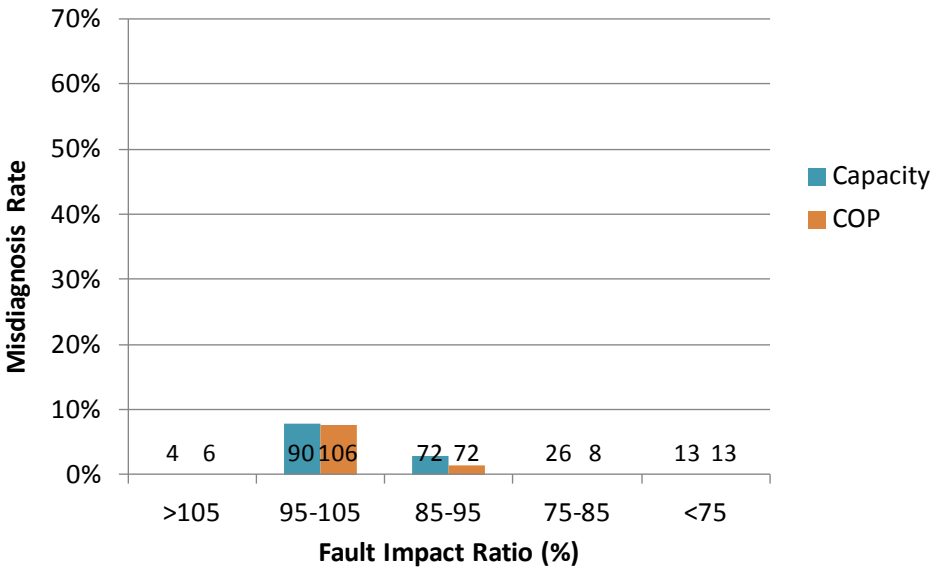

Figure 45: RCA 2008 Installer *Misdiagnosis (b)* rates as a function of Fault Impact Ratio (FIR)

The *Misdiagnosis (b)* rates, which use only test cases that have refrigerant charge or evaporator airflow faults, are shown in Figure 45. The results are markedly improved compared to the rates for *Misdiagnosis (a)*. Overall only 9 of 205 tests have a Misdiagnosis. These nine include undercharge diagnosed as overcharge and vice versa, evaporator airflow diagnosed as overcharge or undercharge, and one case of overcharge diagnosed as an evaporator airflow fault.

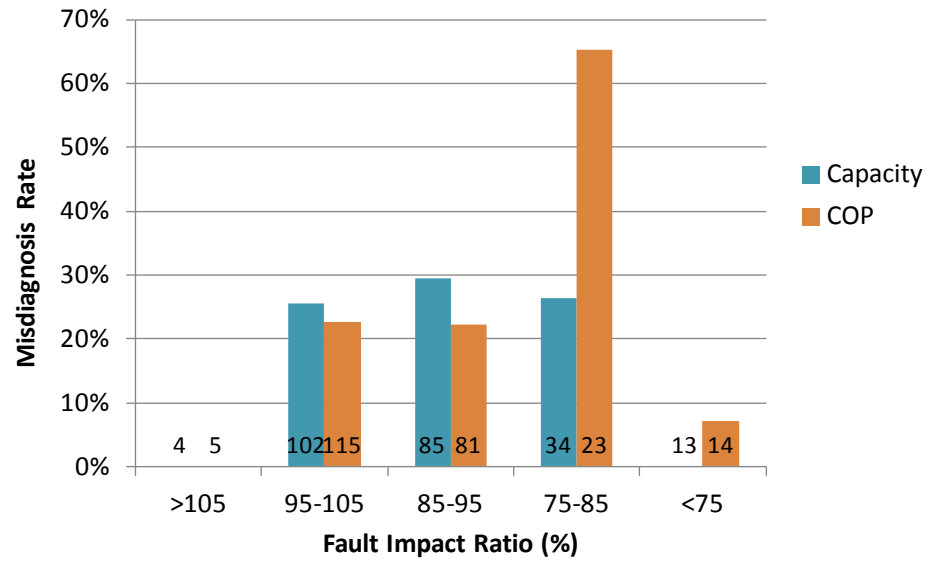

Figure 46: RCA 2008 HERS *Misdiagnosis (a)* rate as a function of Fault Impact Ratio (FIR)

The relaxed criteria for the HERS version of the 2008 protocol means that less cases are flagged as faults – 238 versus 266 for the installer protocol. The results, shown in Figure 46, are otherwise quite similar to the Installer version results, shown in Figure 44. The overall Misdiagnosis rate here is 25%.

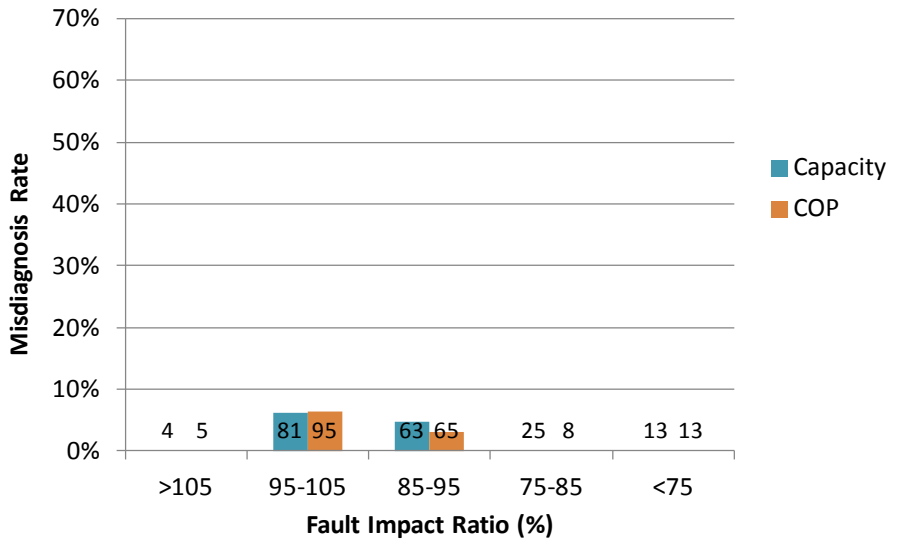

Figure 47: RCA 2008 HERS *Misdiagnosis (b)* rate as a function of Fault Impact Ratio (FIR)

The results for the 2008 HERS *Misdiagnosis (b)* analysis, shown in Figure 47, are also very similar to the 2008 Installer version. The number of misdiagnoses is eight (compared with nine for the Installer version). This suggests that the Misdiagnosis rate is not very sensitive to the fault diagnosis tolerances used by the RCA protocol.

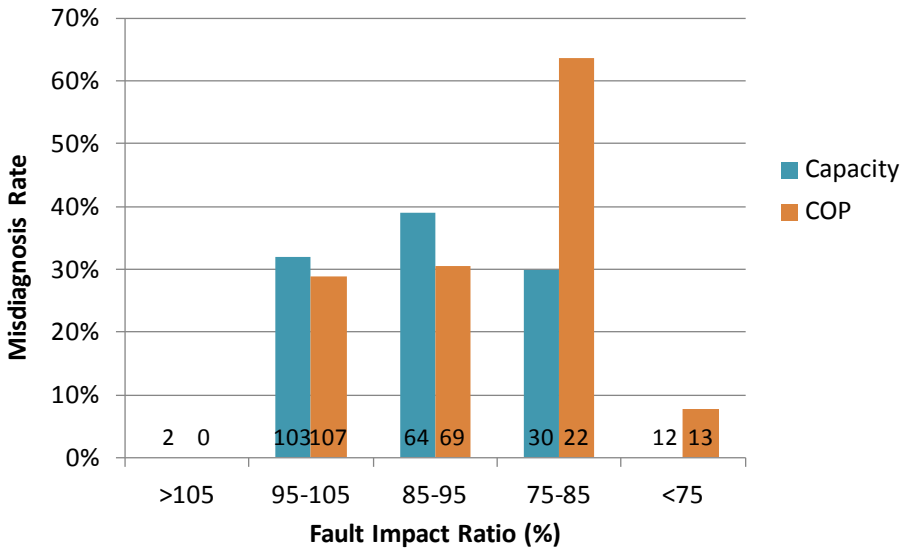

Figure 48: RCA 2013 Installer *Misdiagnosis (a)* rate as a function of Fault Impact Ratio (FIR)

In Figure 48 the RCA again uses the Installer tolerances, but differs from the evaluation in Figure 44 in that there is no longer any airflow diagnostic. Also, all cases with evaporator airflow below 300

CFM/nominal ton are removed from the inputs. The overall Misdiagnosis rate here is 32%. This is slightly higher than the 2008 Installer version's 26% (Figure 44) despite the removal of the airflow diagnostic and the removal of input cases. This suggests that the *Misdiagnosis* rate for the airflow diagnostic may be lower than that of the charge diagnostic for the full range of fault types.

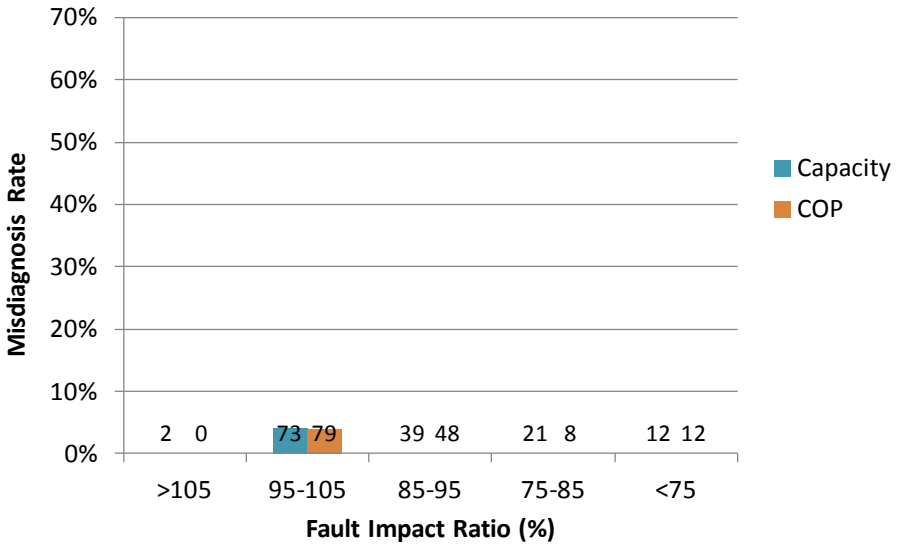

Figure 49: RCA 2013 Installer *Misdiagnosis (b)* rate as a function of Fault Impact Ratio (FIR)

As with the 2008 versions of the protocol, Figure 49 shows *Misdiagnosis (b)* rates that are much better than *Misdiagnosis (a)*. For the 2013 Installer version, there are only 3 misdiagnoses overall among 147 test cases.

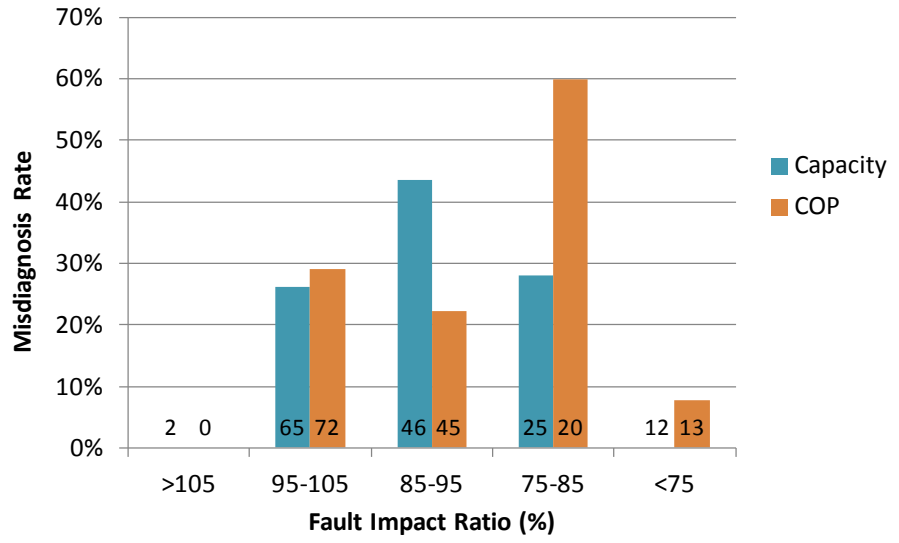

Figure 50: RCA 2013 HERS *Misdiagnosis (a)* rate as a function of Fault Impact Ratio (FIR)

In Figure 50 the results slightly better than the results in Figure 48, suggesting that the looser tolerance provides a small improvement to the Misdiagnosis rate. The overall rate for the 2013 HERS version of

the RCA is 29%. The spike in the 75 – 85% FIR_{COP} bin remains, but is reduced to 60% compared with 64 or 65% for the other versions of the protocol.

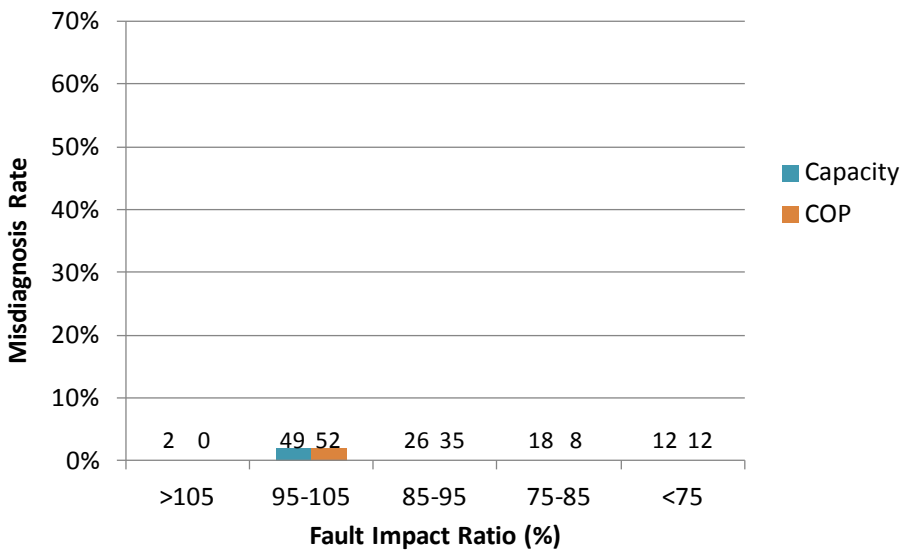

Figure 51: RCA 2013 HERS *Misdiagnosis (b)* rate as a function of Fault Impact Ratio (FIR)

The rates presented in Figure 51 are the best among the four protocol versions, with just 1 of 107 tests misdiagnosed. The one Misdiagnosis is an undercharged case diagnosed as overcharged. It is a fixed-orifice unit with high indoor humidity (80°F dry-bulb and 74°F wet bulb), and with 95°F outdoor temperature. The charge level is 92% of nominal, and the measured superheat is 15°F.

In terms of *Misdiagnoses* the RCA performs quite poorly for each of the four versions. The aggregated Misdiagnosis rates are summarized in Table 11. For the all versions, more than 1/4 of the times it's applied to a system with a fault, it reports that a different fault is present. This will result in a maintenance or installation technician performing the wrong corrective action, which may make the performance worse or at the very least cause the technician to repeat the diagnosis, then apply different corrective actions.

One might argue that the protocol performs extremely well when used for diagnosing charge faults (and evaporator airflow faults, in the case of the 2008 versions), as shown in the *Misdiagnosis (b)* results. However, as noted above, the *Misdiagnosis (b)* results give insight into the workings of the protocol, but don't give a good indication of the utility of the protocol for FDD. It's difficult to imagine a situation in which it is known that other faults don't exist, but charge faults (and evaporator airflow faults) may exist. If the user only wants to check charge using the 2013 RCA, for example, then it is important that the protocol not be affected by the presence of other faults. It should report "No Fault" for cases that don't have a charge fault. If a protocol reports "No Fault" for all faults that it is not intended to diagnose, then the *Misdiagnosis (a)* and *Misdiagnosis (b)* results would be the same (because a "No Fault" response is not categorized as a *Misdiagnosis*).

Table 11: Summary of aggregated Misdiagnosis rates for the four RCA versions

2008		2013	
Installer	HERS	Installer	HERS
26%	25%	32%	29%

Missed Detections

Calculation of *Missed Detection* rate

Missed Detections are cases in which two criteria are met:

- The experimenter identifies a fault (or a charge fault has been determined based on comparison with the charge giving maximum COP, as discussed in the section "Charge effect on COP and capacity" on page 22)
- The RCA response is "No Fault"

The test cases are grouped by Fault Impact Ratio into the same bins as *Misdiagnosis*, as described above. The *Missed Detection* rate is calculated by dividing the number of *Missed Detections* by the total number of tests in which the experimenter identifies a fault. It addresses the question: when the protocol is applied to a system with a fault, how often does it miss the fault and report that the system is operating properly?

As with the *Misdiagnosis* evaluation described above, a second quantity, *Missed Detection (b)*, is also calculated, in which only the faults that RCA is intended to diagnose are considered (charge and evaporator airflow for the 2008 versions, and charge for the 2013 versions). This addresses the question: how often does the protocol miss the faults it's intended to detect?

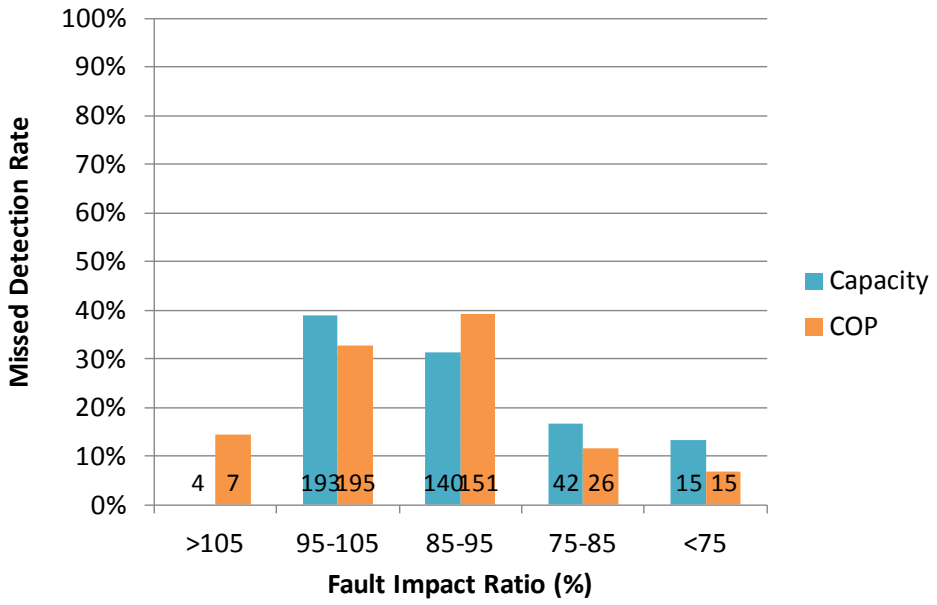

Figure 52: RCA 2008 Installer *Missed Detection (a)* rate as a function of Fault Impact Ratio (FIR)

The *Missed Detection* rates in Figure 52 are 30 to 40% for the low impact faults – those with FIR above 95%. These faults are of lesser importance than the higher impact faults, so the high rate is not very alarming. However, the 85-95% FIR bin still has this high rate of *Missed Detections*, and represents a significant missed potential for energy savings. The overall *Missed Detection* rate is 32%.

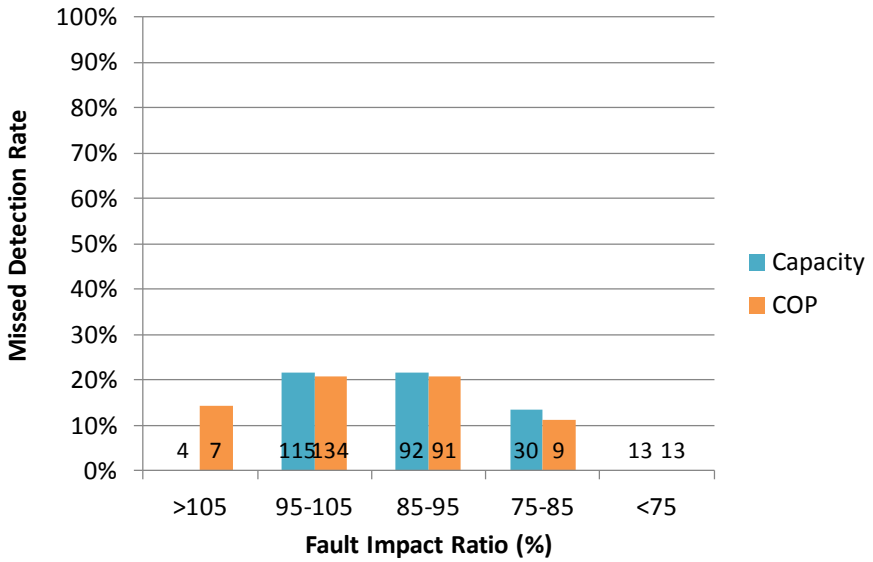

Figure 53: RCA 2008 Installer *Missed Detection (b)* rate as a function of Fault Impact Ratio (FIR)

Figure 53 presents the *Missed Detection (b)* rates – the *Missed Detection* rates for refrigerant charge and evaporator airflow faults only. These results are better than the results in Figure 52, but the 85-95% bin still has at least 20% *Missed Detections* for both $FIR_{capacity}$ and FIR_{COP}.

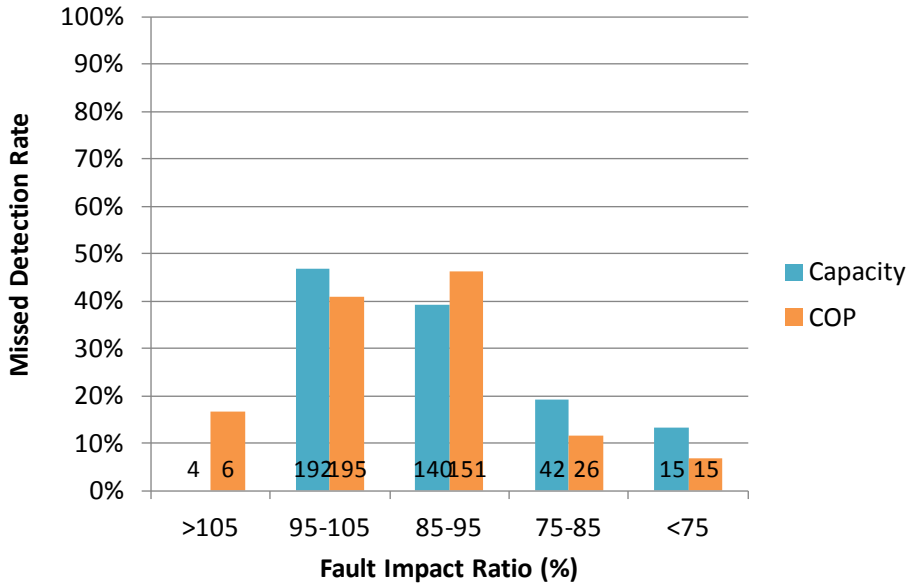

Figure 54: RCA 2008 HERS *Missed Detection (a)* rate as a function of Fault Impact Ratio (FIR)

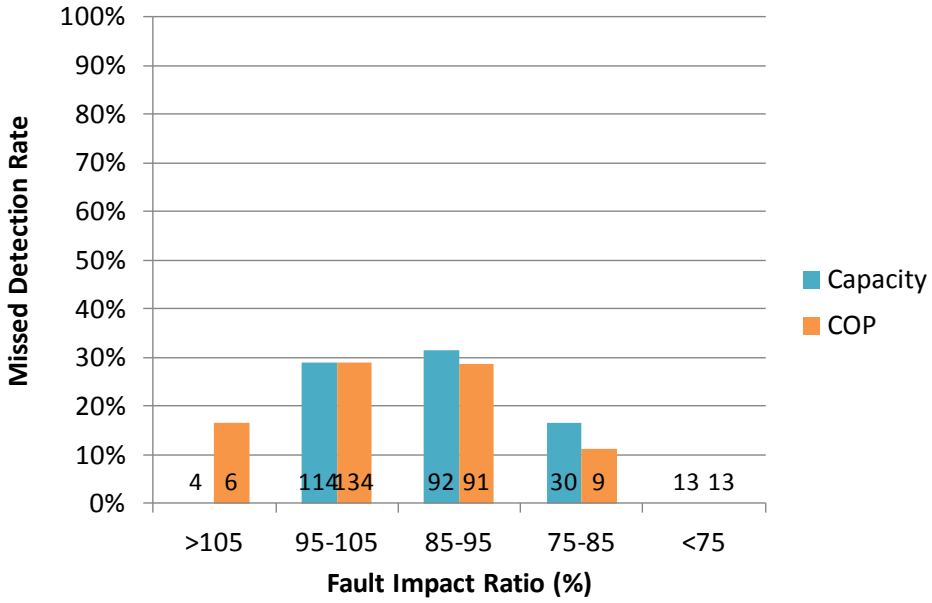

Figure 55: RCA 2008 HERS *Missed Detection (b)* rate as a function of Fault Impact Ratio (FIR)

Comparing the *Missed Detection* rates in Figure 54 and Figure 55 with the rates in Figure 52 and Figure 53 shows that the looser tolerances of the HERS protocol cause many more faults to be missed, raising

the rate in most FIR categories by 5 to 10%. This is a tradeoff with the improved *False Alarm* rate that is associated with looser tolerances. The overall rate of *Missed Detection (a)* for the RCA 2008 HERS protocol is 39%.

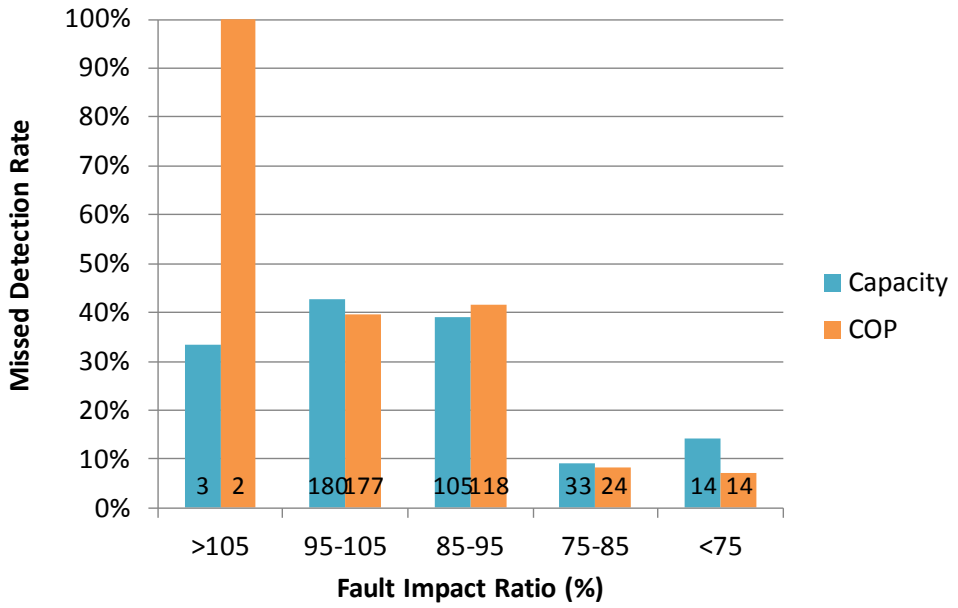

Figure 56: RCA 2013 Installer *Missed Detection (a)* rate as a function of Fault Impact Ratio (FIR)

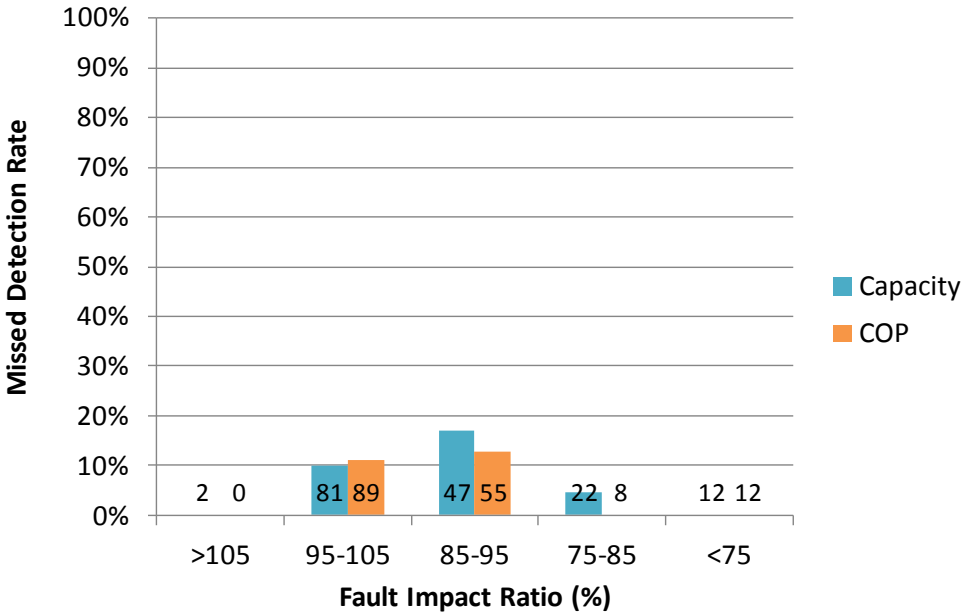

Figure 57: RCA 2013 Installer *Missed Detection (b)* rate as a function of Fault Impact Ratio (FIR)

In Figure 56 we see the effects of removing the airflow diagnostic, by comparing with Figure 52 since the 2008 and 2013 Installer protocols use the same tolerances for charge diagnostics. The overall performance is slightly worse for the 2013 protocol (even ignoring the result for FIR > 105%, which are

not very meaningful). This could suggest that the airflow diagnostic in the 2008 version is less likely to miss a detection than the charge diagnostics. However, comparing Figure 57 with Figure 53 we see that the Missed Detection rate has gone down when only RCA-diagnosed faults are considered. From this we can conclude that the airflow module was misdiagnosing faults, rather than missing detections, and this is why the rates are lower in Figure 52.

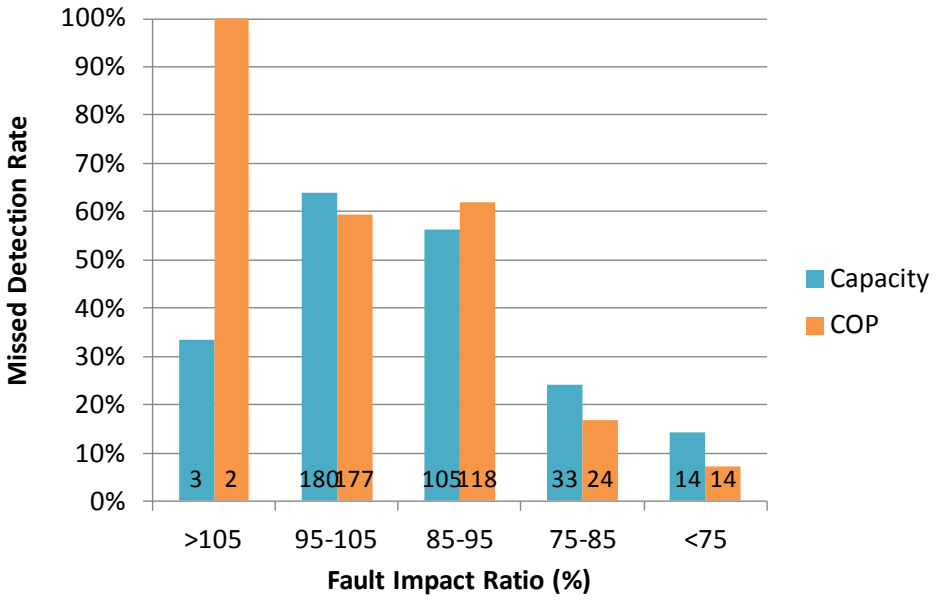

Figure 58: RCA 2013 HERS *Missed Detection (a)* rate as a function of Fault Impact Ratio (FIR)

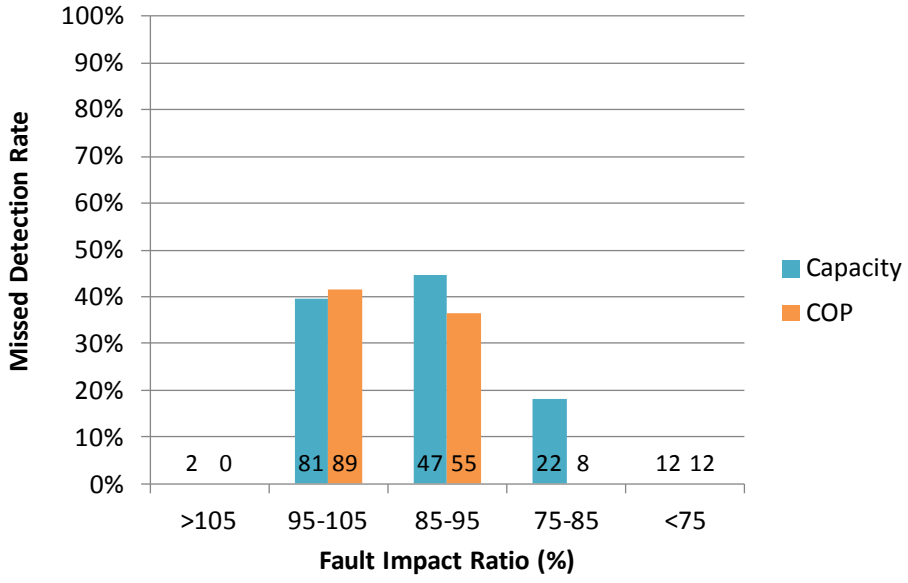

Figure 59: RCA 2013 HERS *Missed Detection (b)* rate as a function of Fault Impact Ratio (FIR)

Finally, the plots showing the Missed Detection rates for the 2013 HERS version, which has the loosest tolerances, show quite poor performance. In Figure 58 almost two thirds of the faults that cause an 85 –

95% $FIR_{capacity}$ are missed. The steady increase in *Missed Detection (b)* rates (which only include faults that the RCA is intended to diagnose) tracks the loosening tolerances as we go from Figure 53 (middle categories at about 20%) to Figure 55 (middle categories at about 30%) to Figure 59 (middle categories at about 40%).

Summarizing the *Missed Detection* evaluation, performance can be characterized as poor, with significant faults being missed in all versions of the protocol. A summary of the aggregated *Missed Detection* rates is given in Table 12.

Table 12: Summary of aggregated Missed Detection rates for the four RCA versions

2008		2013	
Installer	HERS	Installer	HERS
32%	39%	37%	55%

Conclusions of case study

The case study of the RCA protocol has demonstrated that the evaluation method developed in this project can effectively evaluate the strengths and weaknesses of an FDD protocol in a way that reflects the overall usefulness of the protocol to a user. This is done by using a fault-impact based analysis, and by providing results across a range of FIR. A user can select his own sensitivity to fault impact based on either capacity or COP, and read the results in each outcome from the charts. For example, if a user feels that all faults that reduce capacity by less than 10% should be tolerated, she can read the evaluation results from *False Alarm* rate, *Misdiagnosis* rate, and *Missed Detection* rate at those values, and have a reasonable idea of how the protocol will perform. If these results are available for several different protocols they can be compared so that the best protocol for that user can be selected.

One issue that hasn't been discussed is the distribution of faults by type and intensity. The performance of the RCA, and of any protocol, will vary by fault type and by intensity. This means that the results of the evaluation are dependent upon the distribution of faults in the data library. Ultimately, it would be best if this distribution matched the likely distribution of faults that occur in the field. However, this distribution is largely unknown. Even if the distribution were known with some confidence, it would be difficult to get data from the data library to match the expected distribution in the field because it is a finite set. In the next stage of development of FDD evaluation methods, simulation data will be used, which will allow the fault distribution to be controlled. At that time any fault distribution data that become available can be incorporated into the evaluation.

The fault distribution of the current data library is shown in Table 13. This distribution has a heavy concentration of charge faults, with more than 1/3 of all tests, and 44% of faulted tests having charge faults. This distribution may skew some results in favor of the RCA protocol, since charge is a fault that it is intended to diagnose.

Table 13: Distribution of fault types in data library as a percentage of all tests

Fault Type	% of library
No Fault	18%
Undercharge	27%
Overcharge	9%
Evaporator Airflow	17%
Condenser Airflow	11%
Liquid Line Restriction	8%
Non-condensables	2%
Valve Leakage	8%

Besides being an example for application of the evaluation method developed in this project, the case study provides evaluation results for the RCA protocol. The protocol's main strength may be that it is simple to apply, not requiring any difficult computations that require a computer. The protocol's weaknesses are many. Although there is no yardstick for FDD performance, it seems safe to conclude that the results are not good. The current (2008) protocol's *False Alarm* rates of 40% to 50% for all FIR thresholds below 100% are very troubling. It seems unlikely that the net benefit of this protocol could be positive, when it has such a high *False Alarm* rate.

It is tempting to consider using looser tolerances to improve this *False Alarm* rate, but even if we apply the loosest tolerances (from the 2013 HERS version) we get *False Alarm* rates above 15% for all thresholds. (This is an imperfect comparison because the 2013 HERS version also has no airflow diagnostic). This rate, 15%, is still unacceptable. Furthermore, the tradeoff with looser tolerances is that we will have increases in the *Missed Detection* rate. Again using the 2013 HERS tolerances, we have *Missed Detection* rates in Figure 59 that are over 70% in the 85 – 95% FIR_{COP} bin. Even if we only consider charge faults, in this same bin we see that the RCA misses more than half of the faults. One needs to question whether the cost of having 15% *False Alarm* rate is worth the benefit of catching half of the charge faults.

Given this poor performance, it seems that the potential for salvaging the RCA protocol is not very good, and that consideration should be given to replacing it or removing it from the standard.

Conclusions

A FDD protocol evaluation method for protocols applied to unitary air-conditioning systems at steady-state operation has been developed and described in this report. This includes a database of measurement data, and a simulation tool that can be used to reliably generate additional input data to eliminate the need for measurement data.

Several concepts related to the evaluation of FDD have been defined in this project, such as Fault Impact Ratio, Fault Intensity, False Alarms, Misdiagnoses, etc. The evaluation method developed is based on a fault's impact on the performance of a unitary system, and provides outputs over a range of impacts that could be of interest to a potential FDD protocol user. A system has been developed to categorize and enumerate the outcomes of an evaluation.

A case study was conducted in which the RCA protocol was evaluated. It was found to perform poorly, with unacceptable levels of *False Alarms*, regardless of the threshold used to differentiate faulted from unfaulted performance.

Some of the main conclusions of the project:

- The evaluation method developed here should be applied to FDD protocols of interest to determine whether their performance is acceptable to potential users
- Model data should be used instead of measurement data in future evaluations, to:
    - control the distribution of faults
    - remove the uncertainty from experimental error
    - widen the field of potential systems, faults, fault intensities, fault combinations, and driving conditions
    - provide datasets that can't be learned, hence gamed, by unscrupulous developers
- More understanding of the likely distribution of faults in the field is required
- The RCA protocol performs quite poorly, and consideration should be given to removing it from the standard

Moving forward, we are hopeful that this tool can provide a path to improved performance of FDD. It can do this by illuminating poorly performing FDD, to spur further developments and improvement, and by providing a tool for developers to use as they explore improvements in their protocols. It is important to evaluate FDD, because poorly performing FDD is costly, in that it can cause improper corrective actions to be taken, or wasted maintenance service, and can hinder more widespread future adoption of FDD if users don't find FDD benefiting them. The potential for FDD to reduce energy consumption and peak power, and to improve equipment life is still largely untapped, and this potential should be pursued.

Next Steps

The current project spurred interest from the National Institute of Standards and Technology (NIST), who have provided additional funding in support of pursuing effective evaluation methods for FDD protocols applied to unitary systems. This collaboration with NIST has allowed us to take a more ambitious approach to this project. We significantly expanded the scope beyond what was originally proposed, and were more meticulous in the development of the methods and data library than would otherwise have been possible.

The work described in this report will continue under the NIST funding. Future work will include:

(a) evaluation of other protocols, as a way of testing and refining our evaluation approach

(b) evaluations using simulation data

(c) assessment of simulation data as a replacement for experimental data

(d) assimilation of the simulation (or simulated data) into the software

(e) development of simplified figures of merit for FDD protocols

The results of these ongoing efforts will be made available to NBI and the CEC.

Definitions

There are several terms that do not yet have consensus definitions, but which are necessary or convenient when discussing FDD for unitary equipment. The definitions below describe the meaning of some applicable terms as used within this report. The definitions for terms in italics are proposed as standard definitions.

Driving Conditions – the dry-bulb temperature of the air entering the condenser, and the dry-bulb temperature and humidity of the air entering the evaporator

Fault – an operating condition in a unitary air conditioner that causes degradations in performance. This may include degradations in efficiency, capacity, equipment life, maintenance costs, or ability to maintain comfort conditions.

Fault detection – determination that a fault is present in the system

Fault Assessment – A quantification of the severity of the fault. This may be expressed as a fault intensity, a fault impact, or in broader terms, such as "low charge", "very low charge", etc.

Fault Diagnosis - Fault diagnosis consists of two processes: fault isolation and fault assessment

Fault Isolation – determination of the type of fault that is present or the component that is faulted.

Fault Impact – the effect caused by a fault on a variable of interest, such as capacity, EER, subcooling, supply air temperature, cost, thermal comfort, etc.

Fault Impact Ratio **(FIR)** – the ratio of COP or capacity under faulted conditions to COP or capacity under unfaulted operation at the same operating conditions.

Fault Intensity **(FI)** – the level of a fault expressed with reference to physical measurements

Protocol – the algorithm that generates outputs in a FDD tool

Return Air – in the context of this report, return air refers to the air entering the evaporator coil or in cases where the indoor fan is immediately upstream of the indoor coil, return air is the air entering the fan

Test Case – a set of input values, including pressures, temperatures, etc. for a system that is operating at steady-state

Threshold – with respect to Fault Impact Ratio, a threshold is the dividing point between faulted operation and unfaulted operation; the FIR above which a test case should be considered unfaulted

Unitary system – in the context of this report, a unitary system is an air-cooled direct-expansion vapor compression cycle air-conditioner with a single-speed compressor and single-speed fans.

Nomenclature

adp	Apparatus dew point
BF	Bypass factor
CA	Condenser Airflow fault
CEC	California Energy Commission
CFM	Cubic feet per minute
COP	Coefficient of performance
EA	Evaporator Airflow fault
EEV	Electronic expansion valve
EER	Energy efficiency ratio
FDD	Fault detection and diagnostics
FI	Fault Intensity
FIR	Fault impact ratio
FXO	Fixed orifice expansion valve
HERS	Home Energy Rating System
IP	Inch-pound system of units
LL	Liquid Line fault
NBI	New Buildings Institute
NC	Non-condensable gas in the refrigerant fault
NIST	National Institute of Standards and Technology
OC	Overcharge fault
psia	Pounds per square inch, absolute
RA	Return air
RTU	Rooftop unit
SA	Supply air
SEER	Seasonal energy efficiency ratio

SI	International system of units
T	Dry bulb temperature
T_{amb}	Ambient air dry bulb temperature
TXV	Thermostatic expansion valve
UC	Undercharge fault
VL	Compressor Valve Leakage fault
WB_{RA}	Return air wet bulb temperature

References

AHRI. 2008. *AHRI Standard 210/240: Performance Rating of Unitary Air-Conditioning & Air-Source Heat Pump Equipment*. Air-conditioning, Heating, and Refrigeration Institute.

ASHRAE. 2009. *ANSI/ASHRAE Standard 37 – 2009: Methods of Testing for Rating Electrically Driven Unitary Air-Conditioning and Heat Pump Equipment*. American Society of Heating, Ventilating, and Air-conditioning Engineers, Inc.

Armstrong, P.R., C.R. Laughman, S.B. Leeb, and L.K. Norford. 2006. Detection of Rooftop Cooling Unit Faults Based on Electrical Measurements. *HVAC&R Research*, 12(1):151-175.

Brandemuehl, M.J. 1993. *HVAC2 Toolkit: Algorithms and Subroutines for Secondary HVAC System Energy Calculations*. ASHRAE, Inc., Atlanta, GA: 402 p.

Bell, I. H., E.A. Groll and H. König. 2012. Experimental Analysis of the Effects of Particulate Fouling on Heat Exchanger and Air-side Pressure Drop for a Hybrid Dry Cooler", *Heat Transfer Engineering*, 32 (3): 264 - 271

Braun, J. E. 1989, *Methodologies for the Design and Control of Central Cooling Plants*, Ph.D. Thesis. University of Wisconsin – Madison, WI

Breuker, M. S. 1997. *Evaluation of a Statistical, Rule-based Detection and Diagnostics Method for Vapor Compression Air Conditioner*, MSME dissertation, Ray W. Herrick Laboratories, Purdue University, Ind. Report No. 1796-6 HL97-29

Breuker, M.S. and J.E. Braun. 1998a. Common Faults and Their Impacts for Rooftop Air Conditioners. *HVAC&R Research* 4(3):303-318.

Breuker, M.S. and J.E. Braun, 1998b. Evaluating the Performance of a Fault Detection and Diagnostic System for Vapor Compression Equipment. *HVAC&R Research* 4(4):401-425.

Breuker, M.S., T.M. Rossi, and J.E. Braun. 2000. Smart Maintenance for Rooftop Units. *ASHRAE Journal* 42 (11):41-46.

California Energy Commission (CEC), 2008. *2008 Building Energy Efficiency Standards for residential and nonresidential buildings*. CEC-400-2008-001-CM. Sacramento: California Energy Commission.

Cheung, H. and J.E. Braun. 2012a. Inverse Modeling to Simulate Fault Impacts for Vapor Compression Equipment Part 1: Component Modeling and Validation. International Refrigeration and Air Conditioning Conference, West Lafayette, IN, July 2012.

Cheung, H. and J.E. Braun. 2012b. Inverse Modeling to Simulate Fault Impacts for Vapor Compression Equipment Part 2: System Modeling and Validation. International Refrigeration and Air Conditioning Conference, West Lafayette, IN, July 2012.

Comstock, M.C., and J.E. Braun. 1999. *Development of analysis tools for the evaluation of fault detection and diagnostics in chillers, ASHRAE Research Project RP-1043*; HL 99-20: Report #4036-3. Ray W. Herrick Laboratories. Purdue University, West Lafayette, IN.

Feng, M.Y, K.W. Roth, D. Westphalen, and J. Brodrick. 2005. Packaged Rooftop Units: Automated Fault Detection and Diagnostics. *ASHRAE Journal* 47(4):68-70.

Himmelblau, D.M. 1978. Fault detection and diagnosis in chemical and petrochemical processes, pp. 343-393. *Elsevier Scientific Publishing Company*: Amsterdam, The Netherlands.

House, J. M.; W.Y. Lee, and D.R. Shin. 1999. Classification Techniques for Fault Detection and Diagnosis of an Air-Handling Unit. *ASHRAE Transactions* 105(1):1987-1997.

Incropera, F. P., D.P DeWitt, T.L. Bergman and A.S. Lavine. 2007. *Fundamentals of Heat and Mass Transfer, 6th Edition*, John Wiley & Sons, New York.

Isermann, R. 1984. Process Fault Detection Based on Modeling and Estimation—A Survey. *Automatica* 20(4): 387-404.

Jähnig, D. I., D.T. Reindl and S.A.Klein. 2000. A Semi-Empirical Method for Representing Domestic Refrigerator/Freezer Compressor Calorimeter Test Data, *ASHRAE Transactions*, 106 (2):122 - 130

Katipamula, S. and M.R. Brambley. 2005. Methods for Fault Detection, Diagnostics, and Prognostics for Building Systems – A Review, Part I. *HVAC&R Research* 11(1):3-25.

Kim, M.; Payne, W. V.; Domanski, P. A.; Hermes, C. J. L. 2006. *Performance of a Residential Heat Pump Operating in the Cooling Mode With Single Faults Imposed*. NISTIR 7350; 173 p.

Kim, M., Yoon, S.H., Payne, W.V., and Domanski, P.A.. 2008. Design of a steady-state detector for fault detection and diagnosis of a residential air conditioner. *International Journal of Refrigeration* 31(5):790-99.

Li, H., and J.E. Braun. 2003. An improved method for fault detection and diagnosis applied to packaged air conditioners. *ASHRAE Transactions* 109(2):683–692.

Li, H. and J.E. Braun. 2007. A Methodology for Diagnosing Multiple Simultaneous Faults in Vapor-Compression Air Conditioners. *HVAC&R Research*, 13(2): 369-395.

MacArthur, J. W. and Grald E. W. 1989, Unsteady Compressible Two-phase Flow Model for Predicting Cyclic Heat Pump Performance and a Comparison with Experimental Data. *International Journal of Refrigeration* 12 (1): 29 - 41

Norford, L.K., J. A. Wright, R. A. Buswell, D. Luo, C. Klaassen, and A. Suby. 2002. Demonstration of Fault Detection and Diagnosis Methods for Air-Handling Units (ASHRAE 1020-RP). *HVAC&R Research* 8(1):41-72

Palmiter, L., J-H. Kim, B. Larson, P.W. Francisco, EA. Groll and J.E. Braun. 2011. Measured effect of airflow and refrigerant charge on the seasonal performance of an air-source heat pump using R-410A. *Energy and Buildings*, 43(7):1802–1810.

Payne, W. V. and O'Neal, D. L. 2004. A Mass Flow Rate Correlation for Refrigerants and Refrigerant Mixtures Flowing Through Short Tubes. *HVAC&R Research* 10 (1): 73 – 87

Reddy, T.A. 2007. Development and evaluation of a simple model-based automated fault detection and diagnosis (FDD) method suitable for process faults of large chillers. *ASHRAE Transactions* 113(2):27-39.

Rossi, T.M. 2004. Unitary Air Conditioner Field Performance. *Proceedings of the 8th International Refrigeration and Air Conditioning Conference at Purdue*, July 2004. Paper 666.

Rossi, T. M., and J.E. Braun. 1997. A Statistical, Rule-Based Fault Detection and Diagnostic Method for Vapor Compression Air Conditioners. *HVAC&R Research*, 3(1):19–37.

Roth, K.W., D. Westphalen, and J. Brodrick. 2006. Residential Central AC Fault Detection & Diagnostics. *ASHRAE Journal* 48(5):96-97.

Shen, B., E.A. Groll and J.E. Braun. 2006. *Improvement and Validation of Unitary Air Conditioner and Heat Pump Simulation Models for R-22 and HFC Alternatives at Off-Design Conditions*. Final Report for RP-1173, ASHRAE.

Temple, K.A. 2008. Expanded Test Protocols for Low Ambient Testing of Unitary AC Systems. Final Report – Building Energy Research Grant (BERG) Program of the California Energy Commission.

Temple, K.A. 2012. *Brief Technical Review of Paper 2470 "Evaluating Fault Detection and Diagnosis Protocols Applied to Air-cooled Vapor Compression Air-conditioners",* Second Draft, August 5, 2012. Report for 2013 Residential Building Energy Efficiency Standards. California Energy Commission.

Vachtsevanos, G.J., F.L. Lewis, M.J. Roemer, A. Hess, and B. Wu. 2006. *Intelligent fault diagnosis and prognosis for engineering systems*. Hoboken, N.J.: Wiley.

Veronica, D.A. 2010. Detecting Cooling Coil Fouling Automatically—Part1: A Novel Concept. *HVAC&R Research* 16(4): 413-433.

Wallis, G. B. 1969. *One-dimensional Two-phase Flow*. McGraw-Hill, New York

Wang, H. Y. Chen, C.W.H. Chan and J. Qin. 2011. A robust fault detection and diagnosis strategy for pressure-independent VAV terminals of real office buildings. *Energy and Buildings* 43(7): 1774–1783.

Wiggins, M.C. and J.R. Brodrick. 2012. HVAC Fault Detection. *ASHRAE Journal* 54(2): 78-80.

Yang, L. Braun, J. E. and Groll, E. A. 2007. The Impact of fouling on the performance of filter-evaporator combinations", *International Journal of Refrigeration*, 30:489 - 498

Yuill, D.P. and J.E. Braun. 2012. Evaluating Fault Detection and Diagnostics Protocols Applied to Air-cooled Vapor Compression Air-conditioners, Paper 2470 – Revised July 23, *Proceedings of the 14th International Refrigeration and Air Conditioning Conference at Purdue*, July 16-19.

Zakula, T. Gayeski, N. T., Armstrong, P. R. and Norford, L. K. 2011. “Variable-speed heat pump model for a wide range of cooling conditions and loads”, *HVAC&R Research*, 17(5): 670 – 691

Zhao, X., M. Yang, and H. Li. 2011. Decoupling features for fault detection and diagnosis on centrifugal chillers (1486-RP). *HVAC&R Research* 17(1): 86-106.

Appendices

Capacity and COP vs. charge plots

The plots in this appendix show the effect of charge on performance at different driving conditions. Each plot represents data from a single unit, and each point on the plot is a test case. Since experimental facilities can't achieve exactly the same conditions during every test, the data points show more scatter than the actual experimental uncertainty would provide. The tests grouped into a given series (set of driving conditions, denoted in the series name shown in the legend) may have ambient temperature of ±0.75°F, and indoor wet-bulb and dry-bulb variations up to ±1°F in some units. This doesn't affect the effectiveness of the data for evaluating FDD, but it does make them appear more scattered in these plots than they would be if they could all have had exactly the same driving conditions.

On page 22, in the discussion of charge effects on COP, it was noted that some of the units were found to have a maximal COP value at a charge level different from the experimenter's definition of 100% charge at the rating condition (95/80/67). The plots presented in this appendix show the charge levels *before* adjustments were made to the nominally correct charge level. For example, in Figure 65 it is clear that the COP is highest at the 95% charge level (under all operating conditions). The nominally correct charge level was adjusted prior to using the data in the evaluation.

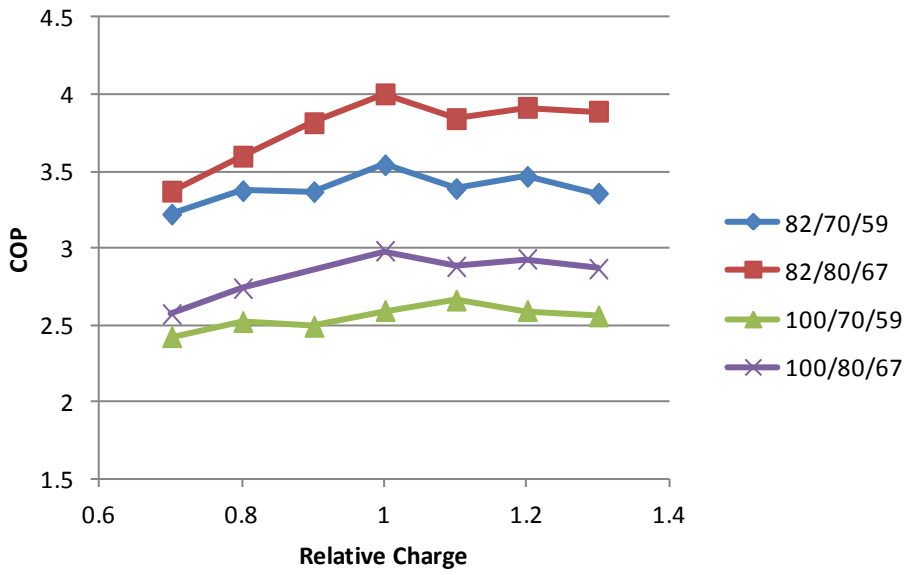

Figure 60: Effect of charge on COP for RTU 2

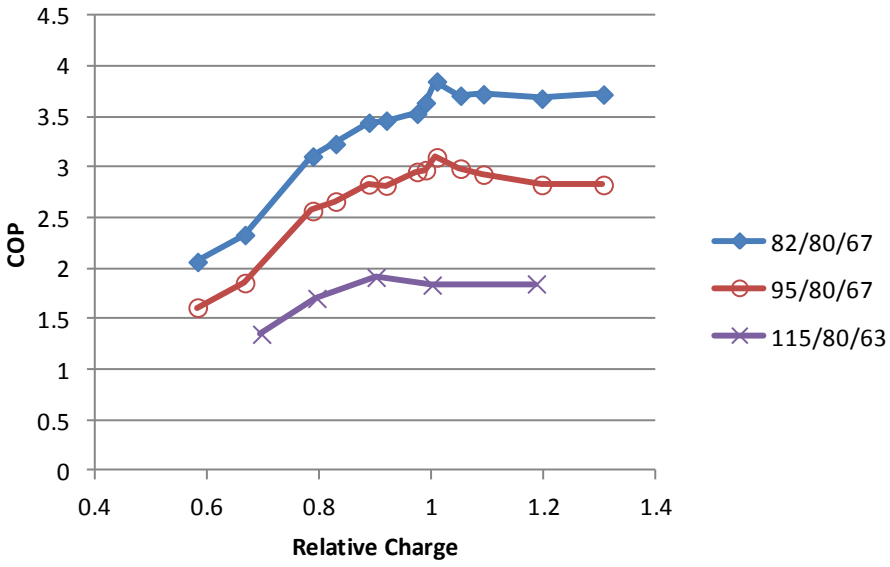

Figure 61: Effect of charge on COP for RTU 3

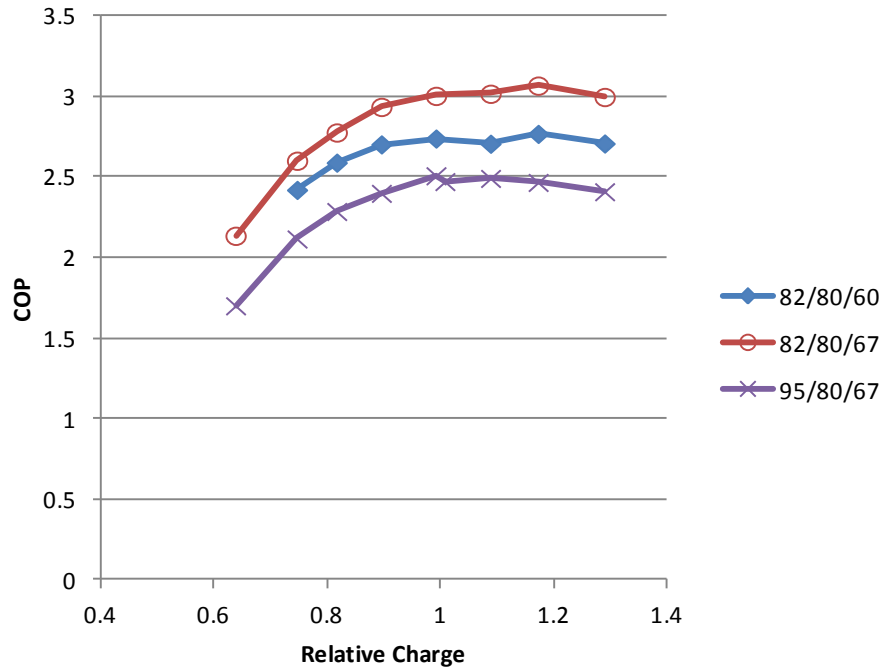

Figure 62: Effect of charge on COP for RTU 4

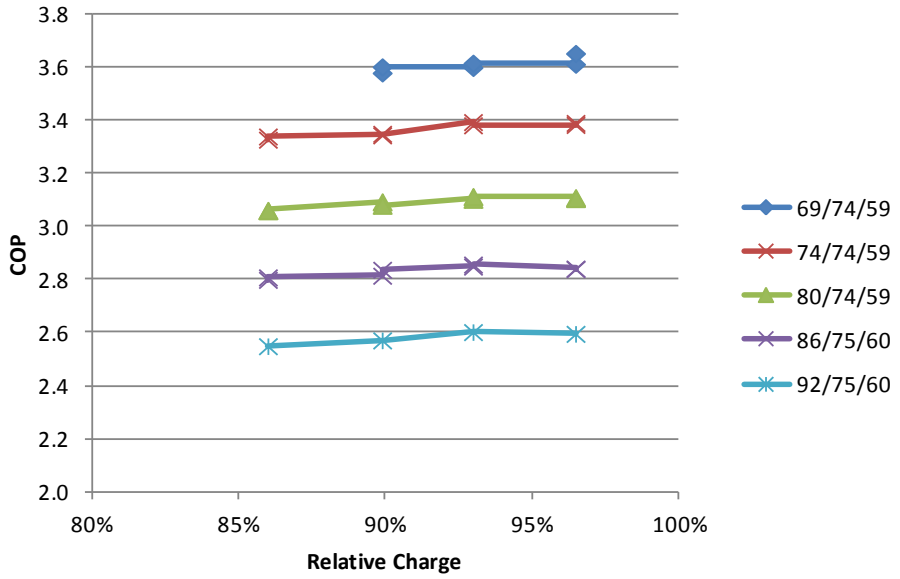

Figure 63: Effect of charge on COP for RTU 7

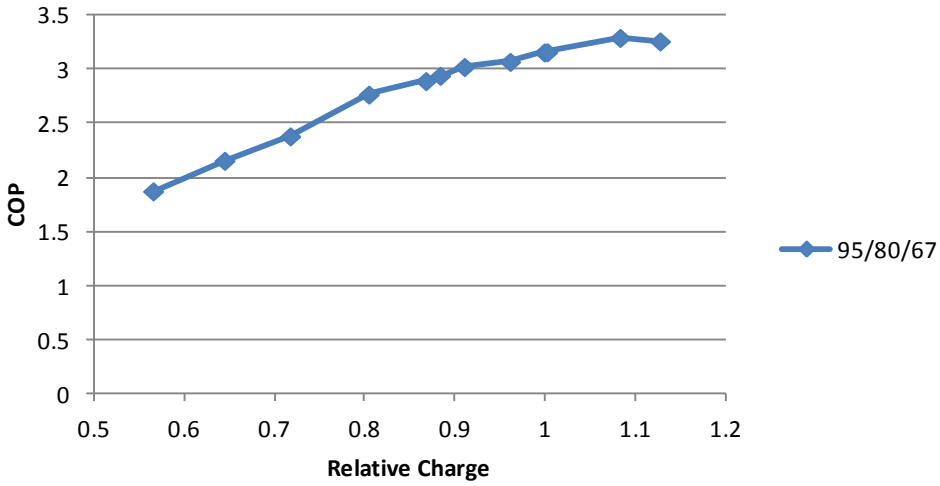

Figure 64: Effect of charge on COP for Split 1

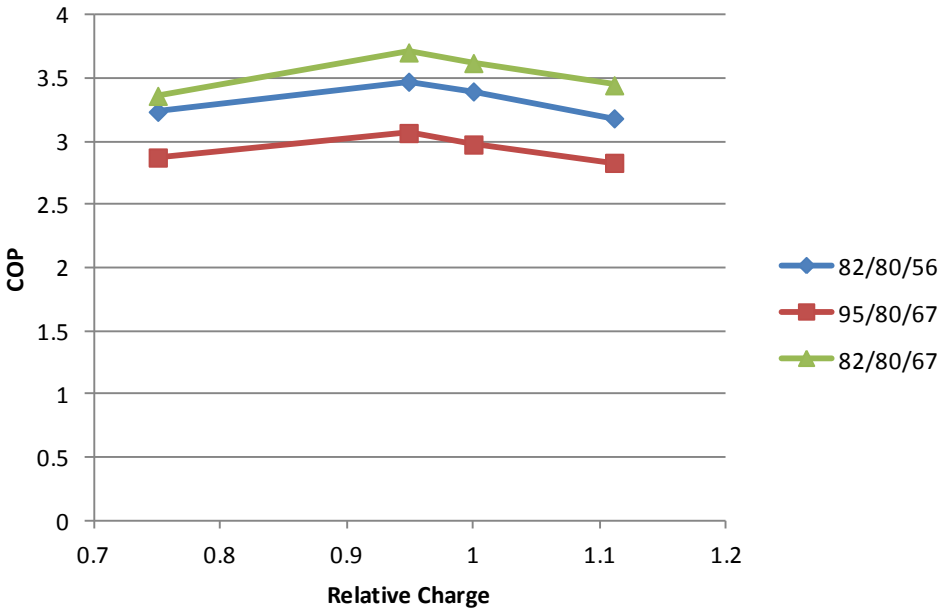

Figure 65: Effect of charge on COP for Split 3

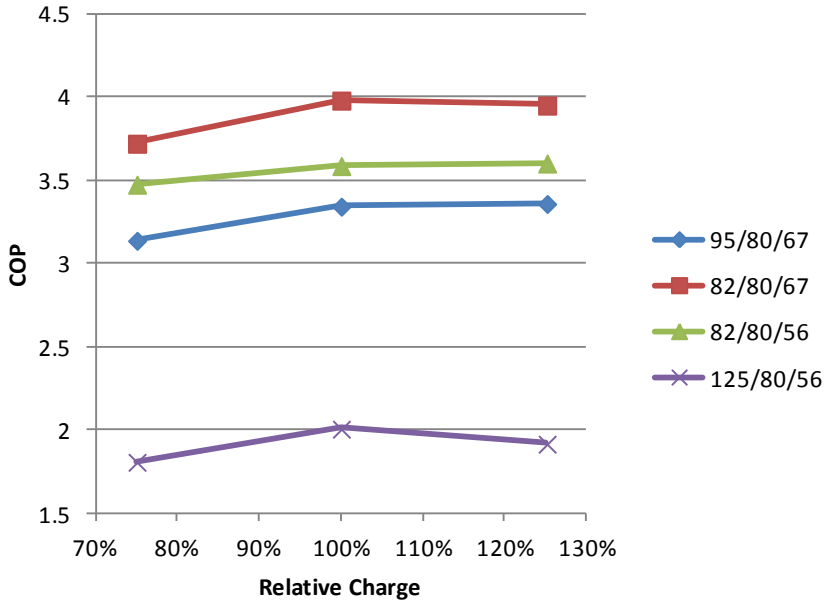

Figure 66: Effect of charge on COP for Split 4

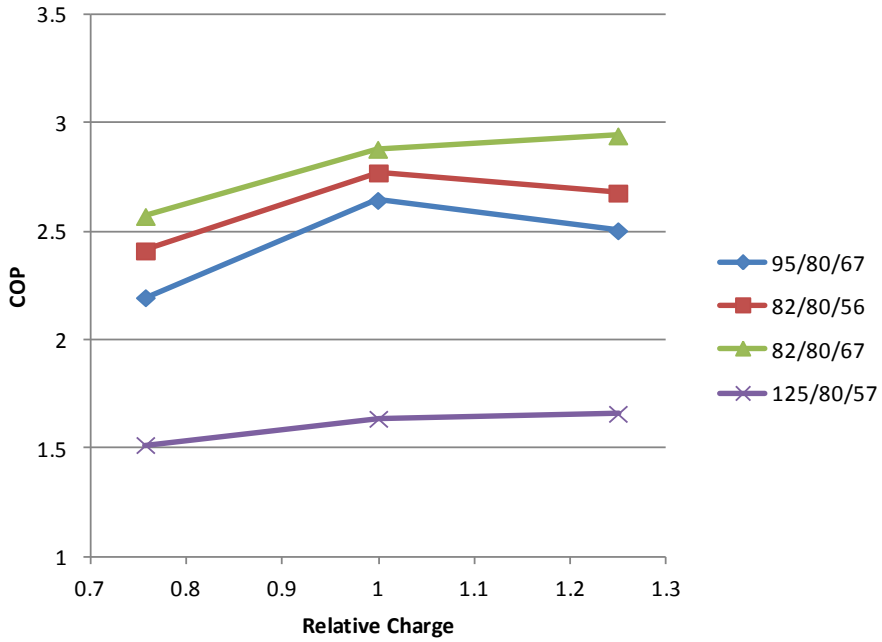

Figure 67: Effect of charge on COP for Split 5

Capacity vs. charge plots

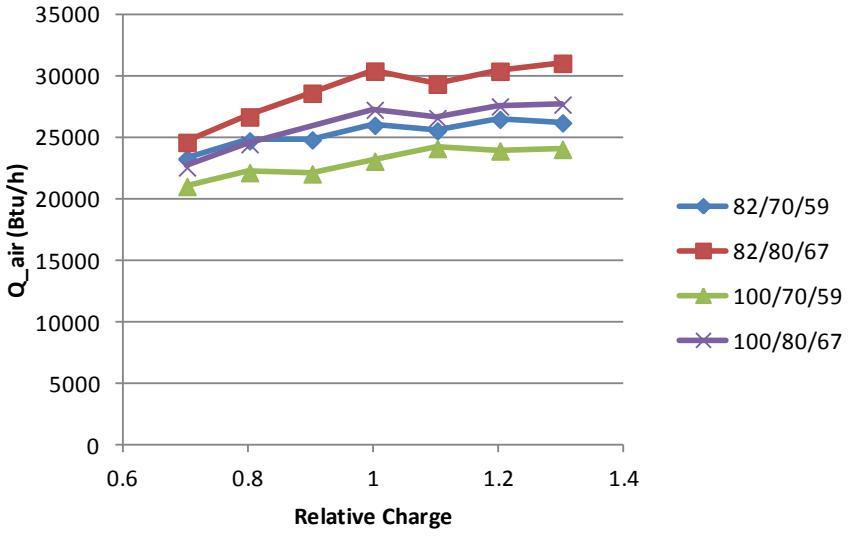

Figure 68: Effect of charge on capacity for RTU 2

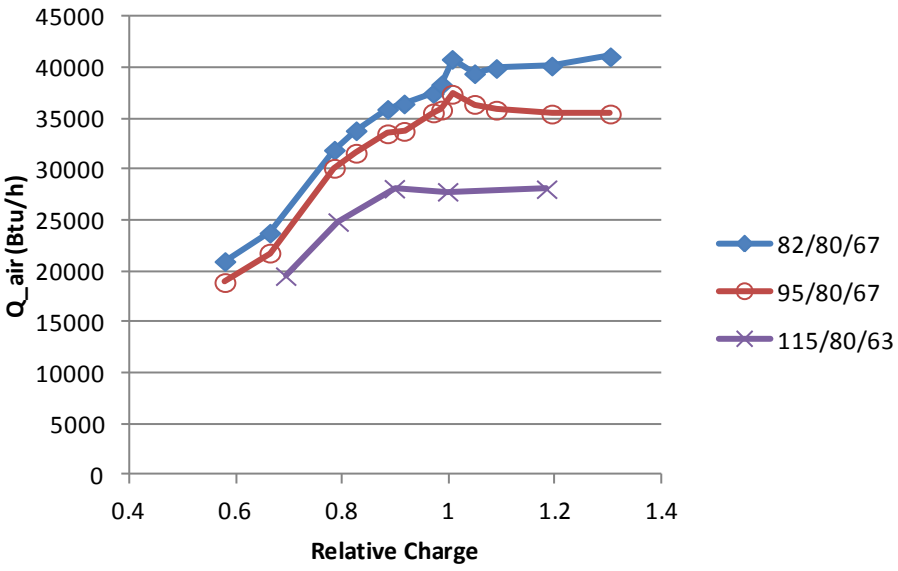

Figure 69: Effect of charge on capacity for RTU 3

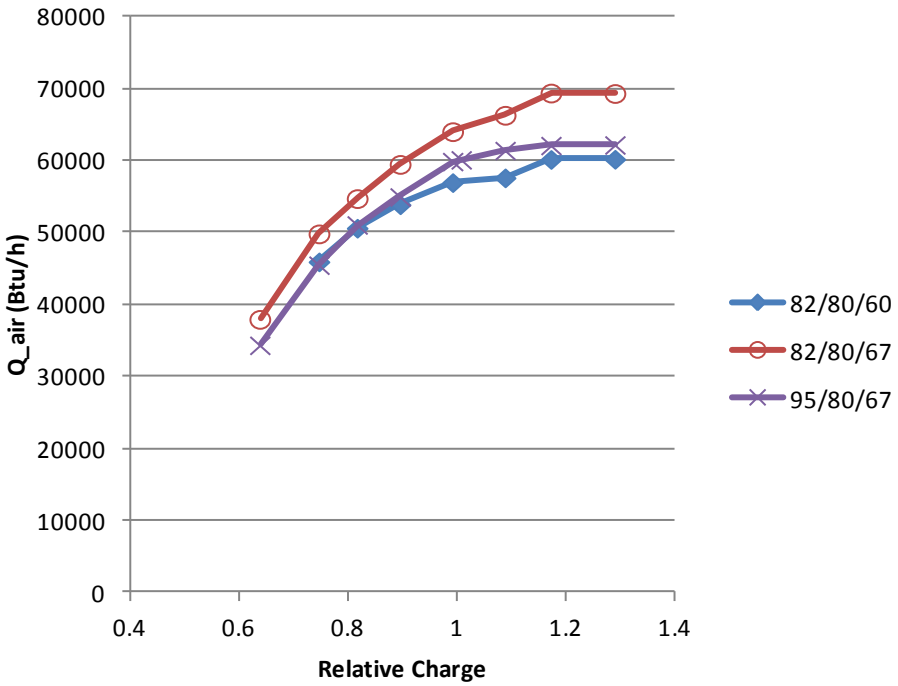

Figure 70: Effect of charge on capacity for RTU 4

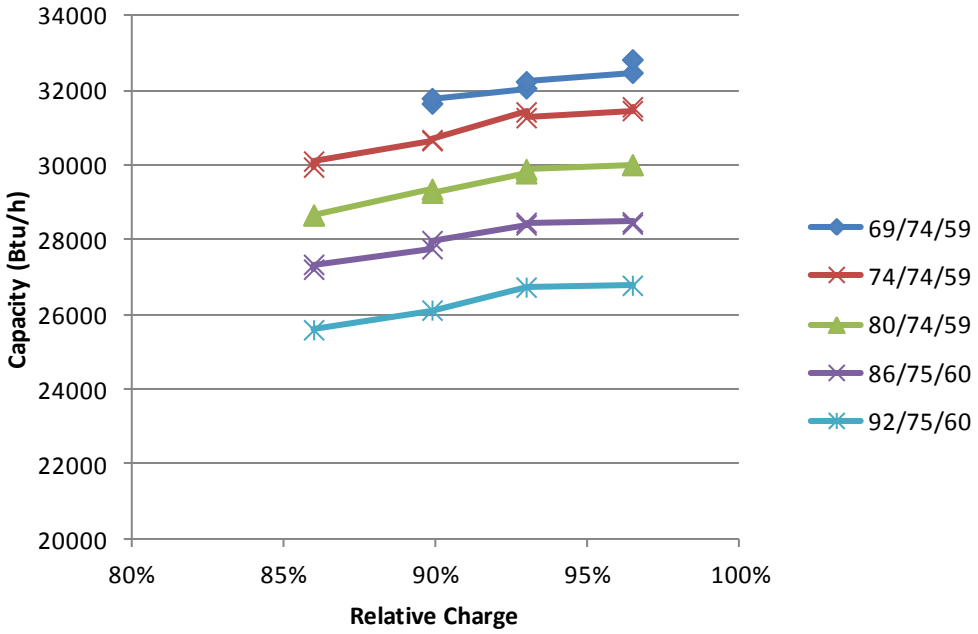

Figure 71: Effect of charge on capacity for RTU 7

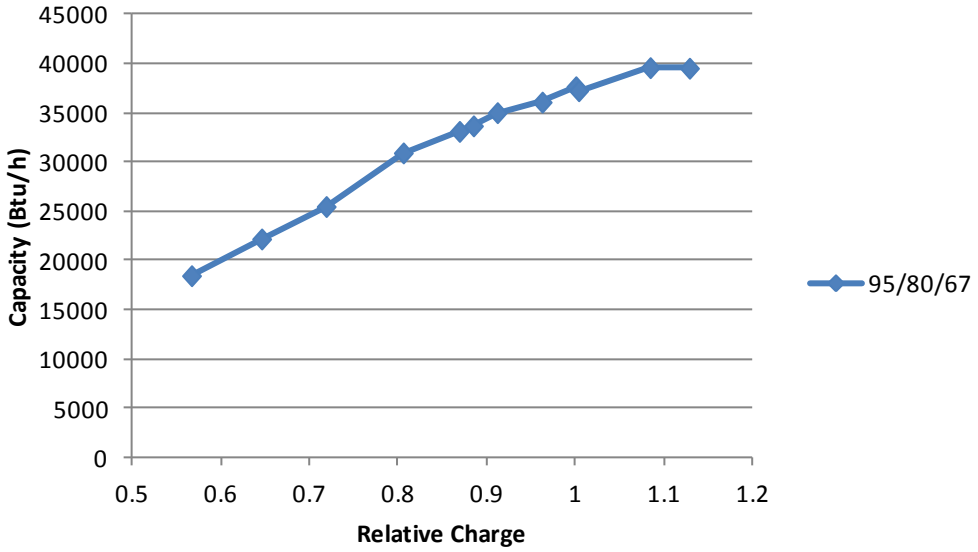

Figure 72: Effect of charge on capacity for Split 1

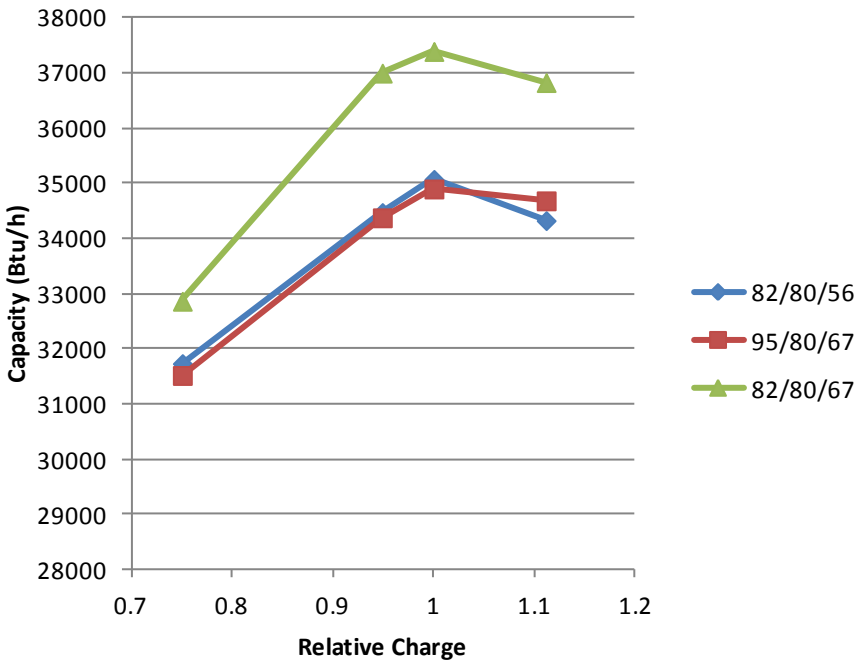

Figure 73: Effect of charge on capacity for Split 3

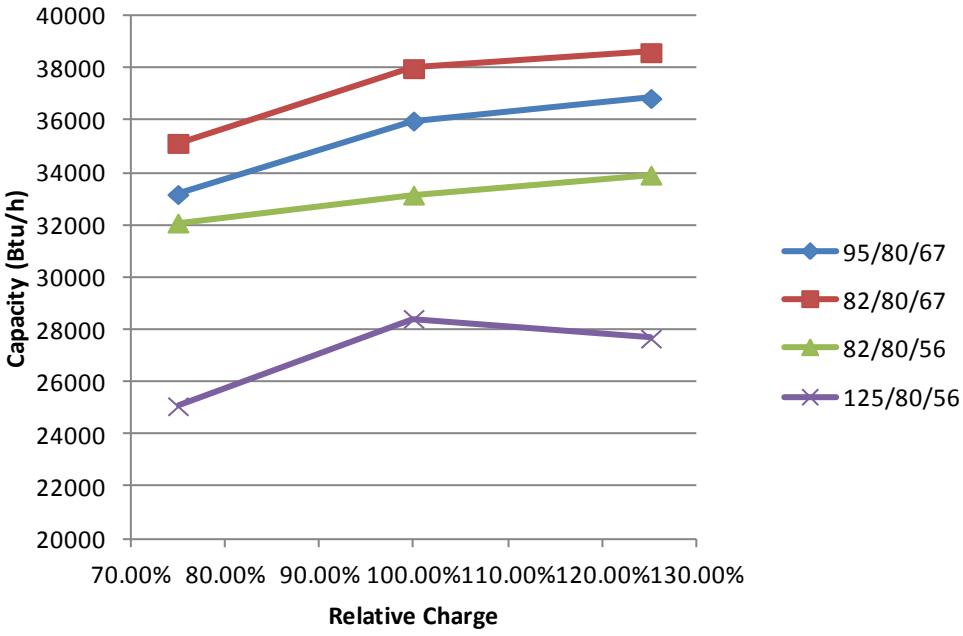

Figure 74: Effect of charge on capacity for Split 4

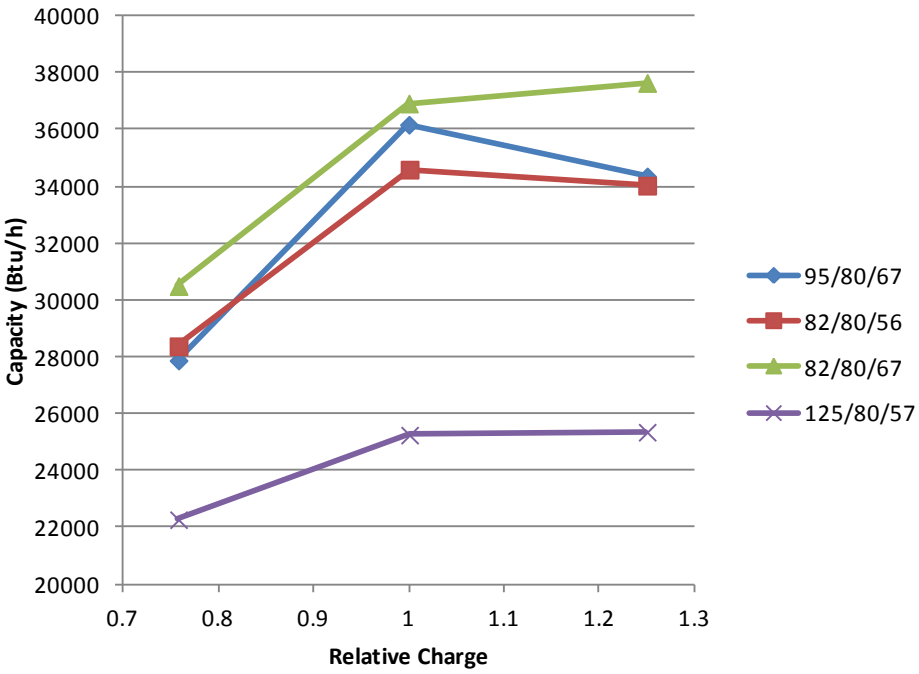

Figure 75: Effect of charge on capacity for Split 5

Normal model plots

This section presents plots of a representative sample of the normal models used in calculation of FIR values for the data library.

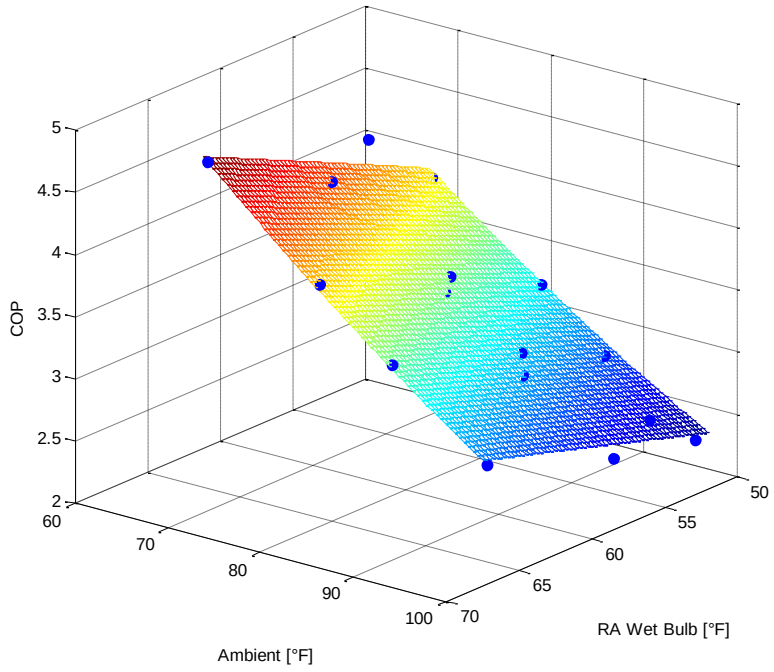

Figure 76: RTU 2 normal model and measurements of COP

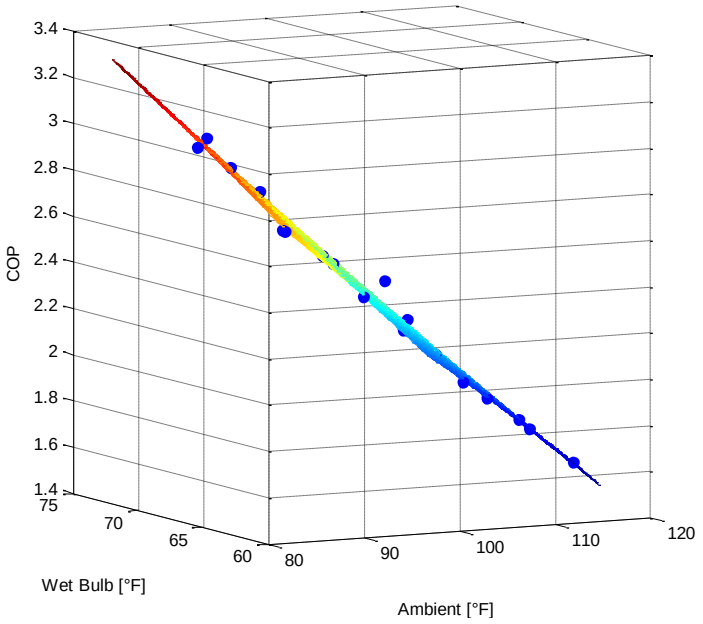

Figure 77: RTU 4 normal model and measurements of COP

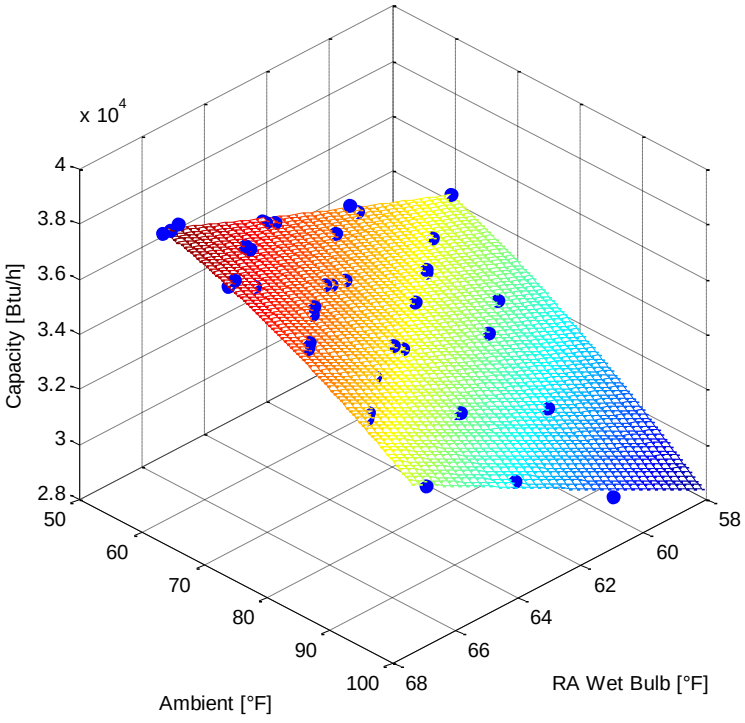

Figure 78: RTU 7 normal model and measurements of capacity

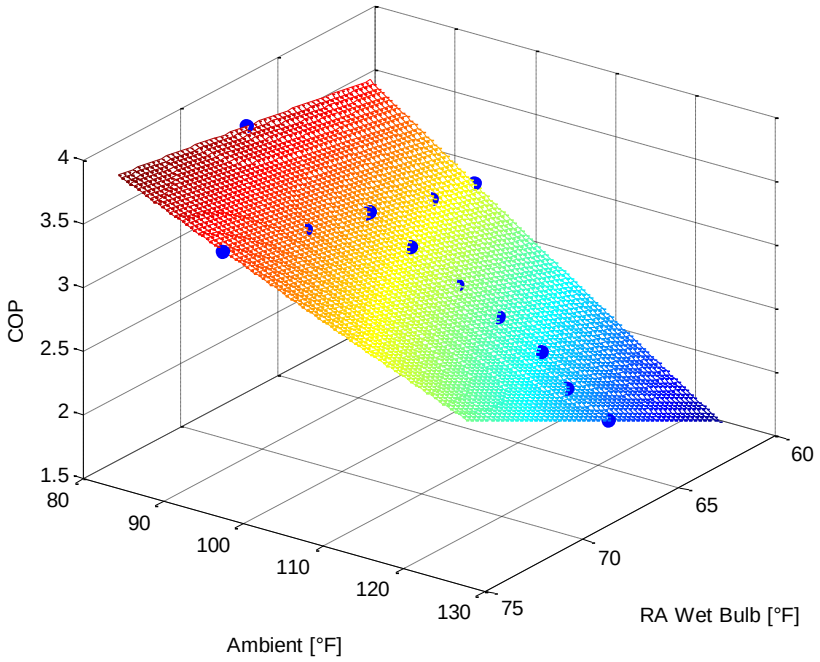

Figure 79: Split 1 normal model and measurements of COP

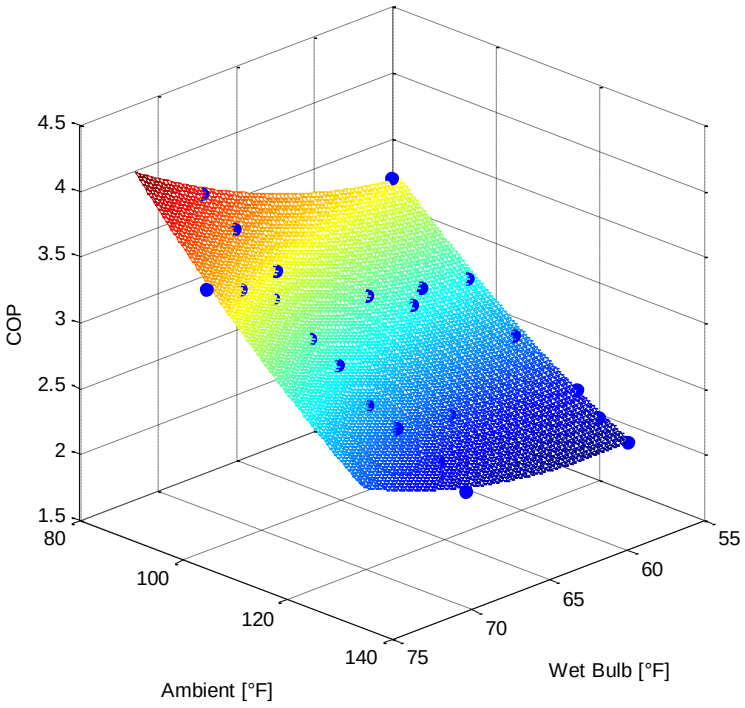

Figure 80: Split 2 normal model and measurements of COP

ATTACHMENTS

A METHOD FOR EVALUATING DIAGNOSTIC PROTOCOLS FOR PACKAGED AIR CONDITIONING EQUIPMENT:

1) EVALUATOR EXAMPLE 0.1.1
2) REVIEWER COMMENTS

FEBRUARY 2013
CEC-500-08-049

nbi new buildings institute

Example Output of *FDD Evaluator 0.1.1*

This appendix contains an example of an evaluation using the software *FDD Evaluator 0.1.1*. In this example, the following situation is evaluated:

Protocol: the 2013 Installer's (Title 24) version of the RCA
Units: All nine of the available HVAC systems
Fault conditions: only cases that have charge faults or no faults
Operating conditions: the full range of operating conditions (*i.e.* no test cases are filtered out because of their operating conditions)

Inputs

The units are selected in the blue region of the user interface. A screenshot of the user interface with the selections from this example is shown below.

The fault conditions are selected in the green region. For this example, only "Unfaulted", "UC (undercharge)" and "OC (overcharge)" are selected.

The purple region contains limits for minimum and maximum operating conditions. In this example, we leave the default values in place, so that we are not filtering out any test cases by specific operating conditions.

The drop-down menu labeled "Protocol Selection" allows us to choose among the four protocols that are coded in this version of the software (four versions of the Title 24 RCA protocol). We choose the 2013 Installer version ("RCA_2013).

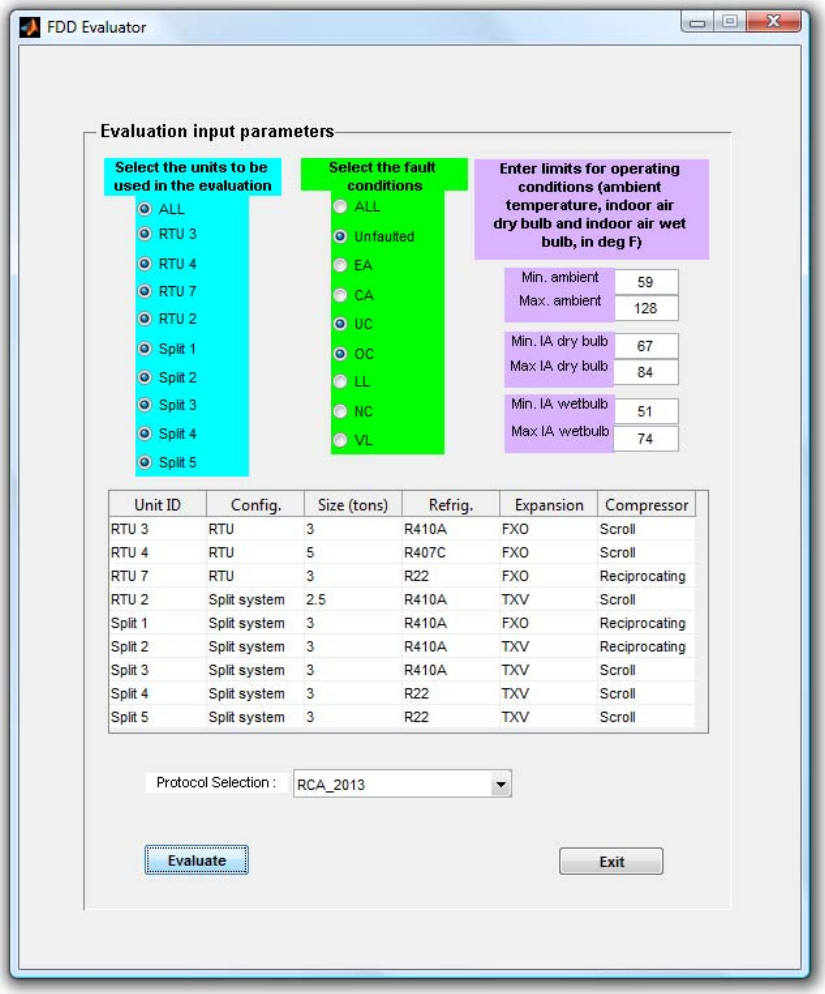

Next, we click "Evaluate" and the output figures are generated.

Outputs and Discussion

The software outputs four plots: 1) Numerical values tables; 2) False Alarm rates figure; 3) Misdiagnosis rates figure; 4) Missed Detection rates figure. The numerical values tables contain all of the data that the figures are based upon. These data may be copied and pasted to other programs for further analysis.

Screenshots of the output screens corresponding to the example situation are shown below.

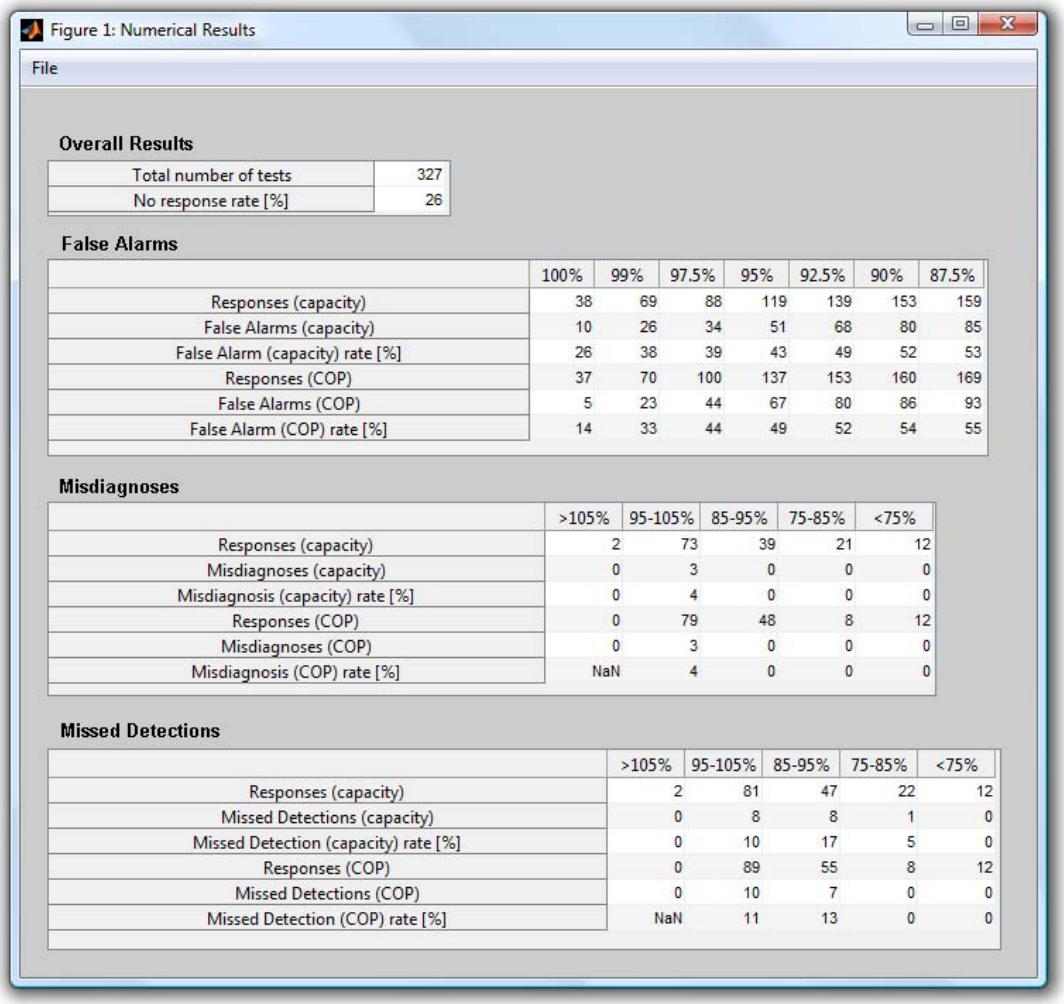

Overall Results

Total number of tests	327
No response rate [%]	26

False Alarms

	100%	99%	97.5%	95%	92.5%	90%	87.5%
Responses (capacity)	38	69	88	119	139	153	159
False Alarms (capacity)	10	26	34	51	68	80	85
False Alarm (capacity) rate [%]	26	38	39	43	49	52	53
Responses (COP)	37	70	100	137	153	160	169
False Alarms (COP)	5	23	44	67	80	86	93
False Alarm (COP) rate [%]	14	33	44	49	52	54	55

Misdiagnoses

	>105%	95-105%	85-95%	75-85%	<75%
Responses (capacity)	2	73	39	21	12
Misdiagnoses (capacity)	0	3	0	0	0
Misdiagnosis (capacity) rate [%]	0	4	0	0	0
Responses (COP)	0	79	48	8	12
Misdiagnoses (COP)	0	3	0	0	0
Misdiagnosis (COP) rate [%]	NaN	4	0	0	0

Missed Detections

	>105%	95-105%	85-95%	75-85%	<75%
Responses (capacity)	2	81	47	22	12
Missed Detections (capacity)	0	8	8	1	0
Missed Detection (capacity) rate [%]	0	10	17	5	0
Responses (COP)	0	89	55	8	12
Missed Detections (COP)	0	10	7	0	0
Missed Detection (COP) rate [%]	NaN	11	13	0	0

The section “Overall Results” presents data that are not shown graphically. The first is the total number of test scenarios that are included in the set. This number is a function of the conditions selected on the user interface. The maximum number is 607. In this example there are 327 tests, each of which is either unfaulted, or has a charge fault.

The second is the “No response” rate – the percentage of tests from the total number for which the protocol cannot be applied because of limitations on its applicability. In this case, there are 85 scenarios (26% of 327) in which the 2013 RCA couldn’t be applied.

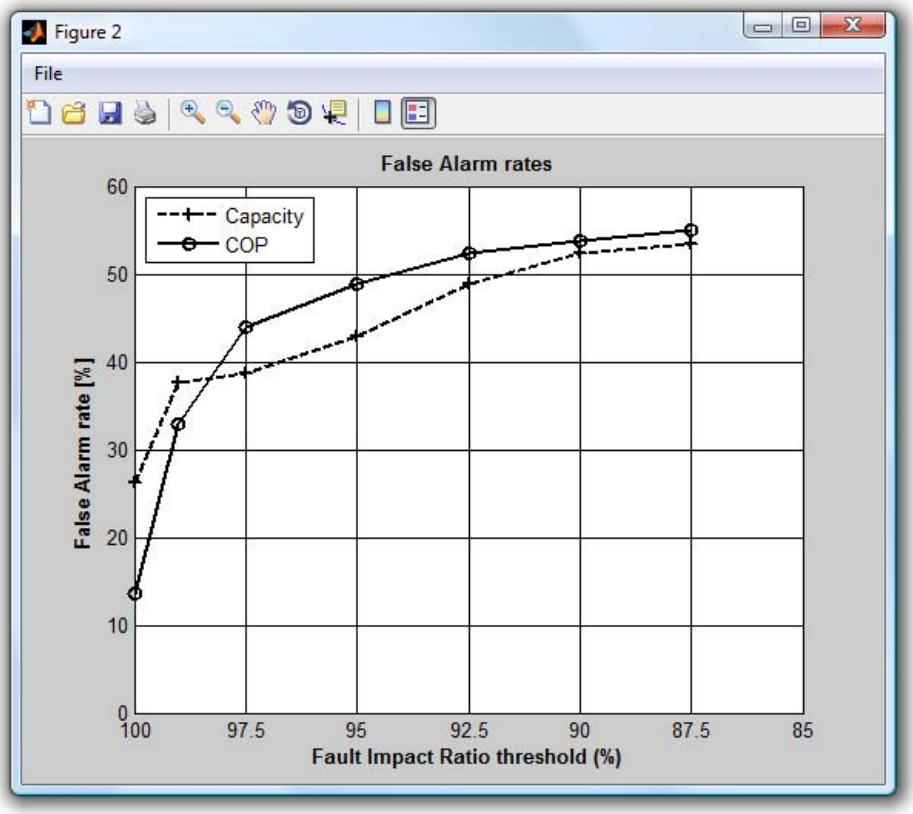

The figure labeled “Figure 2” shows the False Alarm rate at each of the Fault Impact Ratio (FIR) thresholds. For example, if a 2.5% degradation in efficiency (COP) is selected as the minimum degradation that should be considered significant, we look at the COP value at 97.5% FIR and see that a 44% False Alarm rate can be expected.

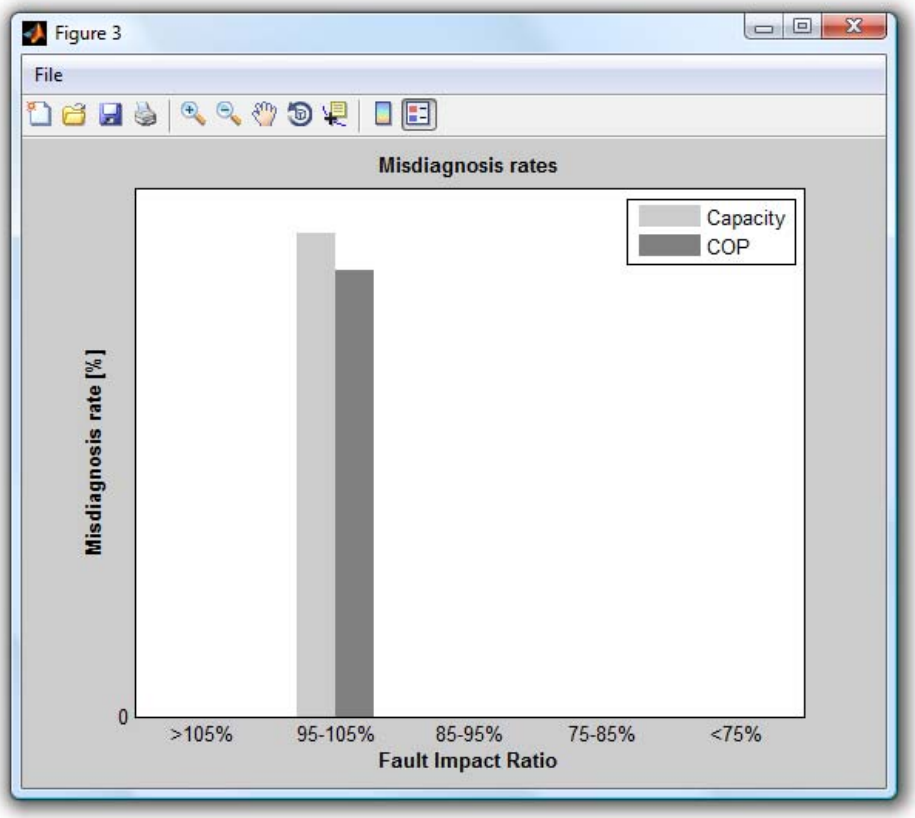

Misdiagnosis and Missed Detection results are presented in bins of FIR. For example, the middle bin contains all of the tests that have faults that reduce capacity or COP by 5 to 15% (i.e. FIR is 85-95%).

In this example, the only faults contained in the input data are overcharge and undercharge, and the only fault diagnoses the protocol can produce are overcharge and undercharge. Therefore, a misdiagnosis has to be an undercharge diagnosed as an overcharge, or vice versa. There are three such cases. In the case of capacity the denominator is 73, so the rate is 3/73 = 4.11%. For COP the denominator is 79, giving a rate of 3/79 = 3.80%. The tables in Figure 1 display integer (rounded) percentage values, but the plots use exact values.

The software's figure generator scales the ordinate (vertical) axis to the resulting values, and has minimum increments of 10%. In this case, the figure has been scaled to the point that the 10% label is not on the plot, so there are no labels on the ordinate except 0. In the next version of the software, the plot scale will be configured to display a minimum value of 10%.

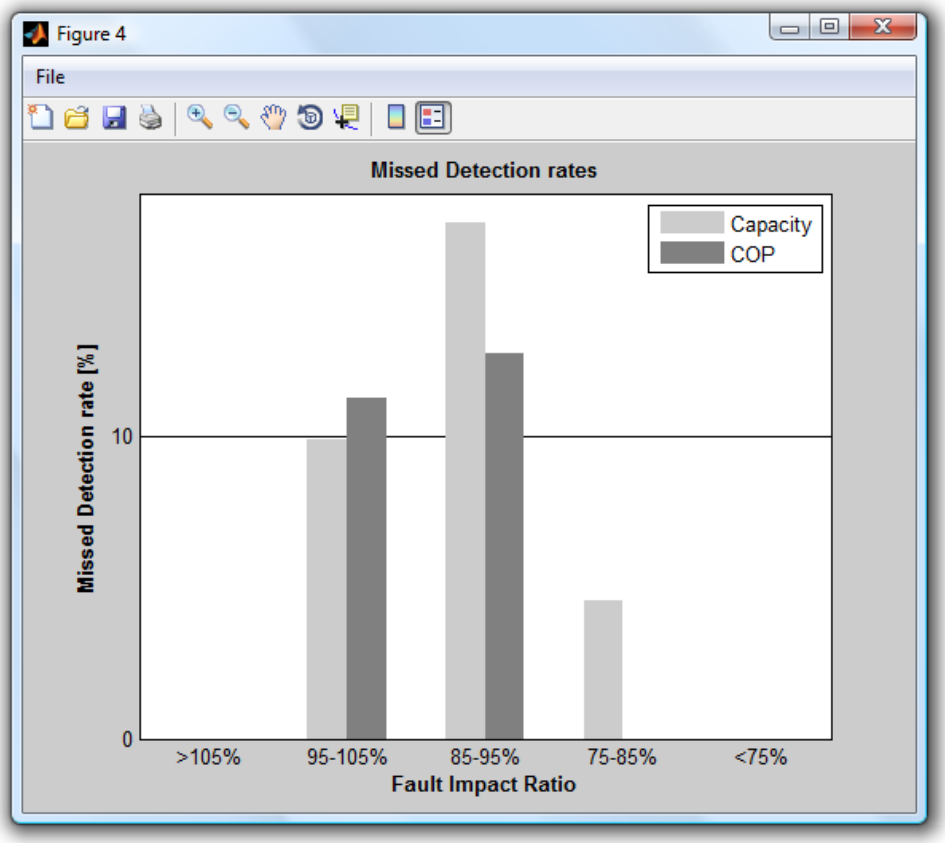

The missed detection rates for the 95-105% bin are roughly 10%. In general, not detecting a fault that has a small impact could be construed as a positive outcome. However, overcharge faults can present a danger to the compressor without having a large effect on capacity or COP. Since the only faults in the current example are charge faults (the unfaulted tests are not used in Missed Detection rate calculations) a large portion of the tests in the 95-105% range will be overcharge cases. Missing these fault detections is important even if the impact on capacity or COP is small.

There are no Missed Detections for cases in which COP is reduced by more than 15%, and none for cases in which capacity is reduced by more than 25%.

Comments and Recommendations on the Heating, Ventilation and Air Conditioning Fault Detection and Diagnostic Tool Evaluator developed by Herrick Laboratories (Purdue University)

March 6, 2013

By
Keith A. Temple, P.E.

Scope

1.1. A technical review of the Draft Final Report "A Method for Evaluating Diagnostic Protocols for Packaged Air Conditioning Equipment" prepared by James E. Braun, PhD, David P. Yuill and Howard Cheung (Ray W. Herrick Laboratories of Purdue University) dated September 30, 2012 was completed and a commented version of the document was submitted on October 18, 2012.

1.2. The present document provides additional comments and recommendations following the project workshops (Workshop on the HVAC Fault Detection and Diagnostic Tool Evaluator) held by NBI (Mark Cherniack) and Purdue University personnel on February 27 and 28, 2013 at WCEC facilities.

2. Comments

2.1. In general I support the methodology of the evaluation tool and the usefulness of such a tool; however, in my assessment the FDD Tool Evaluator requires further development of the data library and validation before it can be implemented as an industry standard.

2.2. The data library needs to be investigated and expanded to address the following:

2.2.1 Several systems in the data library have limited no fault tests which may not be sufficient to adequately determine the no fault performance. Systems 4 and 6 have only 1 and 2 no fault tests respectively making it doubtful that there is sufficient data to establish/confirm performance expectations, especially for system 4 which has a fixed expansion device. Likewise, systems 7, 8 and 9 (TxV systems) each have 4 no fault tests. This may be adequate if the tests represent the operating domain for the fault tests.

2.2.2 There is limited data for some faults, in particular liquid line restriction and compressor leakage.

2.2.3 The systems in the data library need to address the breadth of systems in the field and currently being manufactured. This includes a range of rated steady-state efficiencies from approximately 8 EER to 16+ EER and system characteristics such as finned-tube coils versus microchannel coils.

2.2.4 Simulation data would be helpful as long as the simulation model is fully validated for the application. I am not familiar with the published work on the model. Validation of the model predictions for some faults will be difficult based on the limited experimental fault data as noted above. My experience has been that superheat and subcooling are rather sensitive parameters, especially with regards to modeling, and they are often important parameters for FDD. The capability of the model to predict these parameters would need to be demonstrated.

2.3. There may be issues with the alignment of the fault/no-fault region defined by FIR and the evaluation of a real fault which has varying FIR with operating conditions. This may bias the results of the analysis if the FDD tracks fault level as opposed to efficiency or capacity degradation. The impact may not be that great. This would be a good thing to

test. As a related item, it would be useful to discuss the other approaches that were considered and why they were dismissed.

2.4. It seems that the Evaluator needs to be demonstrated/verified with a “good’ protocol or the unexpected behavior with the RCA protocol needs to be explained in more detail to validate the implementation of the evaluation methodology in the tool.

2.4.1 A possible FDD protocol for testing the evaluator is the subcooling/superheat method proposed by Temple (2004) or the method proposed by Li (2004).

2.5. The performance of the RCA protocol needs to be investigated further to understand the results of the evaluation of this protocol. This may not be relevant to the Purdue research team, but it may be helpful to understand why the RCA protocol produces the results it does as a means of further validating the evaluation method and its implementation.

2.6. The validation of the simulation model proposed for expanding the data library should include verification of the prediction of the following parameters which are likely to be used by FDD algorithms:

2.6.1 Suction pressure or corresponding evaporating temperature

2.6.2 Liquid line pressure or corresponding condensing temperature; could also consider discharge pressure

2.6.3 Superheat (or suction temperature)

2.6.4 Subcooling (or liquid line temperature)

2.6.5 Compressor current or power

2.6.6 Some have tried to use discharge temperature for diagnostics, but this is a rather unreliable measure in the field (more so than the others)

2.6.7 Evaporator discharge air temperature (dry-bulb)

2.6.8 Condenser discharge air temperature (dry-bulb)

2.7. The input structure for the systems in the data library should allow for the following system information provided by the manufacturer (refer to Table 6 in the project report):

2.7.1 The input for target subcooling should allow for more than a single subcoooling value based on operating conditions. Target subcooling should also be an allowable input for fixed expansion device systems.

2.7.2 Input of the manufacturer’s target superheat data based on operating conditions should be allowed for both fixed expansion device systems and a fixed superheat value or range should be allowed for TxV systems.

2.8. It is recommended that WCEC help champion the formation of an ASHRAE standards committee that can oversee future research and development of the FDD evaluator as an industry standard. In addition to Kristin Heinemeier, Mark Modera at WCEC has

particular experience with this process. This recommendation is the result of an inquiry from and discussion with Jeff Miller (CEC).

3. Recommendations for Future Research

3.1. Expand the data library to adequately address the identified faults and range of system characteristics corresponding to the current body of unitary air-conditioning systems in operation. This should include the range of rated steady-state cooling efficiencies (EER). Document how the systems in the data library accomplish the objective.

3.2. Investigate the implications of the fault/no-fault definition based on FIR in the context of a FDD protocol that identifies a specific fault level (a real-world fault).

3.3. Demonstrate the performance of the evaluator for another protocol that has an algorithm that is disclosed in the public domain such that the evaluation results can be understood and explained. A possible alternate protocol is the method using both subcooling and superheat proposed by Temple (2004) or the method proposed by Li (2004). Each of these methods is protected by a patent, but is also disclosed in the corresponding patent.

3.4. Provide a summary document of the model validation which demonstrates that the model is suitable for the intended application including prediction of the appropriate performance parameters (refer to notes above) for the range of systems and system faults.

4. References

4.1. Li, H. A Decoupling-based Unified Fault Detection and Diagnosis Approach for Packaged Air Conditioners, Ph.D. Thesis, Purdue University, August 2004.

4.2. Temple, K. 2004. A Performance Based Method to Determine Refrigerant Charge Level for Commissioning Unitary AC and HP Systems. In Proceedings of the ACEEE 2004 Summer Study on Energy Efficiency in Buildings, 1:306-317. Washington, D.C.: American Council for an Energy-Efficient Economy.

Comments on a Method for Evaluating Diagnostic Protocols for Packaged Air Conditioning Equipment Draft Report

Version 2

Prepared by:
John Proctor, P.E.
CEO, Proctor Engineering Group, Ltd.
418 Mission Ave.
San Rafael, CA 94901
john@proctoreng.com
www.proctoreng.com

March 6, 2013
Revised from February 25, 2013

Table of Contents

Executive Summary

Introduction

When this Fault Detection and Diagnostics (FDD) project began and we met with the investigators, we became cautiously enthusiastic that it would yield an open system for evaluating and improving the diagnosis of air conditioners and heat pumps. We looked forward to an available database of laboratory tests that could be used to analyze issues and discrepancies and resolve them with shared data.

Having attended the review meeting on February 28, 2013 and having worked for a number of hours with the product, it appears to us that it cannot address the real needs for developing fault diagnostics that we can all agree meet the needs of the situation.

The product has improved by being able to look at faults based on their effect on efficiency. That is a very positive step forward.

The small number of units in the analysis and the fact that they are hidden behind a curtain of secrecy makes it impossible to agree that they are right or to use the information to improve FDD products. It is akin to a blind person on a hunting trip without a guide or companion.

Proctor Engineering Group trusts the intentions of the investigators. However we cannot say that we trust that they or anyone else is always right.

The report used the manufacturers' diagnostic protocols enforced by Title 24 as a case study. In order to properly evaluate any diagnostic protocol, it is necessary to understand the purpose and milieu of the protocol. Some of these comments discuss the purpose of the Title 24 application of the air conditioning manufacturers' protocols for charge and airflow.

The Title 24 protocol is intended to ensure that newly installed air conditioners in California:

1. Do not have extremely low evaporator airflow, which produces low sensible efficiency
2. Are not undercharged or overcharged to the point that sensible efficiency is seriously degraded.

The milieu of the protocol is that:

1. It must be accepted by most of the manufacturers as identical to, or not in conflict with their factory protocols.
2. It must be cost effective to apply the protocol.

Results

As shown in the table below, when airflow is measured directly, as it is in the 2013 Title 24, the manufacturers' and 2013 HERS protocols seem to achieve what they set out to do. When the Purdue data are visible it will be possible to evaluate the manufacturers' protocols for additional improvements.

Manufacturers' Installation Protocol						
Metering Device	Orifice		TXV		All Metering Devices	
	Errors	Cases	Errors	Cases	Errors	Cases
False Alarms (no Fault – Fault Indicated)	12 #	56	5	23	17	79
Misdiagnosis (Wrong Fault Identified)	0	34	0	34	0	68
Missed Diagnosis (Fault Present > 5% Effect – No Fault Indicated)	6	40	1	35	7	75
HERS Protocol						
Metering Device	Orifice		TXV		All Metering Devices	
	Errors	Cases	Errors	Cases	Errors	Cases
False Alarms (no Fault – Fault Indicated)	1	56	3	23	4	79
Misdiagnosis (Wrong Fault Identified)	0	28	0	27	0	55
Missed Diagnosis (Fault Present > 5% Effect – No Fault Indicated)	12 ##	40	8 ##	35	20 ##	75
# = 9 of the 12 cases are for RTU7, potentially indicating something special about that unit or the test conditions covered by the tests with that unit. ## = 0 Errors at > 15% Effect						

Recommendations

There is a strong need for full disclosure if this project is going to achieve the twin goals of improving FDD and providing a consensus method of evaluating FDD products. In order to achieve these twin goals, Proctor Engineering Group recommends that:

1. The cases in the data library be made universally available.
2. The data library structure be examined to make additions to the library consistent.
3. The data library be expanded with available data from independent researchers.
4. The data library be expanded with data from manufacturers.
5. The data library be expanded with additional elements, such as sensible heat ratio.

Additional Research

There is an urgent need for a field study that identifies:

1. the extent and magnitude of non-condensable contamination in existing and newly installed air conditioners
2. the extent and measured magnitude of liquid line restrictions in California air conditioners
3. the extent and measured magnitude of condenser heat transfer problems in California air conditioners
4. whether or not valve leakage is a significant problem in California air conditioners.

Moving Forward

We look forward to working through the Purdue data library and expanding it with additional laboratory data.

Discussion

A Parable

A cave man asked his wife to get him a rock. While he was out hunting the next day, she looked around and found a really nice rock, which she presented to him when he returned. He said: “No this is not right this rock is too big!”.

The next day while the cave man was hunting, his wife looked around and found a really nice small rock, which she presented to him when he returned. He said: “No this is not right this rock is too small!”

The next day while the cave man was hunting, his wife looked around and found a really nice medium sized rock, which she presented to him when he returned. He said: “No this is not right this rock is white!”

The next day while the cave man was hunting, his wife looked around and found a really nice medium sized black rock, which she presented to him when he returned. He said: “No this is not right this rock is black!”

This continued day after day until one day he did not go hunting. Instead he called together a few of his buddies. They sat with their backs to the cave entrance with the rock collection in front of them. As his wife was entering the cave with the latest rock for him she heard him say: “I am so frustrated!! No matter what I do my wife always brings me the wrong rock. She is so stupid.” The other cavemen agreed some even saying that their wives were stupid too. The wife walked up behind the Caveman and whacked him in the back of the head with the rock.

Limited Test Cases and Secrecy

Table 3 from the study summarizes the test cases within the Purdue data library.

Table 3: Summary of test cases in experimental data library

#	ID	Type	Capacity [tons]	Refrig.	Exp. Device	Comp. Type	Number of tests: No Fault	UC	OC	EA	CA	LL	NC	VL	Temp. Min. [°F]	Temp. Max. [°F]
1	RTU 3	RTU	3	R410a	FXO	Scroll	24	25	12	21	6	0	0	0	67	125
2	RTU 7	RTU	3	R22	FXO	Recip.	39	34	0	26	36	34	0	33	60	100
3	RTU 4	RTU	5	R407c	FXO	Scroll	17	15	12	19	8	0	0	0	67	116
4	Split 1	Split	3	R410a	FXO	Recip.	1	29	1	0	0	0	0	0	82	127
5	RTU 2[1]	Split	2.5	R410a	TXV	Scroll	16	12	12	21	15	16	15	16	70	100
6	Split 2	Split	3	R410a	TXV	Recip.	2	30	7	0	0	0	0	0	83	127
7	Split 3	Split	3	R410a	TXV	Scroll	4	4	7	0	0	0	0	0	82	125
8	Split 4	Split	3	R22	TXV	Scroll	4	8	0	8	0	0	0	0	82	125
9	Split 5	Split	3	R22	TXV	Scroll	4	4	4	6	0	0	0	0	82	125
						Total:	111	161	55	101	65	50	15	49		

Note 1: RTU 2 is a split system, but was named using a previous naming convention.

It is of concern that there are only nine units that provide data to the library. It is of even greater concern that only four units provide data for condenser airflow while only three units provide data for liquid line restriction and compressor valve leakage. Finally a single unit is used to address non-condensable contamination of the refrigerant.

The data library needs to be expanded to be certain of its accuracy and usefulness.

Furthermore, the accuracy of the data in the library and the reasons for different diagnoses by any protocol and the Purdue data is totally hidden.

The data library needs to be open to be certain of its accuracy and to make it useful.

Achieving Improved Performance of Air Conditioners in the Field

It is nearly universally accepted that a large percentage of the technicians do not check for airflow or for refrigerant charge using the manufacturers' methods. Field testing by various entities has verified that airflow is low and refrigerant charge is often incorrect for both newly installed as well as existing air conditioners.

The Title 24 enforcement of the manufacturers' protocols was initiated because there was adequate data on airflow and refrigerant charge faults in newly installed air conditioners. The enforcement set about addressing those two issues within the milieu of manufacturer acceptance and cost effectiveness.

The Title 24 protocol is intended to ensure that newly installed air conditioners in California:

1. Do not have extremely low evaporator airflow, which produces low sensible efficiency
2. Are not undercharged or overcharged to the point that sensible efficiency is seriously degraded.

The milieu of the protocol is that:

1. It must be accepted by most of the manufacturers as identical to, or not in conflict with their factory protocols.
2. It must be cost effective to apply the protocol.

Looking at the results of this study, this author characterizes the results of the manufacturers' protocols in Title 24 as better than adequate. The changes in the 2013 Standard wherein airflow is measured and verified to be in excess of 350 CFM per ton is a substantial improvement.

Results as Contained in the Purdue Report

False Alarms

The Purdue paper calls false alarms as: "no significant fault is present, but the protocol indicates the presence of a fault."

Orifice Units – Running the Evaluator for the situations that there is no fault present against the 2013 Installer (2013eye) protocol, there are 12[1] out of 56 cases where 2013eye indicates a fault where the Purdue data library identified no fault. Rerunning the Evaluator for the same scenario against the 2013 HERS (2013H) protocol, there is only 1 out of 56 cases where 2013H indicates a fault. This points to the effectiveness of the wider acceptance band in avoiding contractors having come back to work on a unit that was passed by the installer.

TXV Units – Running the Evaluator for the situations that there is no fault present against the 2013 Installer (2013eye) protocol, there are 5 out of 23 cases where 2013eye indicates a fault where the Purdue data library identified no fault. Rerunning the Evaluator for the same scenario against the 2013 HERS (2013H) protocol, there are 3 out of 13 cases where 2013H indicates a fault. This points to the need to have the data to determine why the TXV protocol performs worse than the Orifice protocol with respect to False Alarms.

Runs that include "insignificant faults" from the Purdue data library -- If one includes the situation where there is a smaller fault, then the "false alarm" rate rises. This points to the need to examine these cases to determine the cause of the differences and whether an action should or should not be taken.

Misdiagnosis

Misdiagnosis is being defined as the situation wherein there is a significant fault present, but the protocol identifies a different fault as present. Given that the only misdiagnosis available is to mistake

[1] 9 of the 12 cases are for RTU7, potentially indicating something special about that unit or the test conditions covered by the tests with that unit.

undercharge for overcharge, or vice versa, it is no surprise that both 2013 protocols make no misdiagnoses when the fault has a 5% or higher impact on efficiency.

Missed Detections

Missed detections are defined as the situation wherein there is a significant fault present, but the protocol does not identify a fault. For 2013eye, there are 7 missed detections out of 55 cases. All but one of these are on orifice machines. For 2013H, there are 20 misses reflecting the wider margin of acceptance. There are no cases where 2013H allows a fault with more than 15% COP error to pass.

Early Considerations

Title 24

The California Energy Commission is mandated to produce changes that save energy in buildings. Increasing airflow and reducing the percentage of units with significantly incorrect refrigerant charge is one of the ways to improve energy efficiency.

When the introduction of refrigerant charge and airflow measures in Title 24 was first considered one of the consultants working on the issue noted that the existing manufacturers' method for diagnosing low airflow (temperature split) was far from perfect and other methods would be better. The consultant also raised the issue that the existing superheat tables for charging air conditioners were not sufficiently documented[2]. Early in conversations about and with manufacturers it became clear that the manufacturers would fight methods that conflicted with their specifications.

In the interest of improving the situation at the time, the temperature split, superheat, and subcooling methods of the manufacturers were written into the code and enforced for the first time in any state.

Implementing the Manufacturers' Specification in Utility Programs

As the manufacturers' specifications were implemented within Title 24 and Utility programs it became increasingly clear that the temperature split method was merely a first step toward improving air conditioner efficiency and that a better method was highly desirable. Based on that understanding, the CEC has changed to airflow protocol to direct airflow measurement along with direct measurement of fan watt draw.

Similarly direct measurement of airflow was a proposed change to utility programs, but that change met significant resistance.

It also became clear that, while the manufacturers' Superheat tolerance[3] of ± 5°F might be desirable for installations from the manufacturers' perspective, the tolerance was too narrow for HERS raters' inspections and for utility programs that seek to obtain significant energy savings. As a result changes were proposed for HERS raters and for utility programs. The first change in that direction was taken with the 2008 Title 24 Standards. These changes were resisted and not implemented in utility programs.

[2] Given the manufacturer's desire for about 12 degrees of superheat at 95/80/67 the concern was whether the published target superheats at other conditions would translate to 12 degrees of superheat at 95/80/67.
[3] As well as the manufacturers' subcooling tolerances of ±3°F or less.

Inside Title 24, the tests are generally done on newly installed air conditioners and therefore the condenser heat exchange (condenser air flow and coil cleanliness) is assumed to be correct. Within utility programs however that is not necessarily a good assumption. Many utility programs instituted coil cleaning either as a prerequisite to a tune up or as a paid portion of a tune up. It became clear that if contractors are allowed to "clean condenser coils" to improve condenser airflow and be paid based on how many they cleaned, that they would "clean" almost every condenser coil. More comprehensive diagnosis is used in some utility programs to reduce unnecessary "coil cleaning".

Inside Title 24 and within utility programs a viable (cost effective) consensus method of determining non-condensables in the system has not been found.

The percentage of units with the following faults and the distribution of fault magnitudes in the population are not known for:

- non-condensables
- liquid line restrictions
- compressor valve leakage

Cost Effectiveness

The cost effectiveness of the applying a protocol is judged basically by the following simplifications:

The value of the measure must be equal to or exceed the cost of applying the measure

Value of Measure ($) = Energy Savings (kWh) × Time Value ($/kWh)

ΔE_F = Energy Savings (kWh) = Excess Energy Use due to the corrected Fault (kWh)

Fault conditions range in magnitude from those with negligible energy consequences to those with large energy consequences.

ΔE_{Fi} = Excess Energy Use for corrected fault condition i

$$\Delta E_F = \sum_{i=1}^{n} \Delta E_{Fi} \times \%Occur\&Repair_{Fi}$$

Cost of Measure ($) = Technician's Cost ($) + HERS Rater's Cost($) × (% Inspections)

The Technician Cost is the cost of the additional time the technician must spend to diagnose and, if necessary, repair the particular fault.

ΔCT_{Fi} = Incremental Technician cost for fault condition i

$$\Delta CT_{Fi} = DiagnosticCost_{Fi} + RepairCost_{Fi} \times \%Occur\&Repair_{Fi}$$

Therefore:

The incremental cost effectiveness of the repair of any fault is:

$$CE_{Fi} = \frac{\Delta \mathrm{E}_{Fi} \times \%Occur\&Repair_{Fi}}{DiagnosticCost_{Fi} + RepairCost_{Fi} \times \%Occur\&Repair_{Fi}}$$

Note that:

1. The less often a fault occurs the less cost effective the measure will be. Therefore it is necessary to have a decent idea of the percentage of the time the fault occurs and the distribution of its magnitude.
2. The higher the diagnostic cost and/or the repair cost the less cost effective the measure will be.

Additional Comments and Clarifications

1. The paper states that the airflow diagnostic is intended to ensure that the evaporator has sufficient airflow for the charge diagnostic to be applied. This statement is derived from Title 24 and manufacturers' write-ups of the temperature split method. In actuality, we were also seeking to improve over the widespread problem of low airflow. Low airflow results in low sensible EER – very detrimental in California.
2. The paper points out that the range of conditions under which the charge tests can be made is limited. It is true that the range of refrigerant charge testing for non-TXV units is limited to conditions that the data and the manufacturers believe that the results are reasonably accurate in determining whether or not a repair should be made. Title 24 has also introduced a method of checking charge for TXV systems that allows checking under a much wider variation of conditions.
3. The study provides a flow diagram of the protocol. There is one missing element in that flow diagram, the recursive return to the start when a change is made.

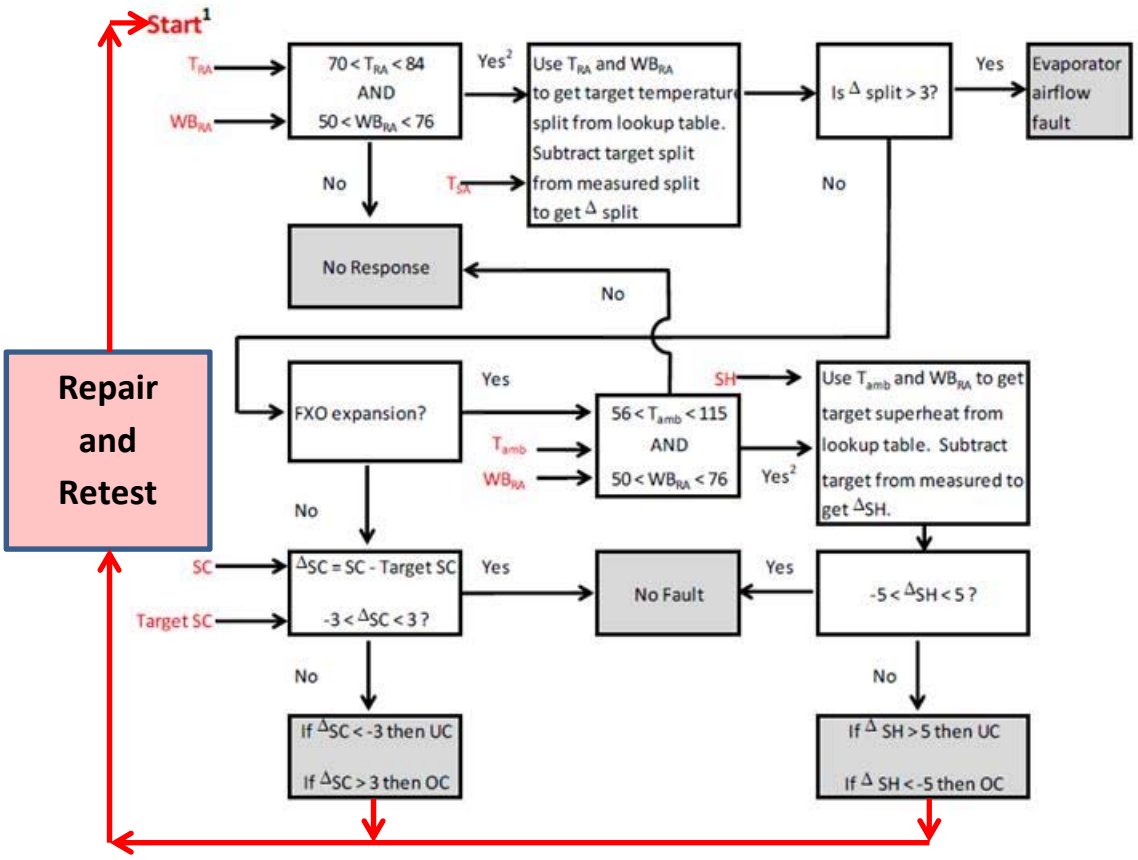

4. The paper provides adequate data to judge the difference between the Purdue definition of proper charge and the manufacturers' definition of proper charge. Specifically the study states:

   " The one Misdiagnosis is an undercharged case diagnosed as overcharged. It is a fixed orifice unit with high indoor humidity (80°F dry-bulb and 74°F wet bulb), and with 95°F outdoor temperature. The charge level is 92% of nominal, and the measured superheat is 15°F."

   The difference in definitions is the cause of this difference in diagnosis. By Purdue's definition the unit is undercharged by 8% however according to the manufacturer's superheat table, the target superheat for these conditions is 25°F. That is 10°F out of specification in the overcharge direction.

5. The paper notes that some evaluations of air conditioning programs based on protocols similar to the manufacturers' had energy savings that fell short of expectations. It should also be noted that other evaluations in California and elsewhere show energy savings in the expected range. The causes of any shortfalls are more likely to be misapplication of the basic methods (superheat, subcooling, and airflow) rather than to the effectiveness of those methods.
6. The paper points out that an ideal evaluation would produce typical economic benefit from deploying the fault detection and repair. Further it notes that this economic benefit is dependent on the prevalence of the faults. To that thought we add the distribution of the magnitudes of the fault as well as the costs to diagnose and repair those faults.
7. The study noted that the amount of laboratory data available and used in the study was limited and that a simulation model would built based on that data as well as engineering modeling. When the model is built it will need to be determined whether it is as good as or better than other models. It is essential that the model be compared to other models and, more importantly, to additional laboratory data.